

CONFIGURATION AND ANALYSIS OF
PIEZOELECTRIC-BASED IN-SOCKET SENSORY SYSTEM
FOR TRANSFEMORAL PROSTHETIC GAIT DETECTION

FARAHYAH BINTI JASNI

FACULTY OF ENGINEERING
UNIVERSITY OF MALAYA
KUALA LUMPUR

2018

**CONFIGURATION AND ANALYSIS OF
PIEZOELECTRIC-BASED IN-SOCKET SENSORY
SYSTEM FOR TRANSFEMORAL PROSTHETIC GAIT
DETECTION**

FARAHYAH BINTI JASNI

**THESIS SUBMITTED IN FULFILMENT OF THE
REQUIREMENTS FOR THE DEGREE OF DOCTOR OF
PHILOSOPHY**

**FACULTY OF ENGINEERING
UNIVERSITY OF MALAYA
KUALA LUMPUR**

2018

UNIVERSITY OF MALAYA
ORIGINAL LITERARY WORK DECLARATION

Name of Candidate: Farahiyah binti Jasni

Matric No: KHA130094

Name of Degree: Doctor of Philosophy

Title of Project Paper/Research Report/Dissertation/Thesis ("this Work"):

Configuration and analysis of piezoelectric-based in-socket sensory system for transfemoral prosthetic gait detection

Field of Study: Rehabilitation Engineering

I do solemnly and sincerely declare that:

- (1) I am the sole author/writer of this Work;
- (2) This Work is original;
- (3) Any use of any work in which copyright exists was done by way of fair dealing and for permitted purposes and any excerpt or extract from, or reference to or reproduction of any copyright work has been disclosed expressly and sufficiently and the title of the Work and its authorship have been acknowledged in this Work;
- (4) I do not have any actual knowledge nor do I ought reasonably to know that the making of this work constitutes an infringement of any copyright work;
- (5) I hereby assign all and every rights in the copyright to this Work to the University of Malaya ("UM"), who henceforth shall be owner of the copyright in this Work and that any reproduction or use in any form or by any means whatsoever is prohibited without the written consent of UM having been first had and obtained;
- (6) I am fully aware that if in the course of making this Work I have infringed any copyright whether intentionally or otherwise, I may be subject to legal action or any other action as may be determined by UM.

Candidate's Signature

Date:

Subscribed and solemnly declared before,

Witness's Signature

Date:

Name:

Designation:

CONFIGURATION AND ANALYSIS OF PIEZOELECTRIC-BASED IN-SOCKET SENSORY SYSTEM FOR TRANSFEMORAL PROSTHETIC GAIT DETECTION

ABSTRACT

Sensory system is one of the important components in micro-processor controlled (MPC) prosthetic leg. It provides the information to the controller on the current phase of the device and, in some applications, the signals from the sensory system are used to predict the intended movement of the amputee. Hence, the quality of the sensory system for the MPC prosthetic leg is very important. The challenge is to balance between the practicality and the efficiency of the sensory system. This study investigated the feasibility and efficacy of an in-socket sensory system which uses multiple piezoelectric sensors as a sensory system for transfemoral (TF) MPC prosthetic leg. The methodology comprised of selecting: (a) the best piezoelectric sensor to be used in terms of the material, size and shape, (b) the method of mounting the sensors onto the socket, and (c) the placement of the sensors. The finalized configuration that resulted in the best response was adopted and used to collect data for training and classifying the gait phase using pattern recognition method. The performance of the proposed sensory system was evaluated by checking the accuracy of the pattern recognition algorithm in detecting the gait phases at different speeds of normal walking. Findings from the simulation study suggested that Polyvinylidene Fluoride (PVDF)-based, small rectangular piezoelectric sensor yielded the highest output voltage. The cantilever with elastic foundation mounting configuration should be adopted and the sensors should be positioned in a zig-zag orientation from top to bottom on the anterior and posterior socket wall to cover the quadriceps and hamstring muscle groups. The sensory system that has been configured was tested and consistent signals across multiple trials were found as the average

Frobenius norm, $\|A\|_F$, calculated for all sensors was 4.5 out of 5.0. The response from the sensory system was proven to be feasible to be used to identify TF gait phases and it could be used to characterise different walking types or speed. For the analysis of gait detection using pattern recognition method through signals from the novel sensory system, it can be concluded that the ensemble classifier method, with a window size of 100 ms, produced the best training and testing performance with an average of 95.6% and 88.32% classification accuracy, respectively. The accuracy increased by 0.1% when the number of sensors was optimized to 14 sensors. In conclusion, this thesis presents the configuration for the in-socket sensory system for TF prosthesis, and proved that the proposed system is feasible to be used to detect gait phases for level walking. In addition, this thesis offers the foundation for more studies on utilization of in-socket sensory system for the MPC prosthetic leg control.

Keywords: Sensory system, prosthesis, Transfemoral, gait analysis

**KONFIGURASI DAN ANALISIS SISTEM SENSORI DALAM SOKET
BERASASKAN PIEZOELEKTRIK UNTUK PENGESANAN GAYA BERJALAN
PROSTETIK TRANSFEMORAL**

ABSTRAK

Sistem penderiaan adalah salah satu komponen penting dalam kaki prostetik yang dikendalikan oleh mikropemproses (MPC). Ia memberikan maklumat kepada sistem pengawal tentang keadaan terkini untuk kaki prostetik tersebut, dan dalam sesetengah aplikasi, isyarat dari sistem penderiaan digunakan untuk meramalkan pergerakan yang dimaksudkan pengguna kaki prostetik tersebut. Oleh itu, kualiti sistem deria untuk kaki prostetik MPC adalah sangat penting. Cabarannya adalah untuk mengimbangi antara praktikaliti dan kecekapan sistem deria. Kajian ini dijalankan untuk menyiasat kebolehlaksanaan dan keberkesanan sistem penderiaan di dalam soket yang menggunakan sensor piezoelektrik sebagai alternatif kepada sistem penderiaan untuk kaki prostetik transfemoral (TF) MPC. Kaedah yang digunakan terdiri daripada memilih: (a) penderia piezoelektrik yang terbaik untuk digunakan dari segi bahan, saiz dan bentuk, (b) cara memasang penderia ke soket, dan (c) penempatan penderia. Konfigurasi yang menghasilkan tindak balas yang terbaik telah digunakan untuk mengumpulkan data untuk latihan dan mengklasifikasikan fasa berjalan menggunakan kaedah pengenalan corak. Prestasi sistem penderiaan yang dicadangkan telah dinilai dengan memeriksa ketepatan algoritma pengenalan corak dalam mengesan fasa berjalan untuk aktiviti berjalan dengan kelajuan yang berbeza. Dapatan menunjukkan bahawa penderia piezoelektrik segi empat tepat kecil PVDF, menghasilkan amplitud tertinggi berbanding dengan pilihan lain. Julur dengan konfigurasi pendudukan asas elastik harus diadaptasi dan penderia harus diletakkan di orientasi zig-zag dari atas ke bawah pada dinding soket anterior dan posterior untuk menutupi kumpulan otot kuadrisep dan hamstring. Sistem penderiaan

yang telah dikonfigurasi telah diuji dan ia dapat memberikan isyarat yang konsisten merentasi pelbagai ujian dengan norma Frobenius purata, $\|A\|_F$, yang dihitung untuk semua penderia adalah 4.5 daripada 5.0. Respons dari sistem deria telah terbukti dapat digunakan untuk mengenal pasti fasa pergerakan kaki prostetik TF dan dapat digunakan untuk membezakan jenis atau kelajuan fasa gaya berjalan yang berlainan. Untuk analisis pengesanan gaya berjalan menggunakan kaedah pengenalan corak melalui isyarat dari sistem penderia asli, dapat disimpulkan bahawa kaedah klasifikasi bersekumpulan, dengan saiz tingkap 100 ms, menunjukkan prestasi latihan dan ujian terbaik, dengan masing-masing purata 95.6% dan ketepatan klasifikasi 87% masing-masing. Ketepatan meningkat sebanyak 0.1% apabila bilangan penderia dioptimumkan kepada 14 penderia. Kesimpulannya, tesis ini membentangkan konfigurasi untuk sistem penderiaan soket untuk TF prosthesis, dan membuktikan bahawa sistem yang dicadangkan itu boleh digunakan untuk mengesan fasa-fasa gaya berjalan. Tesis ini juga menawarkan asas bagi lebih banyak kajian tentang pemanfaatan sistem penderiaan soket untuk kawalan kaki prostetik yang dikendalikan oleh mikropemproses.

Kata kunci: sistem sensori, prosthesis, Transfemoral, analisis cara berjalan

ACKNOWLEDGEMENTS

Alhamdulillah, prayers to Allah s.w.t for giving me the courage, strength, and health to finally complete this thesis as the final outcome of my PhD journey.

I would like to convey my gratitude to my supervisor, Dr. Nur Azah Hamzaid for her passion, and patience in supervising and guiding me to do research and write academic papers. I learned a lot from her, and I do not think it is possible for me to complete my study without her assistance. She is not only a supervisor, but she is also a mentor and a sister! For that, I thank Dr. Azah very much! May Allah bless her and her family! Aamin.

To my co-supervisors, Dr. Ng Siew Cheok and Dr. Asan Gani, thank you for your guidance and assistance throughout the journey.

And thank you to all my mySmartLeg team members, Hanie, Athirah, Zafirah, Anur, Hidayah, Tawfik, and Elle for being such a wonderful teammate for me. It's been a pleasure working with all of you! And my special thanks to my subject, Mr Suparjo @ Asan, thank you very much for your cooperation!

Special thanks to my beloved husband, Mohd Rozaidi Abu Bakar, and to my parents, Fuziyah Abd Wahab and Jasni Mohd Diah, for their endless support.

To my beautiful children, Fatin Amani, Faris Rusydi, and Fahim Imran, thank you for being my strength and motivation.

I would also like to thank my brothers and sister for their support.

Finally, I would like to thank and congratulate my 'partners in crime', Diyana and Azni, who fought together with me in this PhD journey! Thank you! We finally made it!

TABLE OF CONTENTS

Abstract	iii
Abstrak	v
Acknowledgements	vii
Table of Contents	viii
List of Figures	xii
List of Tables.....	xvi
List of Symbols and Abbreviations.....	xviii
List of Appendices	xix
CHAPTER 1: INTRODUCTION.....	1
1.1 Overview.....	1
1.2 Problem statement	7
1.3 Research significance	9
1.4 Research objectives	9
1.5 Thesis organization.....	10
CHAPTER 2: LITERATURE REVIEW.....	12
2.1 Overview of Microprocessor controlled (MPC) prosthetic leg	12
2.2 Sensory system in MPC prosthetic leg and the state-of-the-art.....	14
2.2.1 Prosthetic-device oriented sensory system.....	16
2.2.2 User's-biological-input oriented sensory system	22
2.2.3 Neuro-mechanical fusion sensory system	28
2.2.4 Discussion	30
2.3 Piezoelectric application in prosthesis field	33
2.4 Conclusion	36

CHAPTER 3: CONFIGURATION AND ANALYSIS OF PIEZOELECTRIC-BASED IN-SOCKET SENSORY SYSTEM FOR TRANSFEMORAL PROSTHETIC LEG37

3.1	Introduction.....	37
3.2	Literature review.....	37
3.3	Methods	40
3.3.1	Analysis of the piezoelectric sensors properties.....	40
3.3.2	Piezoelectric sensors mounting configuration.....	42
3.3.3	Sensors placement	45
3.3.4	Gait experiment	47
3.4	Results and Discussion	49
3.4.1	Simulation results to determine piezoelectric properties.....	49
3.4.2	Mounting configuration method experiment.....	52
3.4.3	Sensors placement orientation experiment.....	53
3.4.4	Results for consistency study of the sensors' output signal	55
3.4.4.1	Quadriceps.....	56
3.4.4.2	Hamstring.....	56
3.5	Summary.....	58

CHAPTER 4: ANALYSIS OF PIEZOELECTRIC-BASED IN-SOCKET SENSORY SYSTEM RESPONSE AS A GAIT DETECTION TOOL: A FEASIBILITY STUDY60

4.1	Introduction.....	60
4.2	Literature review.....	60
4.3	Mathematical modelling of the relationship between the in-socket sensory system and forces on the stump	64
4.3.1	Piezoelectric as a dynamic force sensor	64

4.3.2	Input force	66
4.3.2.1	Reaction force from the ground.....	67
4.4	Experiment methodology.....	69
4.4.1	Subject and prosthetic leg.....	70
4.4.2	Lab setup	72
4.4.3	In-socket sensory system data acquisition and signal processing	73
4.4.4	Experimental procedure	74
4.4.4.1	Single stride routine	75
4.4.4.2	Continuous walking routine	77
4.5	Results.....	78
4.5.1	Single stride walking	79
4.5.2	Continuous walking.....	82
4.5.3	Continuous walking vs single stride walking.....	84
4.6	Discussion.....	89
4.7	Summary.....	91

CHAPTER 5: CLASSIFICATION OF SENSORY SYSTEM RESPONSE USING STATISTICAL PATTERN RECOGNITION METHOD FOR TRANSFEMORAL AMPUTEE GAIT DETECTION

5.1	Introduction.....	92
5.2	Literature review.....	92
5.3	Material and methodology	97
5.3.1	Data collection.....	97
5.3.1.1	Subject and material	97
5.3.1.2	Experiment procedure	97
5.3.2	Feature extraction	100
5.3.3	Classifier.....	102

5.3.4	Off-line Testing method	103
5.3.5	Reduction of number of sensors	103
5.4	Results	104
5.4.1	Training performance	104
5.4.2	Test performance	106
5.4.2.1	Normal vs Fast walking test	106
5.4.2.2	Between sessions analysis	111
5.4.3	Reduced number of sensors performance.....	111
5.5	Discussion.....	112
5.6	Summary.....	114
CHAPTER 6: CONCLUSIONS AND RECOMMENDATIONS.....		115
6.1	Summary of the findings	115
6.2	Limitations of the study	117
6.3	Future recommendations	118
References		120
List of Publications		137
APPENDIX.....		138

LIST OF FIGURES

Figure 1.1: The illustration of amputation levels of the lower extremity (Seymour, 2002).	1
Figure 1.2: Findings from a study conducted by Waters to show that transfemoral amputee utilized more metabolic energy based on oxygen consumption (Waters et al., 1976). AK refers to Above-Knee (Transfemoral), BK refers to Below-Knee (Transtibial) and Symes refers to foot amputation.	2
Figure 1.3: The relationship between controller, sensory system and actuator in an active prosthetic leg.	4
Figure 1.4: Gait cycle phase. A: The new gait phase based on Rancho Los Amigos gait analysis committee. B: The classis gait terms. C: The percentage of gait cycle. (Physiopedia contributors, 6 June 2017).....	7
Figure 1.5: Gait cycle illustration (Bonney-Mazure & Armand, 2015).	7
Figure 2.1: The framework of the MPC prosthetic device (Varol et al., 2010).	13
Figure 2.2: The ‘Human Gait Oscillation Detector’ (HGOD) using potentiometers and 2 aluminum links proposed by Nandi et al. (2009).	16
Figure 2.3: The performance of the MPC TF prosthesis driven by the neuromuscular control proposed by Thatte and Gayer (2016) as compared to the classic impedance control. (a) the result for robustness test of the prosthetic leg, (b) the tripping test performance.....	17
Figure 2.4: The features distribution in space for standing, walking and sitting activity in Varol et al. (2010) study. The features were extracted from the sensory system's signal. It can be seen that the features were separated from one activity to another.	19
Figure 2.5: Placement of EMG electrodes in study reported in Hardaker et al. (2013a) 25	
Figure 2.6: The chart of the sensory system adopted or possible to be adopted in prosthesis control system.	31
Figure 3.1: Unimorph and bimorph piezo devices.....	38
Figure 3.2: Flowchart of in-socket sensory system.....	39
Figure 3.3: Model in COMSOL. Left: Model for rectangle shape patch. Right: Model for circle shape patch.	41
Figure 3.4: Illustration of the cantilever with elastic foundation beam configuration....	42

Figure 3.5: The test configurations. (a) Cushion-All Fit (CA FIT). (b) Cushion End Fit (CE FIT). (c) Cushion All Extra (CA XTRA). (d) Cushion End Extra (CE XTRA).	44
Figure 3.6: Sensor's response for knock and push input using CA FIT configuration. (a) Knock input force and sensor's response (voltage). (b) Push input force and sensor's response (voltage).	45
Figure 3.7. F-Scan sensor (Tekscan, Inc., USA) (Tekscan Inc.).....	46
Figure 3.8: Box allocation on the Tekscan sensor area for analysis purposes. Left: Quadriceps, Right: Hamstring.....	47
Figure 3.9: Fabricated socket with instrumented in-socket sensor. (a) interior view, (b) exterior view.....	48
Figure 3.10: Output voltage signal of Sensor P1 for 1 trial.	49
Figure 3.11: Results for simulation of different shape and size for the bicep femoris input.	50
Figure 3.12: Results for simulation of different shape and size for rectus femoris input.	50
Figure 3.13: Piezofilm sensor by Measurement Specialties (Measurement Specialties).	51
Figure 3.14: The mounting configuration adopted in the design.	53
Figure 3.15: Piezo sensors placement for in-socket sensory system.	55
Figure 3.16: Output signal and the correlation table of 5 trials, Sensor P5.	56
Figure 4.1: Illustration of axis assignation (Moheimani & Fleming, 2006)	64
Figure 4.2: Free body diagram for piezo as dynamic force sensor	66
Figure 4.3: Example of free body diagram of the forces acting on one anterior sensor. Note: F_r could be in either direction depending on the body/leg position and gait phase	67
Figure 4.4: Leg model.....	67
Figure 4.5: Diagram of leg model links. (a) thigh-socket link, (b) shank link, and (c) foot link.	68
Figure 4.6: F_R to the wall of the socket.....	69
Figure 4.7: Sensor mounting. The negative side is facing upward.	71

Figure 4.8: Sensor response with respect to the sensor's strain. (a) rest condition, (b) strain downward, and (c) strain upward.....	71
Figure 4.9: Sensors response for quiet standing for all 15 sensors	72
Figure 4.10: Prosthetic leg used in this experiment.	72
Figure 4.11: VICON Motion system. Left: Force plates, Right: VICON Nexus software GUI.....	73
Figure 4.12: Active low pass filter circuit diagram.....	73
Figure 4.13: Data acquisition setup from sensors to computer	74
Figure 4.14: Data synchronization method. Top: The data for GRF. Bottom: Trigger sensor data. It can be seen that force plate was knocked at X=881 after the recording started and the trigger sensor was activated 1658 samples after recording started.....	76
Figure 4.15: Illustration of how the 1 st and 2 nd heel strike was identified.	77
Figure 4.16: Illustration of the walking path for the experiment. Circular path with ~1.5 m radius measured from the centre.	78
Figure 4.17: Anterior sensors responses for single stride walking for Sensor A1 to A4 with respect to the GRV and AP GRF. The vertical dashed line represents the separator of gait phases.....	79
Figure 4.18: Anterior sensors responses for single stride walking for Sensor A5-A8 with respect to the GRV and AP GRF. The vertical dashed line represents the separator of gait phases.	80
Figure 4.19: Posterior sensors response for single stride walking for Sensor P1 to P4 with respect to the GRV and AP GRF. The vertical dashed line represents the separator of gait phases.....	81
Figure 4.20: Posterior sensors response for single stride walking for Sensor P5 to P7 with respect to the GRV and AP GRF. The vertical dashed line represents the separator of gait phases.	82
Figure 4.21: Anterior sensors response for continuous walking. The vertical dashed lines represent the separator of gait phases.....	83
Figure 4.22: Posterior sensors response for continuous walking. The vertical dashed lines represent the separator for gait phases.	84
Figure 4.23: Anterior sensors response for continuous walking and single stride walking for Sensor A1 and A2.....	85

Figure 4.24: Anterior sensors response for continuous walking and single stride walking for Sensor A3 and A4.....	86
Figure 4.25: Anterior sensors response for continuous walking and single stride walking for Sensor A5 and A6.....	86
Figure 4.26: Anterior sensors response for continuous walking and single stride walking for Sensor A7 and A8.....	87
Figure 4.27: Posterior sensors response for continuous walking and single stride walking for Sensor P1 and P2.....	87
Figure 4.28: Posterior sensors response for continuous walking and single stride walking for Sensor P3 and P4.....	88
Figure 4.29: Posterior sensors response for continuous walking and single stride walking for Sensor P5 and P6.....	88
Figure 4.30: Posterior sensors response for continuous walking and single stride walking for Sensor P7.....	89
Figure 5.1: Illustration of the gait detection process.....	93
Figure 5.2: Flowchart of the experimental procedure.....	98
Figure 5.3: Experiment using treadmill to collect walking data.....	99
Figure 5.4: The segmentation process of the data that has been collected.....	100
Figure 5.5: The average training accuracy percentage for different classifiers.....	104
Figure 5.6: The confusion matrix for Bagged Trees classifier. Class 1=LR, Class 2=MSt, Class 3=TSt, Class 4=PSw and Class 5=Sw.....	105
Figure 5.7: Average accuracy rate for 10 trials of normal walking test using BT classifier that was trained with different window size and training dataset.....	107
Figure 5.8: Average accuracy rate for 10 trials of fast walking test using BT classifier that was trained with different window size and training dataset.....	107
Figure 5.9: The average accuracy rate for 25 ms, 50 ms, and 100 ms in normal and fast walking test.....	109
Figure 5.10: The average computing time for BT classifier with 25, 50 and 100 ms window size to classify a 1.434 s long testing data.....	109
Figure 5.11: The average accuracy rate for NW dataset, FW dataset and Combined dataset in normal and walking test.....	110

LIST OF TABLES

Table 2.1: The performance of CYBERLEGs in detecting the states of the leg using the proposed sensory system.....	19
Table 2.2: Summary of the literature review on the prosthetic-device oriented sensory system.....	20
Table 2.3: Summary of the literature review on user's-biological-input oriented sensory system.....	26
Table 2.4: The performance of classifier in detecting ambulation mode transitions	28
Table 2.5: Summary of the literature review on neuro-mechanical fusion sensory system.	29
Table 2.6: Summary of the literature review on the utilization of piezoelectric in the prosthesis.....	34
Table 3.1: Piezoelectric properties	41
Table 3.2: Size and shape of the piezo patches used for the simulation.	41
Table 3.3: The pressure input used for the simulation study	42
Table 3.4: DAQ CARD SPECIFICATION (National Instruments Corporation, 2015).48	
Table 3.5: Tabulated results for voltage output (V) of different shapes and sizes for the bicep femoris input.....	49
Table 3.6: Tabulated results for voltage output (V) for different shapes and sizes for rectus femoris input.	50
Table 3.7: Signal parameters of the mounting configuration experiment.....	52
Table 3.8: Average pressure difference (kpa) of 5 trials for quadriceps muscle group ..	53
Table 3.9: Average pressure difference of 5 trials (kPa) for hamstring muscle group ...	53
Table 3.10: The minimum R-value in the correlation table and the norm value for Sensor A1- Sensor A8.....	56
Table 3.11: The minimum R-value in the correlation table and the norm value for Sensor P1 - Sensor P7	57
Table 4.1: Percentage range of closeness to the normal curve	61

Table 4.2: Definition of abbreviation in equations (1)-(8).....	65
Table 4.3: Description of the subject	70
Table 4.4: Gait phase percentage for both walking types.	79
Table 4.5: Summary of the significant sensor during respective gait phase and transition from phase to phase.....	89
Table 5.1: Accuracy rate (%) for 6 classifiers with different training data set and window sizes.....	105
Table 5.2: Accuracy rate (%) and p-value for Normal Walking test using BT classifier.	106
Table 5.3: Accuracy rate (%) and p-value for Fast Walking test using BT classifier...	107
Table 5.4: The classification accuracy for different sessions.	111
Table 5.5: Summary of the performance comparison between the proposed in-socket sensory system classifier and other studies.....	113

LIST OF SYMBOLS AND ABBREVIATIONS

TF	:	Transfemoral
TT	:	Transtibial
MPC	:	Micro-processor Controlled
IC	:	Initial contact
LR	:	Loading response
MSt	:	Mid-stance
TSt	:	Terminal stance
PSw	:	Pre-swing
Sw	:	Swing
GRF	:	Ground reaction force
GRV	:	Vertical GRF
AP-GRF	:	Anterior-posterior GRF

LIST OF APPENDICES

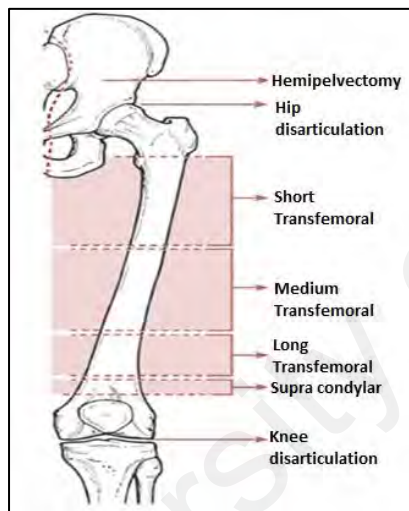
APPENDIX A: INTELLECTUAL PROPERTIES.....	138
APPENDIX B: ETHICS APPROVAL FOR THE STUDY	139
APPENDIX C: PUBLICATION 1	140
APPENDIX D: PUBLICATION 2	141
APPENDIX E: AWARDS RECEIVED	142

University of Malaya

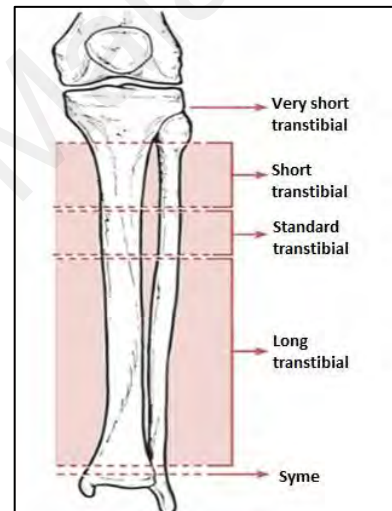
CHAPTER 1: INTRODUCTION

1.1 Overview

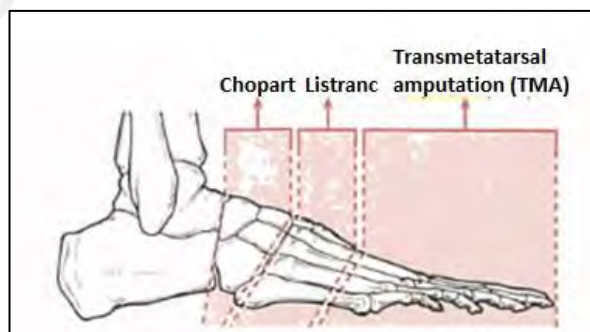
Lower-limb amputation can cause a great change to one's life. Depending on the level of the amputation, the amputee loses his mobility to certain degree, and consequently limits his ability to live an active life. In general, the amputation level of the lower extremity can be divided into three groups, namely transfemoral (above-knee), transtibial (below-knee), and foot amputations. The groups can be further divided into several levels. Figure 1.1 illustrates the extended levels of amputation for transfemoral (TF), transtibial (TT), and foot amputations.



(a) Transfemoral amputation levels



(b) Transtibial amputation levels



(c) Foot amputation levels

Figure 1.1: The illustration of amputation levels of the lower extremity (Seymour, 2002).

A study conducted by Waters, Perry, Antonelli, and Hislop (1976) reported that transfemoral amputee consumed a relatively higher metabolic energy to walk using a prosthetic leg as compared to a normal person and transtibial amputees because of the missing knee joint. The level of metabolic energy consumption comparison is shown in Figure 1.2. The knee joint plays a major role in moving the leg because it controls the muscles' extension and flexion activity to move the leg. Therefore, the absence of knee joint will lead to extra work to the adjacent joint (the hip joint). As a result, most of the transfemoral amputees choose to live an inactive life after amputation. However, a good prosthetic leg system may assist them to regain their normal life.

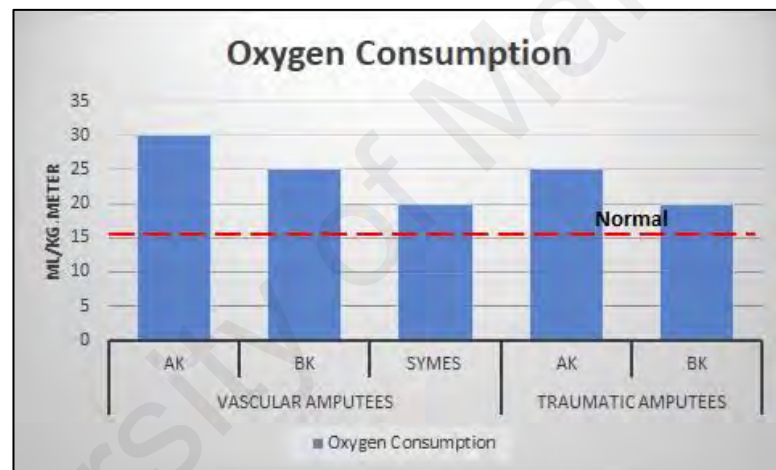


Figure 1.2: Findings from a study conducted by Waters to show that transfemoral amputee utilized more metabolic energy based on oxygen consumption (Waters et al., 1976). AK refers to Above-Knee (Transfemoral), BK refers to Below-Knee (Transtibial) and Symes refers to foot amputation.

Prosthetic leg is one of the technologies invented since 1500 B.C to help the unfortunate people who lost their legs for various reasons. Among the popular reasons are trauma, infection, congenital limb deficiencies and diseases, such as peripheral vascular disease (PVD), diabetes and tumours (Seymour, 2002). A complete set of transfemoral prosthetic leg consists of four main components, namely, the socket, the limb, the prosthetic knee, and the prosthetic foot (Level Four, 2017).

Transfemoral prosthetic leg is classically categorised into two types, particularly passive and active type, based on the method of constraining or causing the rotation to

the artificial knee joint as the amputee moves (Popovic, Tomovic, Tepavac, & Schwirtlich, 1991). The pure passive prosthetic leg is mechanically designed to mimic the lost leg. This type of prosthetic leg is not equipped with any controller or actuator. Despite their advantages in offering a great assistance in stabilising the body to the amputee while he stands and providing body support while he walks, a passive prosthetic leg still holds major drawbacks. A few researches have highlighted the drawbacks of passive prosthetic legs in their articles (Buckley, De Asha, Johnson, & Beggs, 2013; Kapti & Yucenur, 2006; Wentink, Beijen, Hermens, Rietman, & Veltink, 2013). The drawbacks are mainly related to energy consumption, gait performance as compared to the normal gait and failure to correspond with the user's daily activities.

The other type of TF prosthetic leg is called the active prosthetic leg. An active prosthetic leg is designed to support the needs of the user that a passive prosthetic fails to cater. It is commonly equipped with adaptive electronic controller and actuator/s to replace the missing joint (Popovic & Kalanovic, 1993). Some people addressed active prosthetic leg as a Micro-processor controlled (MPC) prosthetic leg due to the presence of an electronics controller unit to control the mechanism of the leg. Popovic et al. (1991) has outlined four basic rules that need to be considered in designing MPC prosthesis, which are:

- 1) Sudden and uncontrolled knee joint (by the actuator) should be avoided.
- 2) The kinetics and kinematics of a normal gait pattern should be duplicated as much as possible.
- 3) The mechanical design should be able to support full body weight.
- 4) Any undesirable pressure at the socket-stump interface that may cause painful contact and gait abnormalities must be avoided.

The findings from this study led to the conclusion that a good active prosthetic leg must have a good mechanical design and an efficient control system to control the knee so that

the safety (i.e. ensure the user is not falling while using the leg), comfort, and symmetrical gait are guaranteed.

There are three important components in the control system of an MPC prosthetic leg system, namely the controller, the sensory system and the actuators. The correlation between the components is described in Figure 1.3.

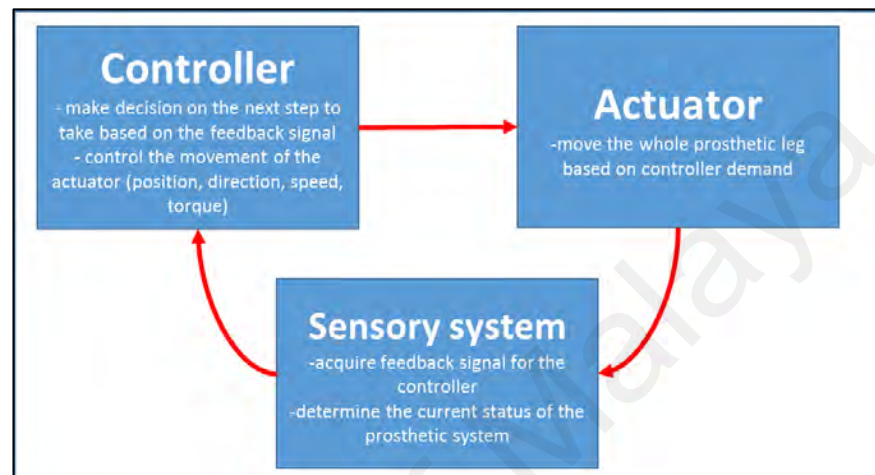


Figure 1.3: The relationship between controller, sensory system and actuator in an active prosthetic leg.

The presence of the actuator in the system acts as the replacement to the muscles that control the knee joint to move the leg. Hence, it reduces the amount of metabolic energy consumption by the amputees to move their prosthetic legs. In addition, Tura, Raggi, Rocchi, Cutti, and Chiari (2010) claimed in their article that asymmetry gait can reduce the quality of amputees' life because it causes comorbidities and falling risk, therefore, it is crucial to reduce the degree of asymmetry in gait. A study conducted by Segal et al. (2006) proved that MPC prosthetic leg can provide improvement in terms of gait symmetry as compared to passive prosthetics.

In order for the controller to work efficiently, it must have the sensory system that will update the status of the prosthetics from time to time. Therefore, an efficient sensory system that can supply feedback to the control system is very crucial and important in an active prosthetic leg system. This is to ensure the safety and better gait performance by the active prosthetic leg user.

Gait can be defined as a repeated movement by the body segments to move the body forward or backward and balancing the body at the same time. One gait cycle is usually identified by the first foot strike of one leg on the ground until the same foot strikes the ground again (Bonney-Mazure & Armand, 2015).

Human gait can be divided into two main phases, namely stance and swing. A stance phase is when the foot is on the ground and usually takes up 60% of the total gait period for a normal person. Meanwhile, a swing phase is when the leg is in the air and it takes the remaining 40% of the gait cycle. However, these phases can be further sub-divided into smaller divisions, depending on the activity of the leg during that particular instant. Based on Rancho Los Amigos gait analysis committee, a complete gait cycle consists of eight phases (*Observational Gait Analysis Handbook*, 1989; Tao, Liu, Zheng, & Feng, 2012):

1. Initial contact (IC) – the instant the foot touches the ground. This is the beginning of double limb support phase (both feet on the ground). Muscle activity is mainly on preparing for weight acceptance.
2. Loading response (LR) – the weight acceptance period. It begins with initial ground contact and ends when the other foot leaves the ground. This phase usually represents the first 10% of the gait cycle. Heel will act as a rocker, knee is flexed for shock absorption purposes, and ankle plantar flexion to limit the effect of heel rocker by allowing the forefoot touching the ground.
3. Midstance (MSt) – the first half of single limb support period. The 10-30% of the gait cycle interval. This phase starts when the other foot is lifted from the ground, continues until the body weight is aligned over the forefoot, and finally ends with heel rise. During this period, momentum causes the body mass moves forward over a stationary foot via ankle dorsiflexion, while the knee and

hip extend. This phase requires a relative control because great muscle activity is not required.

4. Terminal stance (TSt) – completes the single limb support period. It takes up 30-50% interval of the gait cycle. The phase begins with heel rise and ends with the foot strike of the opposite foot. During this phase, the body weight moves forward to the forefoot.
5. Pre-Swing (PSw) – the last phase in stance period and the second double limb support phase in the gait cycle. Pre-swing starts when the other foot touches the ground and ends with the toe-off of the ipsilateral foot. The push-off event occurs in this phase, in which the limb is pushing away from the ground for swing. The ankle plantarflexion also happens in this phase.
6. Initial swing (ISw) – the one-third of the swing period. It starts when the foot leaves the ground and ends when the swinging foot is opposite the stance foot. In this phase, the limb moves forward by the hip flexion and increased the knee flexion.
7. Mid-Swing (MSw) – begins when swinging leg is opposite the stance leg and ends when the swinging leg is forward, and the tibia is vertical. In this phase, knee extension occurs in response to gravity, while the ankle continues to dorsiflex to neutral position.
8. Terminal swing (TSw) – the final interval of swing phase, which starts when the swinging leg tibia is vertical and ends with a foot strike. The advancement of the leg is considered complete when the shank is ahead of the thigh and it is done by knee extension. Hip continues in flexion and ankle maintains dorsiflexion to foot neutral position.

Figure 1.4 illustrates the phases of a complete gait cycle described.

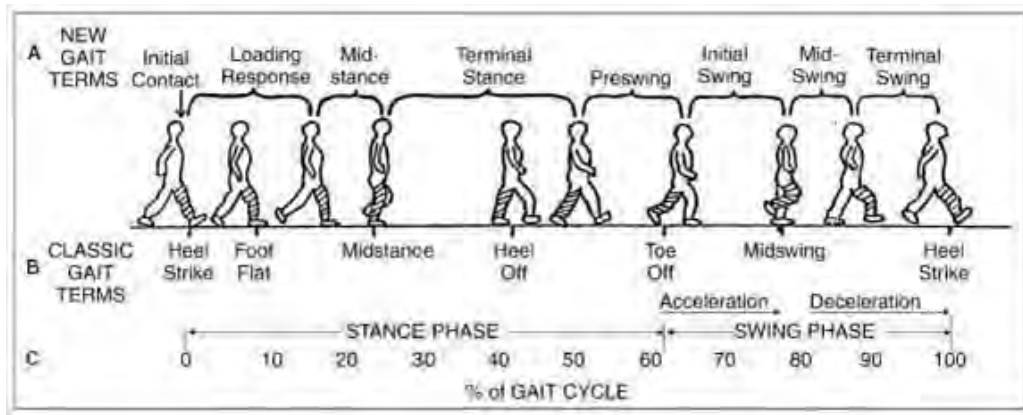


Figure 1.4: Gait cycle phase. A: The new gait phase based on Rancho Los Amigos gait analysis committee. B: The classic gait terms. C: The percentage of gait cycle. (Physiopedia contributors, 6 June 2017)

Another way of dividing the gait cycle is by dividing it to the position of the legs on the ground. When only one leg is on the ground, that phase is called single support phase. Meanwhile, when both legs were on the ground, the phase is named as double support. When the leg of interest is not touching the ground, it is in swing phase. The illustration of the gait cycle is shown in Figure 1.5.

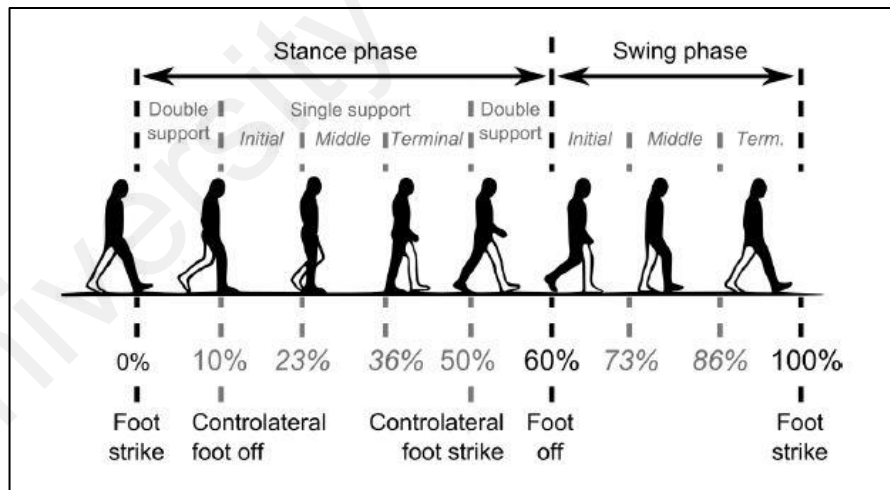


Figure 1.5: Gait cycle illustration (Bonney-Mazure & Armand, 2015).

1.2 Problem statement

Compared to the passive prosthetic leg, an MPC prosthesis offers a wider scope of usage to the amputees in which, it is usually embedded with an actuator to move the knee joint. Hence, less energy is required by the user to do such movements. The sensory system is

one of the important components in MPC prosthesis system. Other than it providing information to the controller about the current status of the leg (position, speed, torque and others), it can also be used to identify the intention of the user, such as gait initiation, gait termination, intention to sit from standing, or to stand from sitting and others.

To date, several methods of sensory system in MPC prosthesis system were reported (Gregg & Sensinger, 2014; Kebin, Qining, & Long, 2015; Pfeifer, Pagel, Riener, & Vallery, 2015). Electromyography (EMG) is utilized to measure and record the muscle's electrical activity in human body. Study by Hudgins, Parker, and Scott (1991a) proved that EMG signal gives a consistent pattern for every movement and can also detect the initial phase of muscle contraction, and hence, it can be utilized to provide feedback to the prosthesis control system. Since then, there have been numbers of research proposing the use of EMG as the sensors in active prosthesis design (Geethanjali & Ray, 2014; Wentink, Schut, Prinsen, Rietman, & Veltink, 2014; Wu, Waycaster, & Shen, 2011). However, one of the unavoidable drawbacks of EMG based sensory system is that it requires careful preparation on the skin to generate an accurate result (Farnsworth, Talyor, Triolo, & Young, 2009; Jamal, 2012). Consequently, it complicates the donning process of the prosthetic devices.

Besides EMG, there are other works proposing the use of mechanical sensor to measure force or pressure in a prosthetic design (Arami et al., 2013; Eshraghi et al., 2013). Mueller et al. (2011) suggested the Inertial Measurement Unit (IMU) sensor to be used in lower limb prosthetic design to acquire kinematic and kinetic data when the amputee moves. The installation of the mechanical sensors on the leg usually results in a more complicated and heavier design of the leg. In addition, the information gained from the mechanical sensors instrumented outside the socket which has no direct contact with the muscles might lead to inaccuracy in detecting the user's intended movement.

A study reported that the accuracy in detecting the continuous locomotion mode increased when information from EMG and mechanical sensors were used together (H. Huang et al., 2011) compared to the performance of the EMG-based sensory system. Considering all the important factors above, a good sensory system for active prosthetic leg must be easy, practical and simple to be used by the user and can provide muscle contraction and forces data to the controller as a feedback to increase its accuracy in controlling the prosthesis' actuator/s.

1.3 Research significance

The motivation of conducting this study is to search for an alternative sensory system that can provide the most informative data in the simplest form for TF prosthesis. Study by Dong et al. (2017) and Suzuki, Soma, González, and Yu (2012) verified that hand motion was successfully classified using piezoelectric sensor in upper-limb application. Based on the findings from these studies, it is hypothesized that piezoelectric sensor's response can also be used to classify the leg motion. Thus, this study was conducted with the intention to propose the piezo-based in-socket sensory system, and to investigate its feasibility and efficacy in providing gait information of the TF prosthetic leg. It is hoped that the outcome of this study would add value to the MPC prosthetic leg state of the art.

1.4 Research objectives

The target of this research is to investigate the feasibility and efficacy of the piezo-based in-socket sensory system to provide gait information of the TF prosthesis. In achieving the target, these objectives were engaged:

1. To configure and analyse the piezoelectric-based in-socket sensory system for transfemoral prosthetic leg application.
2. To analyse the proposed sensory system's response and investigate its feasibility as a gait detection tool.

3. To develop the gait phase classification algorithm using the sensory system response and evaluate the classifier performance.

1.5 Thesis organization

This research work consists of three separate studies that supported one another. Each study covers one of the objectives defined in Section 1.4 is presented in independent Chapter 3, 4 and 5 in this thesis in academic paper format. The chapter division of this thesis is as follows:

Chapter 1: Introduction

This chapter presents the overview of the research area, which are the prosthetic leg, the problem statement of the research work, the significance of the study, the research objectives, and the thesis organization.

Chapter 2: Literature review

This chapter presents the review of the literature that discussed prosthetic leg state of the art. Besides, the literature on piezoelectric sensor utilization in prosthesis technology was also discussed.

Chapter 3: Configuration and analysis of piezoelectric-based in-socket sensory system for transfemoral prosthetic leg using piezoelectric sensors

The methodologies and analysis implemented to configure and design the in-socket sensory system using a set of piezoelectric sensors are reported in this chapter. The methods comprised of determining the piezoelectric material, size and shape to be used in the system, deciding the method of mounting the sensors onto the inner socket wall, determining the orientation of sensor placement, and finally the evaluation method to check the efficacy of the developed in-socket sensory system. Major portion of this chapter was published in IEEE/ASME Transaction on Mechatronics journal (Jasni et al., 2016).

Chapter 4: Analysis of piezoelectric-based in-socket sensory system response as a gait detection tool: a feasibility study

This chapter reports the analysis done to determine the relationship between the response signal from the proposed in-socket sensory system (presented in Chapter 3) and the ground reaction forces components of the prosthetic leg when the subject performed walking motion. This involves data collection process from the sensory system and also ground reaction forces of the prosthetic leg from the force plate.

Chapter 5: Classification of sensory system response using statistical pattern recognition method for transfemoral amputee gait detection

The gait phase detection algorithm using statistical pattern recognition method was developed and analysed based on the understanding that has been drawn from the previous chapter, and the methods and analysis were described in this chapter. The methods comprise of series of experiments with TF subject to collect data from the sensory system, analysis and development of pattern recognition algorithm, which consisted of feature extraction method and classification method, training the developed classifier with the data from the sensory system and finally testing the classifier performance.

Chapter 6: Conclusion and recommendations

The research process and its contribution are concluded in this chapter. Limitations of the work are highlighted and suggestions for the future works are listed.

CHAPTER 2: LITERATURE REVIEW

In this chapter, the review of the literature related to the study is presented. The literature review presented in this chapter are prepared to address two objectives:

1. To understand the state of the art of sensory system utilized in MPC prosthetic leg.
2. To present the utilization of piezoelectric device in prosthesis in terms of its 'how' and 'where'.

2.1 Overview of Microprocessor controlled (MPC) prosthetic leg

To date, the interest in research related to MPC prosthetic leg is expanding. The attention that it attracts is due to its advantage over passive or pure mechanical prosthetic leg. Among the advantages that were highlighted in the literature are; improvement in knee flexion during weight acceptance period (Kaufman et al., 2007), reduction in metabolic energy consumption (Schmalz, Blumentritt, & Jarasch, 2002), and better gait performance (Johansson, Sherrill, Riley, Bonato, & Herr, 2005; Segal et al., 2006). There are many studies conducted on MPC's control efficiency (Gregg & Sensinger, 2014; Shahmoradi & Shouraki, 2017; Sup, Bohara, & Goldfarb, 2007), power optimization (Andrysek, Liang, & Steinnagel, 2009; Dedić & Dindo, 2011), as well as the mechanical design and improvement (Inoue, Wada, Harada, & Tachiwana, 2013).

In brief, the MPC prosthetic device system works based on 4 components that are closely related to each other. They are; the user (the amputee), the prosthetic device mechanical structure and actuators, the environment, and the device's control system. The most important component in MPC prosthetic leg is the control system. This is because, the control system acts as the brain of the prosthetic device and decisions that it makes directly affects the safety, comfort, and confidence of the user. Due to Varol et al. (2010), the control system of prosthetic device can be categorized into 3 phases, namely; the high

level, mid-level, and low-level control. High-level control is responsible for perceiving user's intention based on the sensory data. An example of the high-level control is the activity mode recognition. Meanwhile, the mid-level controller's job is to determine the current state of the device. For instance, the current gait phase that the user is currently on. Finally, the low-level control focused on the actuator control; that is to control the movement of the actuator so that the prosthetic leg is moved according to its current state that has been identified in the mid-level controller for the locomotive task acknowledged by the high-level controller. In a nutshell, the high-level control is the perception layer, mid-level is the translation layer and the low level is the execution layer. The overall framework of the MPC prosthetic device is illustrated in Figure 2.1.

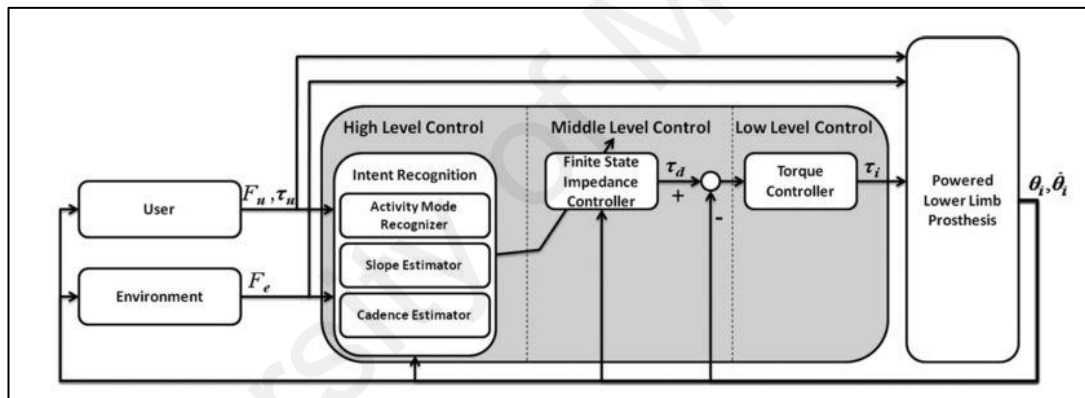


Figure 2.1: The framework of the MPC prosthetic device (Varol et al., 2010).

In order to connect each component in the framework, a sensory system is needed. Sensory system provides information to the controller so that the current stage of the prosthetic leg can be known, and in some application, makes the controller understands the intention of the user. Depending on the type of sensor that is adopted in the system, the type of information provided by the sensory system is different too. Some examples are the angular positions, force, acceleration, Ground Reaction Force (GRF) and electrical activity at the muscles via EMG. These data will be interpreted by the controller and strategize the next move of the MPC prosthetic leg. Thus, it is fair to infer that the efficiency of the control system is closely dependent on the competence of the sensory system that provides the information to the controller. There are various types of sensory

system that has been reported in the literature. Although most of the studies reported are still in research-phase, the growth of the technology is increasingly visible. The state-of-the-art of the sensory system adopted in other studies is discussed in the next section.

2.2 Sensory system in MPC prosthetic leg and the state-of-the-art

The sensory system is crucial in every control algorithm as it provides information about the current state of the control plant. Therefore, it is particularly important to have an effective sensory system to ensure the efficiency of the control algorithm. In MPC prosthetic device, the needs of having an efficient sensory system are even higher. This is because the safety of the user relies on it. There are 2 criteria that need to be optimized in selecting the sensory system for MPC prosthetic device, namely; practicality and quality of the data provided (Tucker et al., 2015). In this aspect, practicality can be understood as the simplicity of the sensors' donning and doffing process, in terms of time, effort and risk. On the other hand, quality of the data involves the richness of the information provided and also the cleanliness of the data signal from external factors such as noise, motion artefacts and etc.

For instance, a study conducted by Farnsworth, Talyor, Triolo, and Young (2009), proposed the utilization of the implanted wireless EMG sensor into the body to control MPC prosthesis. The idea was to eliminate the signal's susceptibility to motion artefacts and perspiration encountered when using the skin surface EMG electrodes. The test was done on a lab rat and the results showed that the implanted sensor had successfully detected the activity of the hind leg of the rat and transmitted the information to the control system wirelessly. Although the proposed system had proven to provide a better signal, it requires a surgical procedure, and the sensors stay in the body, unless the user undergoes another surgery to remove the sensor. Thus, the outcome of the sensory system proposed might seems convincing, but the application is not practical and too risky, hence the balance between the two criteria was not met.

There are many ways of categorizing the sensory technology in MPC prosthetic device. Generally, the sensory system adopted in MPC prosthetic device are categorized based on the type of the sensors used; mechanical sensors and biology-related sensors. Martin et al. (2010) categorized the technology into two classes, namely; the Computational Intrinsic (CI) and Interactive Extrinsic (IE). The computational intrinsic gets the information about the current state of the device using sensors placed on the device itself and it has no interaction with the user, while interactive intrinsic obtains information through interactions with the user in the form of muscle activation and brain signal. Interactive extrinsic usually requires electrography device to get the input from the respective body part. Meanwhile, Tucker et al. (2015) discussed sensor modalities utilization in MPC prosthetic and orthotics device based on the type of the information that the sensor's acquired. The categories are: (i) Supraspinal activity, (ii) Peripheral neural activity, (iii) Joint torques and positions, and (iv) Manual inputs.

In this literature review, the discussion of sensory system state-of-the-art adopted in MPC prosthetic leg was divided into 3 main categories, namely; (i) Prosthetic-device oriented, (ii) user's-biological-input oriented, and (iii) neuro-mechanical fusion approach. The description and discussion for each category can be found in the following subsections.

The review was done on related works within the last 11 years (2007-2018) for both types of lower limb prosthetic device; transfemoral and transtibial. Besides, the review was not limited to the literature that reported on prototyped MPC prosthetic leg only but also covered the proof-of-concept studies related to the field. In addition, some studies that proposed the sensory system that was designed and tested on orthotics and upper-limb prosthesis but had the potential to be implemented on prosthetic were also considered.

2.2.1 Prosthetic-device oriented sensory system

Prosthetic-device oriented sensory system describes the sensors that collect data from the prosthetic device itself and interpret the data, to understand the current stage of the device, to predict the intention of the user or even to understand the environment that the user is moving in. Most of the literature reported the use of mechanical sensors. The mechanical sensors can be further divided into 2 types, namely, kinematics and kinetics sensors.

Kinematics sensor is the sensory device that can extract the kinematics properties, such as joint angle, velocity, and acceleration of the device. The common sensors used for this purpose is accelerometer, gyroscope, goniometer, and magnetometers. The information given by these sensors enables the controller to estimate the position of the device. This information is commonly used for the mid-level controller; in which the identification of the current state the device is currently in is done.

Nandi et al. (2009) proposed an idea of having a simpler sensory system to control active prosthetic leg, which they named as Adaptive Modular Active Leg (AMAL). They proposed the 'Human Gait Oscillation Detector' (HGOD) to measure the joints' oscillation using 8 potentiometers which were connected to 2 rigid aluminium links. The signal from the potentiometers was used to customize biological gait patterns using fuzzy logic classifier. Figure 2.2 below illustrates the joint oscillation detection method using HGOD.

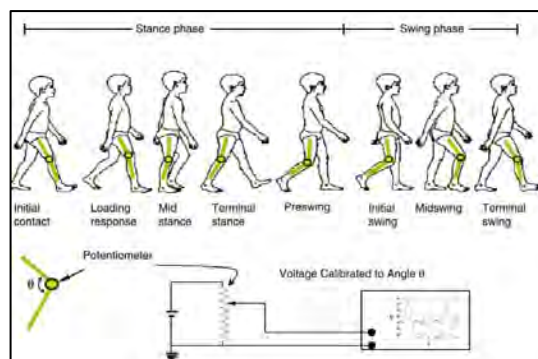


Figure 2.2: The 'Human Gait Oscillation Detector' (HGOD) using potentiometers and 2 aluminum links proposed by Nandi et al. (2009).

Another study conducted by Thatte et al. (Thatte & Geyer, 2016) proposed the utilization of prosthetic device oriented sensory system consists of IMU units and joint encoders to control the MPC prosthetic leg. Although the sensory system used was the same as the others, the application of the information is different in this work. The joints kinematic parameters acquired by the sensors were used to predict the neuromuscular model of human locomotion, and the prosthetic device was controlled by the neuromuscular model, instead of using the signal of the sensor. The idea was to improve the robustness of the prosthetic device. Simulation results shown in Figure 2.3(a) shows that their proposed model is closer to the normal pattern, while Figure 2.3(b) illustrates the performance in response to disturbance of the neuromuscular model is better as compared to the impedance model. Findings from Thatte and Geyer (2016) proved that the proposed control managed to mimic the normal walking patterns and successfully reacted to disturbance to avoid falls.

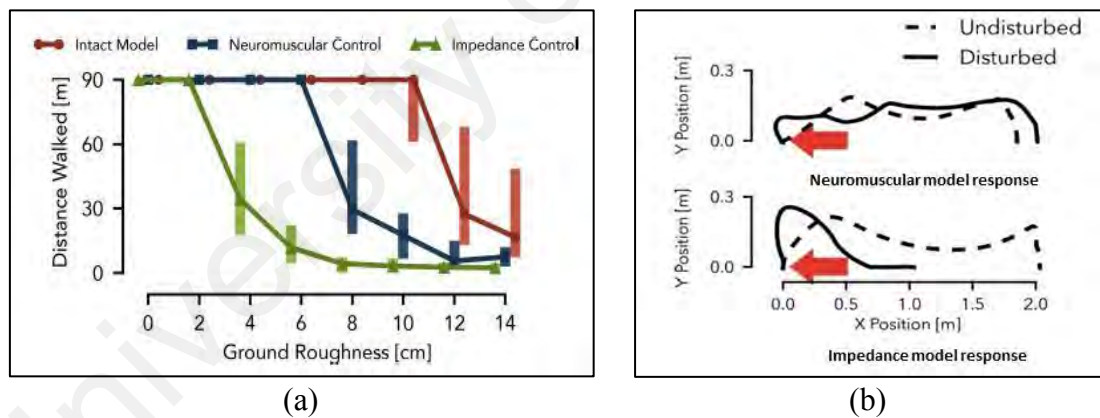


Figure 2.3: The performance of the MPC TF prosthesis driven by the neuromuscular control proposed by Thatte and Gayer (2016) as compared to the classic impedance control. (a) the result for robustness test of the prosthetic leg, (b) the tripping test performance.

A study conducted by Kapti et al. (2014) claimed that the active transtibial prosthesis can be controlled using information provided by 2 tri-axial accelerometers positioned on the shank and the foot of the sound limb. The acceleration data was used to estimate the position of the sound leg, and consequently predicted the ankle angle of the prosthetic leg via echo control method. Echo control method is an MPC prosthesis control approach

which is executed by copying the motions of the sound limb with a delay of half gait cycle (Windrich, Grimmer, Christ, Rinderknecht, & Beckerle, 2016).

On the other hand, kinetics sensors deliver signals that are related to the forces exerted on or by the device, for instance, the Ground Reaction Force (GRF). Examples of the force sensor the strain gauge, load cell, various pressure pad, piezo-resistive and piezo-electric devices.

Most of the literature reported the use of a set of kinematic and kinetic sensors to make a complete sensory system for MPC sensory system. One of the examples is CYBERLEGS, a robotic transfemoral prosthesis, adopted a wearable sensory system consisted of 7 inertial and magnetic measurement units (IMU) that can measure kinematic properties of the CYBERLEGS such as, three-dimensional accelerations, angular velocities, and the magnetic field. In addition to that, the sensory system was also equipped with pressure-sensitive insoles that is sensitive to vertical loads and less sensitive to tangential loads. The insoles measure the kinetic measurement of the prosthetic leg, particularly the vertical GRF (GRV), and the center of pressure (COP) at the bottom of the sole. The information from all sensors in the system was merged and analysed to determine these four states; quiet standing (QS), gait intention (GI), steady-state gait (SSG), and gait termination (GT). The SSG phase was further divided into the prosthetic limb single stance (SS-P), sound limb single stance (SS-S), the double stance with prosthesis leading sound limb to swing (DS-STs), and with the sound limb leading prosthesis to swing (DS-PTS).

Table 2.1 shows the classification rate of all states using the inputs from the sensory system and based on the classification rate, it can be deduced that the sensory system managed to detect the states well, especially during the SSG state (Ambrozic et al., 2014).

Table 2.1: The performance of CYBERLEGs in detecting the states of the leg using the proposed sensory system.

States		Classification accuracy %
SSG	GI	85.2
	SS-P	98.7
	SS-S	98.1
	DS-PTS	97.9
	DS-STs	91.1
GT		64.8

Source: (Ambrozic et al., 2014)

Xie, Li, Sheng, Xu, and Liu (2009) proposed the utilization of 6-axis force sensor located in between the pylon and prosthesis foot, and joint encoder to detect the gait phases for their intelligent bionic leg. The GRF information extracted by the 6-axis force sensor was used to predict the Zero Moment Point (ZMP), and the body posture information gained from the encoders, were used to control the movement of the bionic leg.

Varol et al. (2010) used a prosthetic-device oriented sensory system that consisted of foot-insole to measure GRF under the foot, load cells to measure joint torques, including one custom-made load cell to measure the sagittal-socket interface moment above the knee joint, and potentiometers to measure joint positions in the transfemoral MPC prosthesis to identify the activity of the prosthetic user and the transition between the modes. The activities that were tested were sitting, walking and standing.

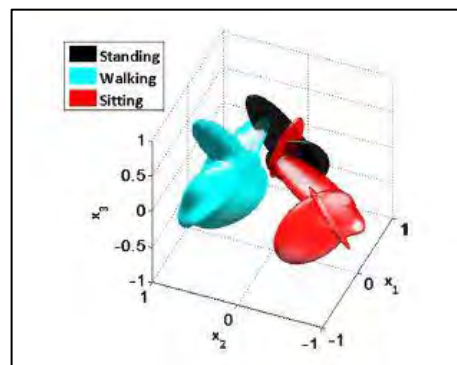


Figure 2.4: The features distribution in space for standing, walking and sitting activity in Varol et al. (2010) study. The features were extracted from the sensory system's signal. It can be seen that the features were separated from one activity to another.

On the other hand, Young et al. (Young & Hargrove, 2016; Young, Simon, & Hargrove, 2014) proposed the use of prosthetic device-oriented sensors such as load cells, gyroscopes, and accelerometers, to classify 5 activity modes (level walking, ramp ascent, ramp descent, and stair ascent and stair descent). There are more literature reported the use of prosthetic device oriented sensory system consisting of a set of kinematic and kinetic sensors to detect either gait events or gait intention (Fite, Mitchell, Sup, & Goldfarb, 2007; Fuhr, Quintern, Riener, & Schmidt, 2008; Khademi, Mohammadi, Simon, & Hardin, 2015; Krut, Coste, & Chablot, 2011; S. H. Lee & Kim, 2017; Shahmoradi & Shouraki, 2017; Stolyarov, Burnett, & Herr, 2018; Sup et al., 2007; Yang & Kim, 2015) and the summary on those works are presented in Table 2.2.

Another application of prosthetic device oriented sensory system was found in detecting the physical of the terrain (e.g. level or un-level, slope, stairs and etc.). Zhang et al. (F. Zhang, Fang, Liu, & Huang, 2011) proposed the use of IMU units with a distance laser sensor to predict the terrain before the user walked on it. Although the experiment was conducted on the able-bodied subject, the researchers claimed that the concept can also be implemented to control MPC prosthetic leg, so that the prosthesis device becomes more adaptive to the environment.

Table 2.2: Summary of the literature review on the prosthetic-device oriented sensory system.

	Type of prosthesis device	Sensors used	Sensor's information application	Other remarks.
(Nandi et al., 2009)	TF	Potentiometers	Proxy	Used sensors' data to develop CPG model to control MPC prosthetic leg.
(Thatte & Geyer, 2016)	TF	IMU and encoders	Proxy	Used sensors' data to feed the neuromuscular model to control MPC prosthetic leg. The findings showed that improvement was monitored in terms of the robustness of the prosthetic leg in rough terrain and in tripping test.

Table 2.2, continued

	Type of prosthesis device	Sensors used	Sensor's information application	Other remarks.
(Kapti & Muhurcu, 2014)	TF	Accelerometers	Proxy	Used sensors' data located on the sound limb to control the prosthetic leg via echo method.
(Torrealba, Cappelletto, Fermin-Leon, Grieco, & Fernandez-Lopez, 2010)	TF	Accelerometers	Impedance control approach	
(Xie et al., 2009)	TF	6-axis load cell and encoders	Impedance control approach	
(Ambrozic et al., 2014)	TF	IMU and pressure-sensitive insole	Hi-level control	Sensors data was used to identify GI, SSG that consists of SS-P, SS-S, DS-STs, and DS-PTS, and GT.
(Varol et al., 2010)	TF	Potentiometers, load cells, foot insole	Hi-level control	Sensors data was used to recognize sitting, walking and standing activity.
(Young & Hargrove, 2016; Young, Simon, & Hargrove, 2014)	TF	Accelerometers, gyroscopes and load cells	Hi-level control	Sensors data was used to identify 5 activities; level walking, ramp ascent, ramp descent, stairs ascent and stairs descent.
(Fite et al., 2007)	TF	Joint motion sensor and force sensor at the heel	Impedance control approach	
(Fuhr et al., 2008)	Neurorehabilitation robotic	Inertial sensor, goniometer, gyroscope, and foot insole	Impedance control approach	
(A. M. El-Sayed, Hamzaid, & Osman, 2014; A. M. El-Sayed, Hamzaid, Tan, & Abu Osman, 2015)	TF	Piezoelectric sensors	Impedance control approach	Investigated the feasibility of using 3 bi-morph piezoelectric sensors, placed on the inner wall of the TF prosthesis wall to detect knee movement.
(Khademi et al., 2015)	Collected on able-bodied	Potentiometers, load cells, foot insole	Hi-level control	Sensors data was used to classify 4 types of locomotion mode; standing, slow walking, normal walking, and fast walking.
(Krut et al., 2011)	TF	Force sensors and encoders	Hi-level control	Focused on developing MPC prosthetic leg for elderly.
(S. H. Lee & Kim, 2017)	TF	Inertial sensors	Impedance control approach	Used the sensors data to adjust the control parameters for posture stabilization on slope terrain and obstacle avoidance.
(Shahmoradi & Shouraki, 2017)	TF	IMU and Force-sensitive resistor (FSR)	Hi-level control	Used sensors data to train the Fuzzy-based classifier to identify different activities; sitting, standing, walking, stair ascent, stair descent, ramp ascent, and ramp descent.

Table 2.2, continued

	Type of prosthesis device	Sensors used	Sensor's information application	Other remarks.
(Stolyarov et al., 2018)	TT	Inertial sensors	Hi-level control	Sensors data was used to predict the intention to change activity by estimating the translational motion of the joints. Results suggested that the intention could be captured by using only the inertial sensors.
(Liu, Lin, Geng, & Yang, 2017)	TF	Accelerometer, gyroscope and pressure sensors on shoe insole	Hi-level control	Sensors data was used to recognize the user's intention of walking on various terrain; level ground, stair ascent, stair descent, up and down the ramp.
(Shultz, Lawson, & Goldfarb, 2016)	TT	Absolute encoder, incremental encoder, and IMU units	Hi-level control and impedance-based control	Position and velocity of the ankle joint, together with shank absolute orientation and angular velocity measured by the sensors were used to identify the 5 state; Standing, Middle stance, Late stance, Early swing and Late swing/Early stance.
(Villalpando, Weber, Elliott, & Herr, 2008)	TF	Digital encoders, Hall effect, IMU	Impedance-based control	

2.2.2 User's-biological-input oriented sensory system

Sensory system that reads the biological activity of the user falls into user's biological input-oriented category. The sensory system usually requires direct contact with the user, and electrography devices such as Electromyography (EMG) were often adopted as the sensor. The information obtained from this type of sensory system is usually reliable for intention detection process because the sensory system records the excitation signal transmitted from the brain to the respected organ or limb when one intends to make any moves.

To date, based on the review made on literatures that reported on the user's biological input measurement for controlling the MPC prosthetic device, and applications that are closely related to the field, the approach of recording the excitation signal can be summarized into two categories, namely; the CNS (i.e. brain) level and Peripheral Nervous System (PNS) level.

The CNS-level sensory system reads the excitation signal directly from the brain. The success in obtaining information for the brain that is correlated to human motion can lead to the success in neuro-prosthesis. In some studies, the approach of acquiring the signal from the brain and analysing it using machine/computer is called the Brain-Machine Interface (BMI). There are many works of literature that reported studies on BMI, but very few described the use of BMI for lower-limb prosthesis field (Murguialday et al., 2007; Presacco, Forrester, & Contreras-Vidal, 2012). Most of the literature reported BMI's development and analysis for the upper-limb prosthesis (Mashal, Shafique, & Khan, 2015; McMullen et al., 2014; Murguialday et al., 2007). The common device used for the CNS level measurement is Electroencephalography (EEG), and functional near-infrared spectroscopy (fNIRS) for surface-based measurement, and Electrocorticography (ECoG) which is more invasive in nature.

Fitzsimmons et al. (2009) and Ma et al. (2017) conducted a separate study to prove the correlation between the cortical activity with the lower-limb muscles during motion by using the intra-cortical invasive electrodes. Both studies recruited monkeys as subjects and implanted multi-array electrodes on the subjects' brain surgically to perform chronic neural data recording. At the same time, EMG sensors were also implanted on the subjects' several lower-limb muscles to monitor muscles activity. Both studies concluded that there was high correlation between cortical ensemble activity and muscles activity during walking (in Fitzsimmons et al. study) and stand and squat motion in Ma et al. study.

A study conducted by Presacco et al. (2012) proposed the use of 12 scalp EEG electrodes to achieve the same research objective outlined in Fitzsimmons et al. (2009). Findings from Presacco et al. proved that the non-invasive electrodes accuracy in decoding the brain's signal was comparable to the study in (Presacco et al., 2012) which

utilized the intra-cortical invasive electrodes. Hence, it led to the inference that non-invasive scalp electrodes are reliable to be adopted in BMI system development.

Bai et al. (2015) have successfully proved the reliability of the use of 7 wireless non-invasive EEG electrodes which was placed on the subject's scalp, to control the knee-lock mechanism of TF prosthesis. The intent of the user to sit, and walking were determined using the information gained from the EEG sensors and good volition-control sensitivity were observed for both activities.

In addition to EEG, the use of the hemodynamic-signal-capturing device such as functional near-infrared spectroscopy (fNIRS) was also found in the literature as an approach to read brain activity that corresponds to the lower limb movement (Rea et al., 2014). Although the implementation was in the rehabilitation of lower-limb of stroke patients, the findings show that fNIRS could detect the brain activity that associated with the motion intention by the lower-limb, and therefore, this study gave an insight that fNIRS could be adopted for neuro-prosthesis control. Findings from those studies gave an insight that controlling an MPC prosthetic leg using the signal from the brain is possible to be implemented in the future.

The second type of user's biology oriented sensory system is the PNS-level sensory system. The famous sensor device that is usually used to acquire the PNS signal from the human body is EMG. Electromyography (EMG) is used to record the electrical signal produced by skeletal muscle. It is favorable to be adopted in prosthetic design because the method directly reads the electrical signal of the muscle which is connected to the nervous system and finally to the brain. To make any motion, the brain sends excitation signal via the Central Nervous System (CNS) to the "motor unit". The activation of the motor unit will produce an electrical signal that is known as "Motor Unit Action Potential" (MUAP) and when the activation continues, a MUAP train is produced. The MUAP train is the signal acquired by the EMG (Jamal, 2012).

In 1991, Hudgins, Parker, and Scott conducted a study to investigate the ability of EMG signal to control the multifunction prosthesis. The EMG electrodes were placed on the different upper extremity muscle group of 15 subjects. In their study, they proved that EMG signal gives a consistent pattern for every movement and can also detect the initial phase of muscle contraction and hence, it can be utilized to control any prosthetic limb (Hudgins, Parker, & Scott, 1991b).

Hardaker, Passow, and Elizondo (2013b) proposed the use of EMG on transfemoral amputee to identify the state of the user either he/she is standing still, walking or running using the acquired EMG signal from the transfemoral amputee residual limb. The electrodes placement is shown in Figure 2.5 below. The EMG signals were processed for feature extraction and pattern recognition and the Artificial Neural Network (ANN) method were utilized in this study.

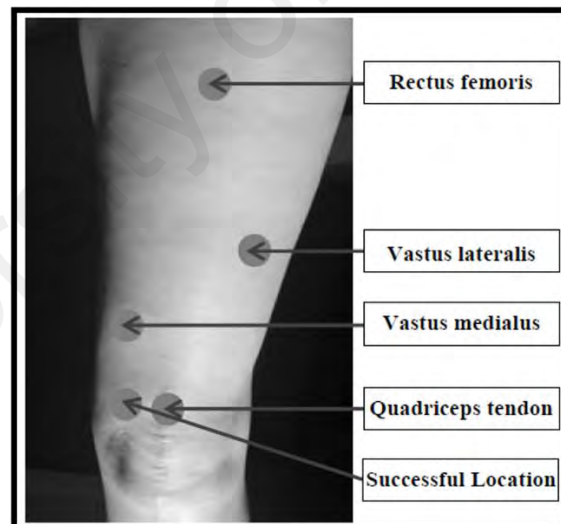


Figure 2.5: Placement of EMG electrodes in study reported in Hardaker et al. (2013b)

Wu, Waycaster, and Shen (2011) presented an ‘active–reactive’ control method that imitates the actuation mechanism of a human biological joint. The EMG signal was used as the input to the control algorithm and based on the input signal, the active and reactive muscle will be determined. The control law was designed to use the connection between active and reactive muscle to operate the actuator (Wu et al., 2011).

Some literature reported the study and analysis on improving the efficiency of myoelectric control in prosthesis application (Hofmann, Jiang, Vujaklija, & Farina, 2016; Q. Huang et al., 2017; Nakamura & Hahn, 2016; Zhu, Liu, Zhang, Sheng, & Jiang, 2017). The summary of the reviewed literature is presented in Table 2.3.

From the review, it can be observed that, most of the studies utilized this type of sensory system response to identify the intention of the user. This indicates that the usage of user's-biological-input oriented sensory system is a popular option for user intention detection purposes and consequently used to develop the high-level controller of the MPC prosthetic leg. However, it can also be noticed that the user's-biological-input oriented sensory system requires tedious donning and doffing. The BMI sensory system, such as EEG, requires at least the utilization of scalp electrodes, while EMG needs electrodes to be properly located on the respected muscles to gain the necessary information. Thus, it can be deduced that, despite of providing rich information, it compromises the practicality of the prosthesis system.

Table 2.3: Summary of the literature review on user's-biological-input oriented sensory system.

	Type of prosthesis device	Sensors used	Sensor's information application	Other remarks.
(Mashal et al., 2015)	Simulated robotics arm	EEG	Control	The EEG signal is used to simulate the robotic arm motion control. The findings can be adopted by neuroprosthesis design.
(McMullen et al., 2014)	Modular Prosthetic Limb (MPL)	ECoG	Brain-control	The sensor information was used to train the BMI to recognise an object and initiate the reach-grasp-and-drop activity by the MPL.
(Murguialday et al., 2007)	Upper-limb	EEG	Brain-control	The information extracted from the EEG was used to train the BMI to do object grasping activity and control the grasping force. The accuracy of the proposed BMI was comparable to the EMG-based control mechanism.
(Fitzsimmons et al., 2009)	-	Invasive implanted EEG	Conceptual study	Used implanted EEG on monkeys to investigate the correlation of brain activity captured by the EEG sensors with muscle activity for walking. The findings gave an insight that EEG sensor can be used to control the neuroprosthesis.

Table 2.3, continued.

	Type of prosthesis device	Sensors used	Sensor's information application	Other remarks.
(Presacco et al., 2012)	-	Scalp EEG electrodes	Conceptual study	Aim on achieving the same objective as Fitzsimmons et al. (2009) but proposed the non-invasive method, the scalp EEG electrodes. Results show that the accuracy of the data was comparable to the results reported in Fitzsimmons et al. (2009).
(Bai et al., 2015)	TF	Wireless scalp EEG electrodes	Brain-control	Proved that the TF prosthesis knee-lock mechanism can be controlled using signal extracted from the brain using 12 wireless non-invasive scalp EEG sensors.
(Rea et al., 2014)	Lower-limb	fNIRS	Brain-control	Proved that fNIRS device can be used to extract brain signal that corresponds to lower-limb motion's intent.
(Hudgins et al., 1991a)	-	Surface EMG	Conceptual study on Myoelectric-control	Proved that EMG signal gives a consistent pattern for every movement and can also detect the initial phase of muscle contraction and hence, it can be utilized to control any prosthetic limb.
(Hardaker, Passow, & Elizondo, 2013a)	TF	Surface EMG	Myoelectric-control	Used the EMG data to classify different activity; standing, walking or running.
(Wu et al., 2011)	TF	Surface EMG	Myoelectric-control	Presented an 'active-reactive' control method that imitates the actuation mechanism of a human biological joint based on the input from EMG.
(Hofmann et al., 2016)	Multi-functional prosthesis	Surface EMG	Myoelectric-control	Proposed a " <i>recursive nonlinear estimator of sEMG amplitude based on Bayesian filtering</i> " to improve the robustness of the control system.
(Q. Huang et al., 2017)	-	EMG	Myoelectric-control	Proposed a Particle Adaptive Classifier (PAC) for to address performance degradation issue in myoelectric-control.
(Nakamura & Hahn, 2016)	TF	Surface EMG	Myoelectric-control	Investigated the variations in muscle activation during locomotion state pre-transition and transition.
(Zhu et al., 2017)	-	Surface EMG	Myoelectric Pattern Recognition (MPR) algorithm	Proposed a Linear Discriminant Analysis (LDA)-based cascaded adaptation (CA) approach, which integrates history-information for calibrating the latest MPR model, in order to address the limitations of current myoelectric pattern recognition (MPR) algorithm; performance degradation caused by the EMG non-stationary signal and the needs of re-training and re-calibration.

Table 2.3, continued.

	Type of prosthesis device	Sensors used	Sensor's information application	Other remarks.
(Tkach, Huang, & Kuiken, 2010)	Upper-limb	EMG	MPR	This study investigated the effects of EMG electrode shift, amount of user effort during muscle contraction, and muscle fatigue, to classification accuracies.
(T. Y. Zhang, 2016)	TF	EMG	Conceptual study on myoelectric control	Proved that the use of sEMG on the residual limb of TF amputee is sufficient to recognize different activity; level-walking, stairs ascending and descending with high classification rate (>95%).

2.2.3 Neuro-mechanical fusion sensory system

Neuro-mechanical fusion sensory system combines the above-mentioned sensory systems in one system. For lower-limb MPC prosthesis, the combination of EMG and mechanical sensors are the popular option found in the literature.

Tkach et al. (2013) investigated the performance of a classifier trained with a neuro-mechanical fusion based sensory data in predicting 8 ambulation mode transitions as compared to mechanical based only and EMG based only sensory data for TT amputees. The findings from the study concluded that of neuro-mechanical fusion sensory system in detecting the ambulation mode transitions outperformed the other 2 approaches in terms of classification accuracy. This is because a significant improvement in terms of classification accuracy was observed for classifier which was trained with neuro-mechanical fusion sensory data. Table 2.4 presented the classification error for all three approaches.

Table 2.4: The performance of classifier in detecting ambulation mode transitions

Method	Classification error %
Mechanical only	7.8±0.9%
EMG only	20.2±2.0%
Fusion	2.3±0.7%

Source: Tkach et al. (Tkach & Hargrove, 2013)

Wentink et al. (2013) proposed the use of inertial sensors and EMG to capture the real-time intention of gait initiation. The motivation is to help the amputees to generate artificial push off by the prosthetic leg and ensuring the stability by early detection of heel-strike and toe-off of the leading limb. Data were collected from 10 able-bodied subjects who were asked to mimic the TF amputee situation using 'knee-walker'. The findings from this study show that the neuro-mechanical fusion sensory system proposed managed to successfully capture the intention to start the gait within 130-260ms before toe-off and heel-strike occurred. The findings can be used as guidance in designing the control algorithm of the prosthetic leg to produce artificial push off.

Another study by Wentink et al. (2014) investigated the reliability of the neuro-mechanical fusion sensory system to detect the onset of gait initiation of TF amputees. In this study, data were collected from 6 TF amputees. The results show that the gait initiation can be captured by the inertial sensors. Meanwhile, the intention of starting the movement was captured by the EMG 138ms prior to the initial movement, if the leading leg is the prosthetic leg. This study gave an insight into MPC prosthetic leg control design.

Table 2.5: Summary of the literature review on neuro-mechanical fusion sensory system.

	Type of prosthesis device	Sensors used	Sensor's information application	Other remarks.
(Tkach & Hargrove, 2013)	TT	Inertial sensors and EMG	Prosthesis control	Investigated the performance of a classifier trained with a neuro-mechanical fusion based sensory data in predicting 8 ambulation mode transitions as compared to mechanical based only and EMG based only sensory data for TT amputees. Findings show that neuro-mechanical fusion sensory system performed better as compared to the other alternatives.

Table 2.5, continued.

	Type of prosthesis device	Sensors used	Sensor's information application	Other remarks.
(Wentink, Beijen, et al., 2013)	TF	Inertial sensors, accelerometers, gyroscopes, magnetometers, and EMG	Prosthesis control	Findings from the analysis of data collected from able-bodied subject showed that the neuro-mechanical fusion sensory system proposed managed to successfully capture the intention to start the gait within 130-260ms before toe-off and heel-strike occurred.
(Wentink et al., 2014)	TF	Inertial sensors, accelerometers, gyroscopes, magnetometers, and EMG	Prosthesis control	Investigated the reliability of the neuro-mechanical fusion sensory system in detecting the onset of gait initiation of TF amputees.
(Joshi & Hahn, 2016)	Lower-limb	Accelerometers, and EMG	Prosthesis control	Used the sensory signals to detect the transition from level ground walking to stairs ascending or descending, and ramp ascending and descending. The findings from this study show that accelerometer and EMG data complemented each other. Therefore, Joshi and Hahn deduced that fusion sensory system is more robust.
(Krausz, Lenzi, & Hargrove, 2015)	Lower-limb	Accelerometers, EMG, and depth sensor	Prosthesis control	Proposed the addition of the depth sensor to the neuro-mechanical fusion sensor to enhance the robustness of the MPR, so that a seamless ambulation transition can be achieved.

2.2.4 Discussion

Figure 2.6 illustrates the sensory systems that were adopted or potentially adopted for prosthesis application. From the literature review, it can be observed that studies involving the prosthetic-device oriented sensory system were more advanced as compared to the other two alternatives. A few of the studies reported the use of the developed MPC prosthetic leg prototype which was equipped with and controlled using the proposed sensory system, for instance, the CYBERLEGs (Ambrozic et al., 2014) and VI Knee (Villalpando et al., 2008). It indicates the confidence of the researchers in the

proposed system in terms of providing safety to the subjects. Meanwhile, research involving the user's-biological-input oriented and neuro-mechanical fusion sensory system, are still in its fundamental phase.

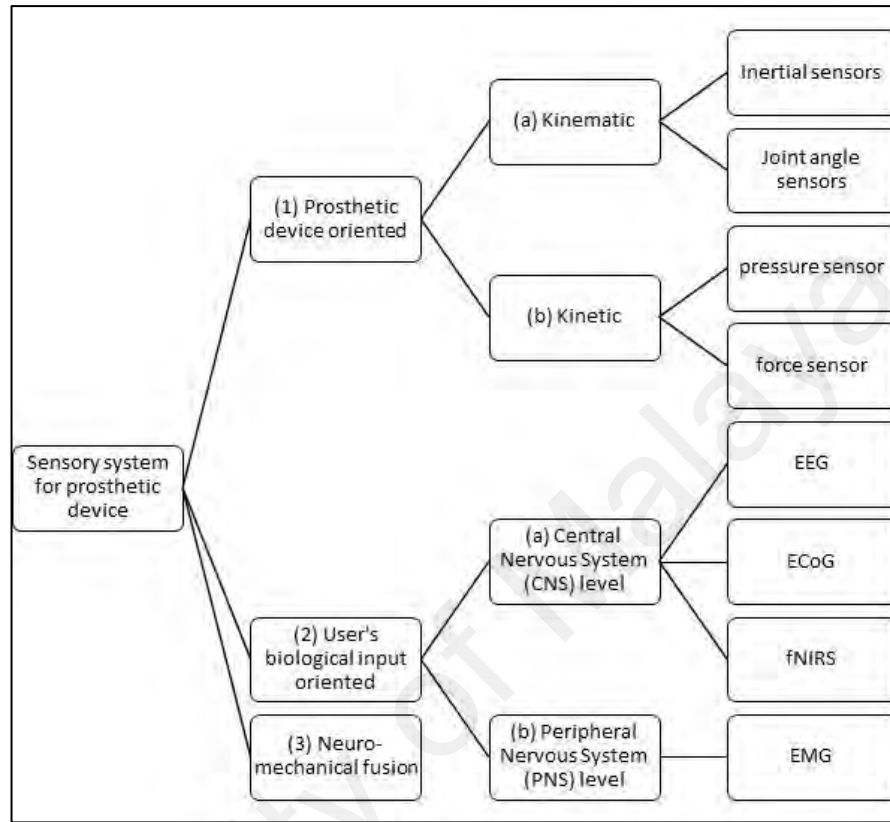


Figure 2.6: The chart of the sensory system adopted or possible to be adopted in prosthesis control system.

Prosthetic-device oriented sensory system was proven to work well in coordinating the device motion via impedance-based control. Besides, it was also seen to be used as input signal to identify the transition between ambulation modes. However, the review shows that only one study reported the use of kinematic sensor only to do the task (Stolyarov et al., 2018), the rest reported the use of both kinematic and kinetic sensors for activity mode transition detection purpose. However, to date, the efficiency of this type of sensory system is still inadequate to be used in predicting the intention of the user. This is because, there is no direct contact between the sensors to the user's body, what more to access the neural input of the user; which was proven to be able to interpret the motion intent before the movement takes place.

Besides, the prosthetic-device oriented sensory system does not integrate the response-to-the-environment data. For instance, for an able-bodied person, the locomotion pattern also depends on the input from the sensory organs (e.g. eyes, and ears) that sense obstacle along the path. Therefore, the brain will signal the muscles to increase the degree of knee flexion, and lengthen the swing period to avoid the obstacle. The absence of this data, might compromise the safety of the prosthetic user. Martin et al. (2010) claimed in his study, compromised user's safety, gait deficiency and eventually prosthetic device rejection are the negative impact that might occur if there is a contradiction between the user's intended motion and the motion set by the prosthetic device controller. One way to avoid this is to use a sensory system that acquires information from the user's biological input, such as EEG and EMG.

The utilization of EMG electrodes is more commonly found in the lower-limb prosthesis. Although many studies proved that EMG signal is reliable in detecting the intention of the user before the movement really takes place, its performance is limited to some drawbacks. It is highly susceptible to electrode-skin conductivity, motion artifacts, misalignment of the electrodes, and cross-talk between the nearby muscles (H. Huang, Kuiken, & Lipschutz, 2009; Tkach et al., 2010). In addition, the don and doff process of EMG sensory system is tedious (Jamal, 2012). Thus, it can be predicted that, unless these signal-quality related issues are really addressed, an EMG-only-based sensory system is not convincing enough to be used in lower-limb MPC prosthesis.

The fusion sensory system provides more informative data to the controller. Both muscle activity and kinetic and kinematic information can be obtained from this type of sensory system, hence, offer a robust control algorithm and provide a seamless transition between ambulation modes for MPC prosthesis. Nevertheless, the complexity of the system to process heavy information from the sensors (i.e. EMG and mechanical sensors)

might reduce the practicality of the sensory system in terms of processing time and RAM and ROM capacity of the processor.

A study conducted by Zhang et al. (2013) reported that data from EMG and GRF/moment were more useful for real-time intent recognition task for TF amputees than the kinematics information. However, a more recent study by Stolyarov et al. (2018) proved that the use of inertial sensors only was sufficient to perform the intent recognition task by adopting the translational motion tracking method. The findings gave an insight that with some creative approach to extrapolate the available sensor information into a larger group of meaningful information, the adoption of a simpler sensory system to control MPC prosthetic leg is possible. Hence, the two criteria of an efficient sensory system; practicality and quality of the sensory information can be fulfilled.

2.3 Piezoelectric application in prosthesis field

The existing sensors incorporated by other studies may cause skin abrasion or redness (Miyamoto et al., 2017). An alternative to this may require sensors that does not protrude onto the skin and does not require any extensive skin preparation. A sensory system that is already incorporated or embedded into the socket may prove to be a good solution. This would not require any skin preparation and the readability of the sensors inside the socket may act like a sensor-shoe that could detect user's movement by just walking in it.

To date, the piezoelectric device is becoming a favourable option to be used in many applications. This is because of the electro-mechanical feature that it possesses. Some application that adopt piezoelectric device is energy harvesting (Hu, Hu, Chen, & Wang, 2008; Li, Jin, & Yang, 2013; H. Liu et al., 2017; Nguyen, Feng, Häfliger, & Chakrabartty, 2014), medicine and biomedical (Choi, Duan, Li, Wang, & Oldham, 2017; Farooq & Sazonov, 2017; Lin et al., 2017), and instrumentation (Búa-Núñez, Posada-Román, Rubio-Serrano, & Garcia-Souto, 2014; Dante, Bacurau, Spengler, Ferreira, & Dias, 2016; Ribeiro et al., 2017).

Prosthesis field is one of the applications that adopt piezoelectric as part of the system. Based on the search done on literature review, the application of piezoelectric device was found on the ear, dental, upper-limb and lower-limb prostheses device. The key findings of the studies were summarised in Table 2.6.

Very few studies reported the use of the piezoelectric sensor in lower-limb prosthesis-related research. Lorenzelli et al. (2017) and Sordo and Lorenzelli (2016) proposed the piezoelectric sensor to be used to measure the interface force between socket and stump for TF amputee. The purpose of the measurement is to optimize the TF socket design. Meanwhile, El-Sayed (2014; 2015) conducted a feasibility study to utilize bi-morph piezoelectric sensors placed inside the socket to detect knee movement. Findings from the study suggested that the piezoelectric-based in-socket sensory system is feasible to be used, hence open the window for further investigations. Further study on configuring the piezoelectric sensors on the socket, and testing the accuracy of the classifier model based on the piezoelectric-based in-socket sensory system to detect and predict motion of the prosthetic leg.

Table 2.6: Summary of the literature review on the utilization of piezoelectric in the prosthesis.

	Type of prosthesis	Piezoelectric device function	Other remarks
(Campanella et al., 2012)	Ear	As middle-ear audio prosthesis	Proposed the use of piezoelectric-based microelectromechanical system (MEMS) transducer as audio prosthesis and method to fabricate the piezoelectric-based audio prosthesis.
(Lacour, Graz, Cotton, Bauer, & Wagner, 2011)	Generic	As a material to develop the prosthetic skin.	Reported the use of multilayer piezoelectric elastomer inserted in between stretchable electrodes and thin-film transistors to develop a stretchable prosthetic skin that can measure pressure.
(Z. X. Huang, X. D. Zhang, & Y. N. Li, 2012)	Hand	As tactile and slipping sensors for finger prosthesis.	Developed a Polyvinylidene Fluoride (PVDF) piezoelectric-based tactile and slipping sensor as a feedback system for adaptive hand prosthesis.

Table 2.6, continued.

	Type of prosthesis	Piezoelectric device function	Other remarks
(Dong et al., 2017)	Generic	Human-Machine Interface (HMI) device	Proposed the use of PVDF piezoelectric sensor as HMI device. The PVDF piezoelectric sensor was laminated on the skin surface and signal was used for motion classification and controlling a mobile robot. Gave an insight that PVDF piezoelectric sensor is reliable to be used as HMI device and can also be implemented in the prosthesis system.
(D. Zhang et al., 2017)	Dental prosthesis	Instrumentation device	The 3-D piezoelectric transducer was used to measure dynamic load in the in-vivo implant-supported fixed partial denture (I-FPD).
(Zhuo et al., 2015)	Hand	As tactile and slipping sensor	Proposed and evaluated the use of piezoelectrets as a tactile and slipping sensor for hand prosthesis. Findings suggested that the piezoelectrets-based sensor reliable to detect both touching and slipping.
(A. Huang, Ono, & Ieee, 2016)	Hand	As a material to develop wearable flexible ultrasonic sensor to monitor muscle activity	Proposed the use of a piezoelectric polymer-based film ultrasonic sensor to estimate the wrist angles by measuring the changes in muscle thickness. Proved that the response obtained from the proposed sensor display comparable pattern with the wrist angles pattern obtained from video image analysis.
(Suaste-Gomez, Rodriguez-Roldan, Reyes-Cruz, & Teran-Jimenez, 2016)	Ear	As an ear prosthesis	Proposed an ear prosthesis that was developed using PVDF piezoelectric.
(Creighton et al., 2016)	Ear	As an ear prosthesis	Proposed the use of PVDF piezoelectric transducer to measure intracochlear pressure. The study proved that intracochlear piezoelectric sensor is feasible to function as an ear prosthesis.
(Suzuki et al., 2012)	Upper Limb	Sensor to detect hand motion	Investigated the feasibility of piezoelectric sensor to classify various hand motion and evaluated the robustness of the sensor to the unintended motion. Findings suggested that piezoelectric sensor is feasible and robust to be used as a sensory system for upper limb prosthesis.
(Lorenzelli et al., 2017; Sordo & Lorenzelli, 2016)	Lower-limb	Sensor to measure the interface force between socket and stump.	These studies used the piezoelectric transducer to develop a low-cost tri-axial force sensor to measure the interaction force between socket and stump. The sensor was placed inside the master socket. The information obtained from the sensor could be expedited the customization of TF socket.
(A. M. El-Sayed et al., 2014; A. M. El-Sayed et al., 2015)	Lower-limb	Sensor to detect prosthetic knee movement	Proposed the use of 3 bi-morph piezoelectric sensors which were placed on the inner wall of the socket to detect the movement of the knee. And proved the feasibility of the in-socket sensory system for knee movement detection.

2.4 Conclusion

The overview of the control system of an MPC prosthetic leg was described in the first section of the chapter. Then, the importance of the sensory system to the MPC control system was elaborated and the criteria of an efficient sensory system was discussed. Besides, this chapter also reports the literature review of the state-of-the-art of the sensory system in MPC prosthetic leg. The sensor technology that was adopted in MPC prosthesis system was divided into three types, namely; the prosthetic-device oriented, user's-biological-input oriented, and neuro-mechanical fusion. The advantages and drawbacks of each type of the sensory system were discussed. In addition, the application of piezoelectric in various types of prosthesis was reviewed. The function of the piezoelectric in the respective prosthesis system was described.

Based on this review, it can be deduced that the sensory technology reported in the literature still does not fulfil the criteria of efficient sensory system, which are; the practicality and quality of the information provided. Most of the sensory system reported is either too complex (e.g. multiple types of sensors, tedious preparation needed) which compromise the practicality of the system, or not informative enough to provide the reliable info to the controller. Hence, a simpler sensory system that can ease the don and doff process of the prosthesis, yet informative to effectively control the prosthesis is needed. Thus, this thesis proposed the use of piezoelectric-based in-socket sensory system to provide information to detect gait phases for TF amputee.

CHAPTER 3: CONFIGURATION AND ANALYSIS OF PIEZOELECTRIC-BASED IN-SOCKET SENSORY SYSTEM FOR TRANSFEMORAL PROSTHETIC LEG

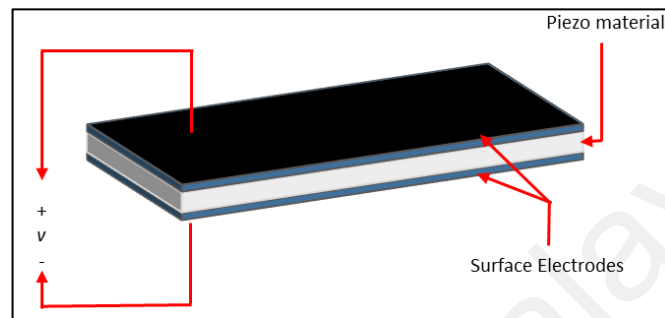
3.1 Introduction

This study focused on determining the best configuration for TF prosthesis in-socket sensory system using a set of piezoelectric sensors. For this application, the piezoelectric sensor was chosen to be used for its electro-mechanical properties. The idea is to place the piezo sensors on the socket wall to detect the force or pressure profile when there is motion and portray it in terms of a voltage signal. The voltage signal would then be used to characterize the motion. Thus, to ensure that the output signals from the piezo were reliable to be used, the suitable piezo sensors and its mounting and placement configuration as in-socket sensors had to be confirmed. This chapter describes the methods used, the analysis conducted on the obtained results and the discussion and conclusion of the findings at the end of this chapter.

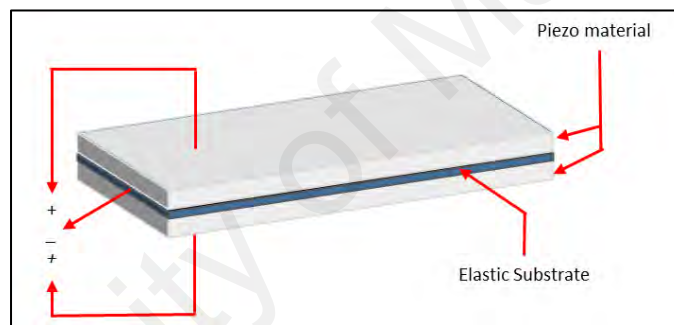
3.2 Literature review

Piezoelectric (piezo) is categorized in the smart material group for its electromechanical feature that can convert electrical to mechanical energy and vice versa. When force is applied to the piezo device, voltage is generated as the output. This is known as “*direct piezoelectric effect*” or also termed as “*sensor mode*”. On the other hand, when the piezo is supplied with voltage and the piezo actuates as the result, this phenomenon is described as the “*converse piezoelectric effect*” or the piezo is in “*actuator mode*”. There are two types of piezo device. Unimorph piezo device is a single layer piezo (Figure 3.1(a)), whereas bimorph is the term for the double layers piezo device (illustrated in Figure 3.1(b)). Study by Ng and Liao (2005) shows that bimorph piezo device yields higher output voltage as compared to unimorph piezo when the same amount of force is applied.

The piezo sensors were used in many areas, including energy harvesting (Muthalif & Nordin, 2015; Romani, Filippi, & Tartagni, 2014), instrumentation (Krajewski, Magniez, Helmer, & Schrank, 2013; Wen-Yang, Chun-Hsun, & Yu-Cheng, 2008), and medical applications (McPherson & Ueda, 2014; Toledo, Fernandez, & Anthony, 2010; Yan, Lu, Ding, & Yan, 2002) due to its unique electromechanical properties.



(a) Unimorph piezo device



(b) Bimorph piezo device

Figure 3.1: Unimorph and bimorph piezo devices

In this work, a set of piezo transducers were used to construct a sensory system inside a prosthetic socket wall that is directly in-contact with the stump to detect any changes in the pressure applied by the thigh's muscle groups (quadriceps and hamstring) while performing locomotion activities. The practical motivation is to eliminate the need of donning and doffing the sensors onto the amputees' skin. The piezo signal would correspond to the movements and the signal could be classified for further decision making (Figure 3.2).

Literature have reported that piezo sensors were utilized in the upper-limb prosthetic control algorithm (Cotton, Chappell, Cranny, White, & Beeby, 2007; Z.-X. Huang, X.-D. Zhang, & Y.-N. Li, 2012; Spanu et al., 2016; Sun et al., 2015) and other types of

prosthesis (Adams, Brillhart, Bushek, & Kroll, 2001; Leysieffer, Hortmann, & Baumann, 1994). However, only few studies proposed the use of piezo transducers as the feedback signal source in controlling the lower-limb prosthesis, especially for TF prosthetic application. El-Sayed performed a feasibility study to use the PZT-type, bi-morph piezo transducers as an in-socket sensor for TF prosthetic leg (Amr M. El-Sayed, Hamzaid, & Abu Osman, 2014; Amr M. El-Sayed, Hamzaid, Tan, & Abu Osman, 2014). While the outcome verified that an in-socket piezo sensor can be useful to characterise the movements, the sensitivity range and the signal-to-movement characterisation accuracy might have been affected by the size, thickness and the number of the sensors attached. Thus, this work utilised smaller and thinner piezo sensors with array setting in the design.

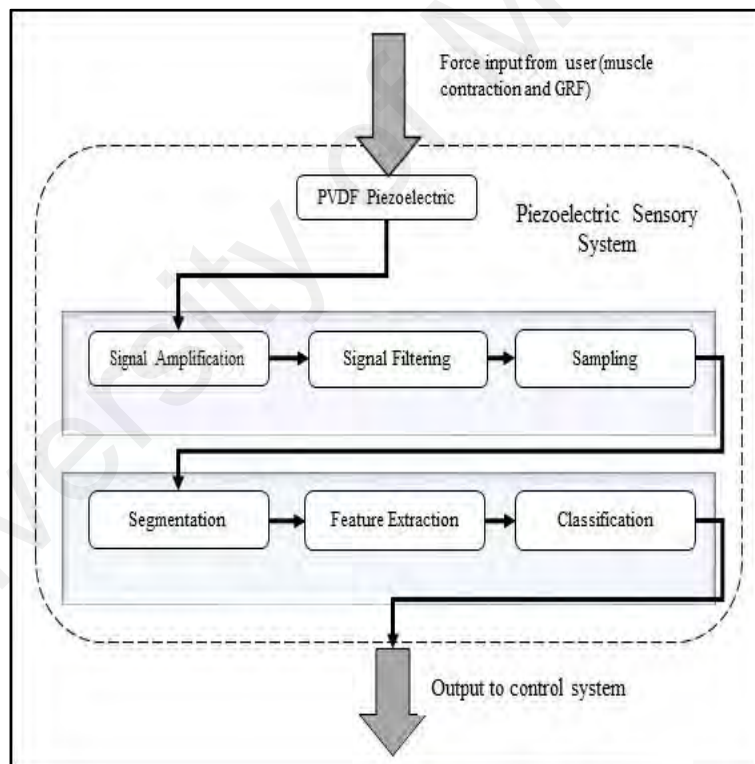


Figure 3.2: Flowchart of in-socket sensory system.

Another major factor that might affect the performance of the output signal is the mounting configuration of the sensor to the host structures (the socket inner wall). The different mounting method would produce dissimilar deformation, stress and strain pattern, and eventually resulted in the sensor's performance. Due to the same reason

explained above, the position and placement of the sensors would also affect the overall sensory system performance.

In this study, Polyvinylidene Fluoride (PVDF)-type piezo, also commonly known as piezofilm was adopted as the sensors. A piezofilm was chosen for its advantages compared to other piezo materials and it was found to be suitable for this application. Ueberschlag (2001) claimed in his paper that among the advantages of piezofilm are flexibility (ability to adapt to non-even surface), durable to mechanical force, dimensional stability, homogenous response within the piezo plane, high piezoelectric and dielectric coefficients, endurance towards temperature factor (up to 80°C), has low acoustic impedance, and usually comes with thin thickness (9 to 100 μm).

Hence, this study aims to investigate the size and shape of the piezo sensors, the mounting configuration and placement orientation of the in-socket sensory system. Then, the efficacy of the proposed configuration and setup was tested by evaluating its performance during gait activities of an amputee.

3.3 Methods

3.3.1 Analysis of the piezoelectric sensors properties

In order to determine that a proper type of piezoelectric sensors was selected, a simulation study using a finite element analysis software, Comsol Multiphysics modelling software (COMSOL Inc, USA) was used to determine the size and shape of the piezo sensors. The simulation was performed with the aim of selecting the piezo features that can yield the strongest output when the same amount of pressure was applied.

The properties of piezofilm or PVDF piezo that were used in configuring the model were presented in Table 3.1. There are four options of different sizes and shapes for the piezo patch that was considered in this study and the options are shown in Table 3.2. The model for both shapes (rectangular and circle shape) used in the simulation is illustrated

in Figure 3.3. The piezo beam was located on top of the sponges (polyethylene material) as the stand. The sponges were set to be linear elastic material.

Table 3.1: Piezoelectric properties

	Density, ρ (g/cm ³)	Relative permittivity, ϵ_{33}/ϵ_0	Strain coefficient, d (pC/N)
PVDF	1.78	12	$\begin{bmatrix} 0 & 0 & 0 & 0 & 23 & 0 \\ 0 & 0 & 0 & 27 & 0 & 0 \\ -21 & -2.3 & 26 & 0 & 0 & 0 \end{bmatrix}$

Source: (Ueberschlag, 2001)

Table 3.2: Size and shape of the piezo patches used for the simulation.

Option #	SHAPE	SIZE
Opt 1	Round	Diameter - 15 mm
Opt 2		Diameter- 25 mm
Opt 3	Rectangular	Width \times Length – 50 mm \times 30 mm
Opt 4		Width \times Length – 30 mm \times 20 mm

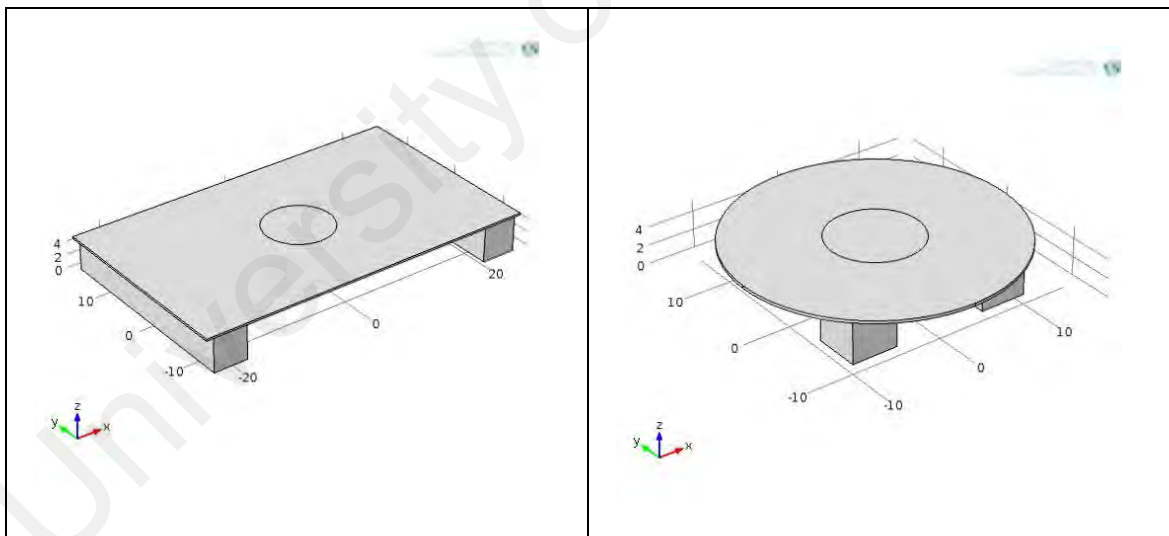


Figure 3.3: Model in COMSOL. Left: Model for rectangle shape patch. Right: Model for circle shape patch.

As investigated by Hing & Mun (2005), the input signal given to the beam is in terms of pressure function exerted on two muscles; Bicep Femoris (BF) and Rectus Femoris (RF), with respect to the gait sub-phase (Initial Contact (IC), Foot Flat (FF), Push Off (PO), Toe Off (TO), and Terminal Swing (TS). The pressure value of Bicep Femoris and

Rectus Femoris for the gait events is presented in Table 3.3. The simulation was run for both input functions (BF and RF) in *Time Dependent Study Mode*.

Table 3.3: The pressure input used for the simulation study

Gait Phase	Pressure	
	Bicep Femoris	Rectus Femoris
IC	25 kPa	90 kPa
FF	210 kPa	250 kPa
PO	70 kPa	180 kPa
TO	10 kPa	60 kPa
TS	45 kPa	100 kPa

3.3.2 Piezoelectric sensors mounting configuration

The piezo sensor can be regarded as a beam. There are multiple ways of mounting a beam to a structure and the stress and strain response is different from one another. This is due to the boundary conditions, which play an important role in determining the response, are different from one mounting method to another. Among the popular methods are ‘simply supported’, ‘fixed end’, continuous, and cantilever (Gere, 2004).

For this application, the cantilever beam configuration was chosen due to its ability to produce higher strain for a given input force (Roundy et al., 2005). The cantilever beam is a configuration that is fixed on one end and free on the other end of the beam (Gere, 2004). The elastic foundation (Figure 3.4) was added to the cantilever configuration to enhance the stability of the sensor’s reading as it would be placed in a tight and closed area (in the socket).

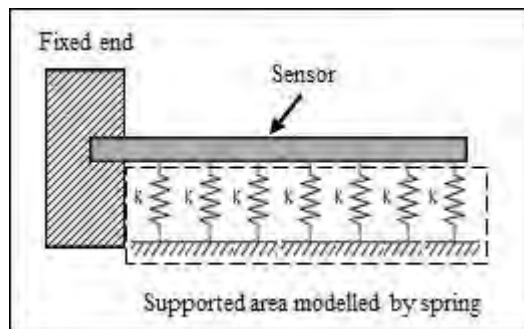


Figure 3.4: Illustration of the cantilever with elastic foundation beam configuration.

To determine the optimal cantilever with elastic foundation configuration for each piezo sensor, bench experiment was performed on the PVDF piezo sensor. In total, four configurations were tested (Figure 3.5). These configurations were classified into two main categories, which were:

- a) Cushion all (CA) configuration – the remaining unfixed area was supported
- b) Cushion end (CE) configuration – only one end of the sensor was supported

One end was fixed onto a hard material named *Pelite* material that is usually used as a liner in the prosthetic, while *Plastazote foam* (commonly used as insoles in the prosthetic leg) were used to provide the elastic support on the other end. For each category, two different sizes of supporting cushion were tested. One was cut to fit exactly the free end area size (FIT) and the other side was bigger (extra ~2 mm for every side) than the sensor size (XTRA).

In order to imitate the real input force, two different types of external force input were applied using the Integrated Electronic Piezoelectric, IEPE-based impact hammer. They were:

- 1) Knock – no initial contact, swing the hammer on the sensor and release
- 2) Push – initial contact, push the hammer on the sensor and back to initial position

Three force points were marked on the sensor with 10 mm apart. The data collection process was done in two phases. First, the force was applied on one point repeatedly (i.e. 50 trials) and the responses were analysed. Second, the force was applied to all three points in one trial (i.e. repeated for 20 times) and the response was analysed. The input force reading and the voltage signal from the sensor were recorded using a 24-bit, 100 kHz DAQ card (NI USB-4431, National Instrument).

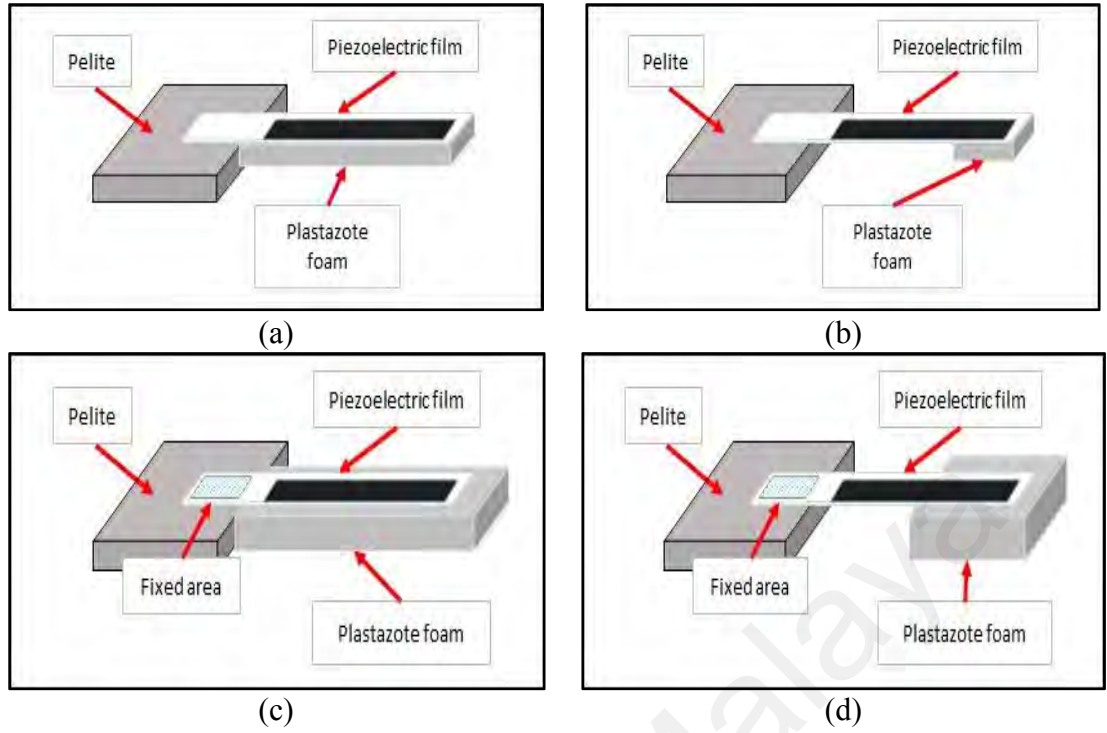
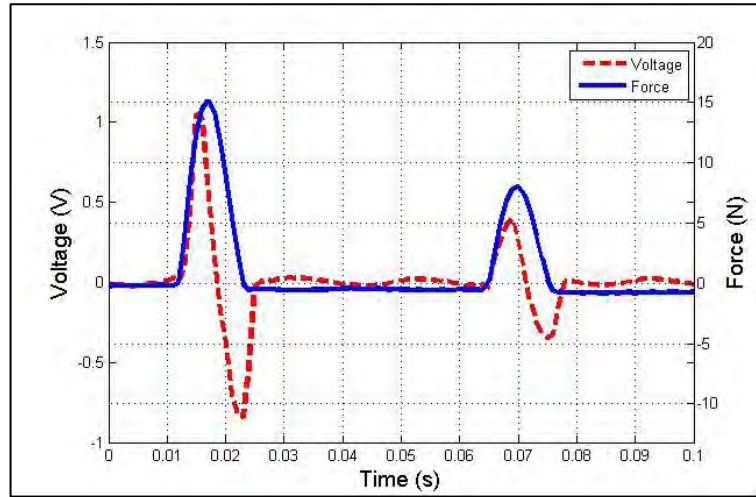
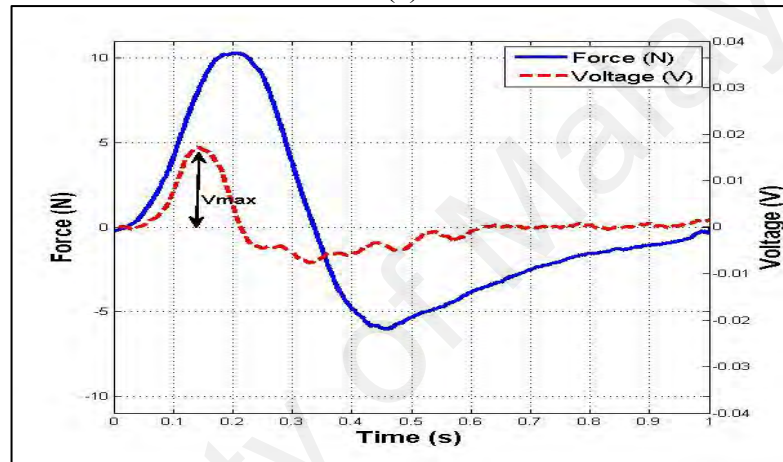


Figure 3.5: The test configurations. (a) Cushion-All Fit (CA FIT). (b) Cushion End Fit (CE FIT). (c) Cushion All Extra (CA XTRA). (d) Cushion End Extra (CE XTRA).

The sample of the sensor responses with respect to different input force patterns was illustrated in Figure 3.6(a) and Figure 3.6(b). For knock force response, the peak-to-peak voltage (V_{p-p}) for every trial was recorded, while for push force response, the maximum voltage was recorded. The sensor's performance was checked for its repeatability, linearity and sensitivity. For repeatability, the average Mean Squared Error (MSE) was calculated. Configuration with the smallest MSE was selected as the most repeatable one. The R^2 and p-value of the output vs input graph were used to determine the linearity of the sensor. Finally, a configuration with the highest mean value of the Voltage (V) / Force (N) indicates the best configuration in terms of sensitivity. The performance of the sensor using these four configurations (CA FIT, CE FIT, CA XTRA and CE XTRA) were compared and discussed in section 3.4.2.



(a)



(b)

Figure 3.6: Sensor's response for knock and push input using CA FIT configuration. (a) Knock input force and sensor's response (voltage). (b) Push input force and sensor's response (voltage).

3.3.3 Sensors placement

The piezo sensors were intended to detect the changes in the muscles contraction level or force. Thus, the location to place the sensors are very critical to ensure its best performance. The best location should be at the most active area, defined as the biggest change in the pressure from rest to active, measured at the skin surface. For this purpose, the quadriceps and hamstring muscle groups were selected because these two are the biggest muscle groups above the knee area and they are located close to the skin surface hence can be measured easily.

To identify the area of the quadriceps and hamstring muscle groups that could manifest the maximum activity, the F-Socket sensor (Tekscan, Inc., USA) as illustrated in Figure 3.7 was used. The patch consisted of 16 rows and 4 columns cells of sensors. A TF amputee with basic to normal mobility (K3-level based on US Health Care Financing Administration's, HCFA classification) was recruited for this experiment. The sensor sheet was located on the amputee's muscle and pressure data was recorded during two conditions. The first baseline pressure was at rest (no muscle contraction) and the second condition was when the patient performed Maximum Voluntary Contraction (MVC). For the second condition, the participant was asked to perform flexion (for quadriceps) and extension (for hamstring), while the motion was resisted by applying force on the stump against the movement to maintain it in the rest position. The pressure readings for both conditions were recorded using the Tekscan software for 5 seconds (500 frames). The experiment was repeated for 5 times for each routine.

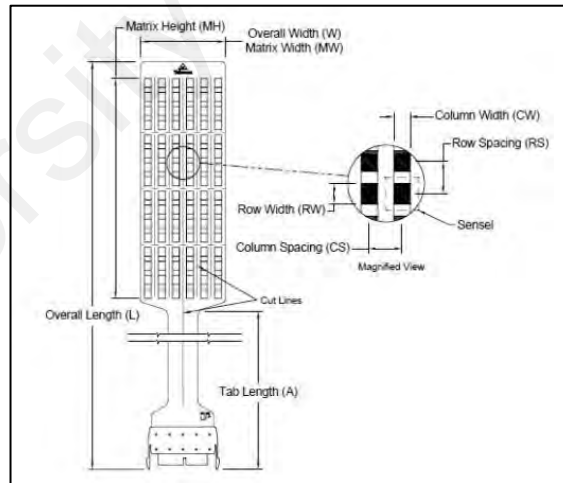


Figure 3.7. F-Scan sensor (Tekscan, Inc., USA) (Tekscan Inc.).

For analysis purposes, the sensor was divided into smaller boxes based on the pressure distribution seen in the MVC condition at $t=0$. Figure 3.8 illustrates the allocation of the boxes for quadriceps (left) and hamstring (right). Based on the pressure distribution seen during the mock trials, the quadriceps region was divided into 11 boxes (Box 1 – Box 11) since the pressure difference could be observed in a smaller area. On the other hand, the

pressure distribution for the hamstring seems to be more uniformed, thus, only 3 boxes were used for the analysis (Box A, Box B and Box C).

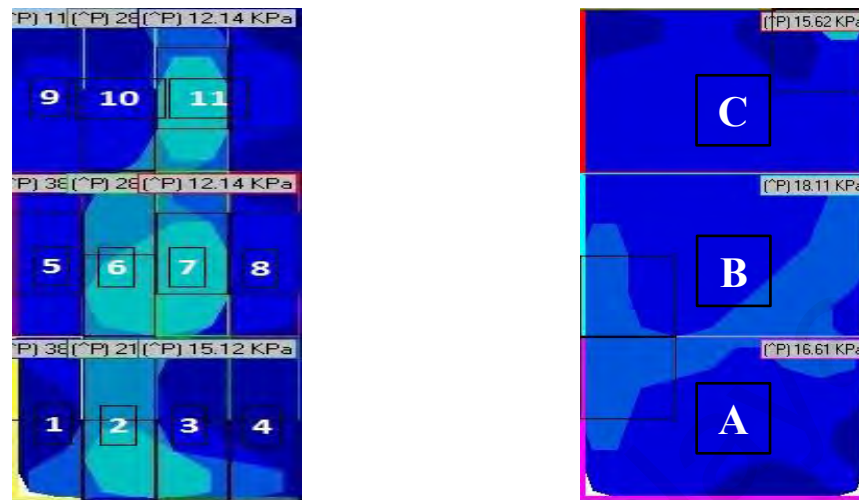
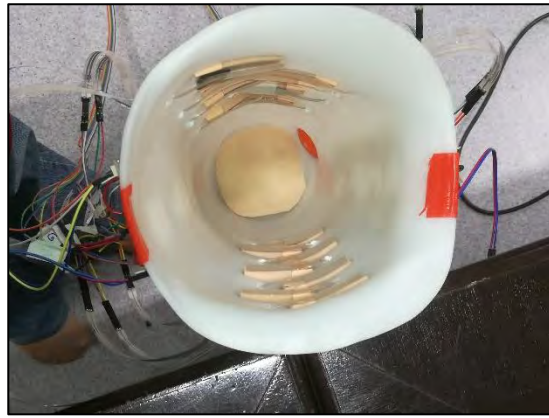


Figure 3.8: Box allocation on the Tekscan sensor area for analysis purposes. Left: Quadriceps, Right: Hamstring.

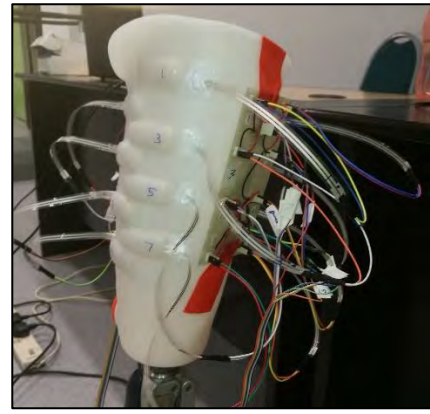
To identify the most active area of the muscle, the difference of the average pressure readings (area under the curve of pressure vs time graph) between MVC and the baseline for 5 trials was calculated. The box that read the highest average pressure difference was identified as the most active area of the muscle and was considered as the targeted position to place the sensors. The results were presented in section 3.4.3.

3.3.4 Gait experiment

Based on the findings presented in section 3.4.1, 3.4.2, and 3.4.3, a socket instrumented with 15 piezoelectric sensors was fabricated (Figure 3.9). The socket was ensured to be in good fit with the user's stump to eliminate external factors that might affect the sensors' response. It was evaluated for its response consistency. The voltage measurements for all sensors were acquired using 2 8-channels DAQ cards; NI 9221 (National Instruments, USA). All sensors were wired to NI-9221 DAQ Card. The sampling rate for both DAQ cards was set to be 1 kHz. The specifications for both DAQ cards are tabulated in Table 3.4.



(a)



(b)

Figure 3.9: Fabricated socket with instrumented in-socket sensor. (a) interior view, (b) exterior view.

Table 3.4: DAQ CARD SPECIFICATION (National Instruments Corporation, 2015).

	NI-9221
Signal ranges	± 60 V
Channels Number	8 single-ended
Sample Rate	800 kS/s
Resolution	12-bit

Since the objective of the experiment was to evaluate the in-socket sensory design, the recruitment of a single subject was deemed sufficient. The same amputee was recruited for the sensors' placement experiment and for the gait trial. The subject was asked to walk at his normal speed on 5 meters levelled, i.e. no slope, pathway. A switch was placed on the pathway to synchronize the starting point of all data collection. Five complete trials were recorded for further processing.

The piezo signals were low-pass-filtered at 10 Hz passing frequency as the muscle activation and deactivations happen at lower frequencies (up to 10 Hz) (Prendergast, Helm, & Duda, 2005). The filtered signal is illustrated in Figure 3.10. One trial consists of more than 1 cycle of walking gait (multiple steps). It could be observed that the signal in Figure 3.10 consists of a repeated pattern. Since the parameter of interest is the consistency of the signals, data from one cycle of multiple trials were used for the analysis.

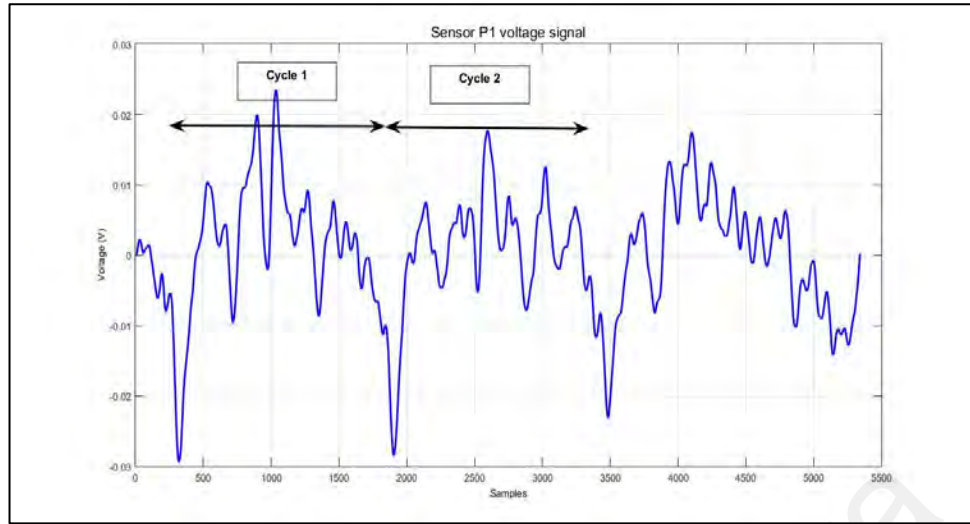


Figure 3.10: Output voltage signal of Sensor P1 for 1 trial.

The consistency of the signals across the 5 trials was determined by the correlation value, while the normalised cross-correlation value was calculated to determine the output signal pattern consistency for every trial. The results of all sensors are presented in section 3.4.4.

3.4 Results and Discussion

In this section, the results for this study and discussion on the findings are presented.

3.4.1 Simulation results to determine piezoelectric properties

Table 3.5 displays the output voltage yielded from different sizes and shapes of the piezo patch for one gait cycle of the bicep femoris pressure and Figure 3.11 illustrates the pattern. Meanwhile, Table 3.6 and Figure 3.12 show the output voltage for rectus femoris.

Table 3.5: Tabulated results for voltage output (V) of different shapes and sizes for the bicep femoris input.

Gait Phase	Pressure (kPa)	Round 15 mm	Round 25 mm	Rectangular 50x30	Rectangular 30x20
IC	25 kPa	0.006	0.083	0.178	0.164
FF	210 kPa	0.05	0.207	1.269	1.4
PO	70 kPa	0.017	0.151	0.438	0.465
TO	10 kPa	0.002	0.055	0.079	0.065
TS	45 kPa	0.011	0.084	0.28	0.299

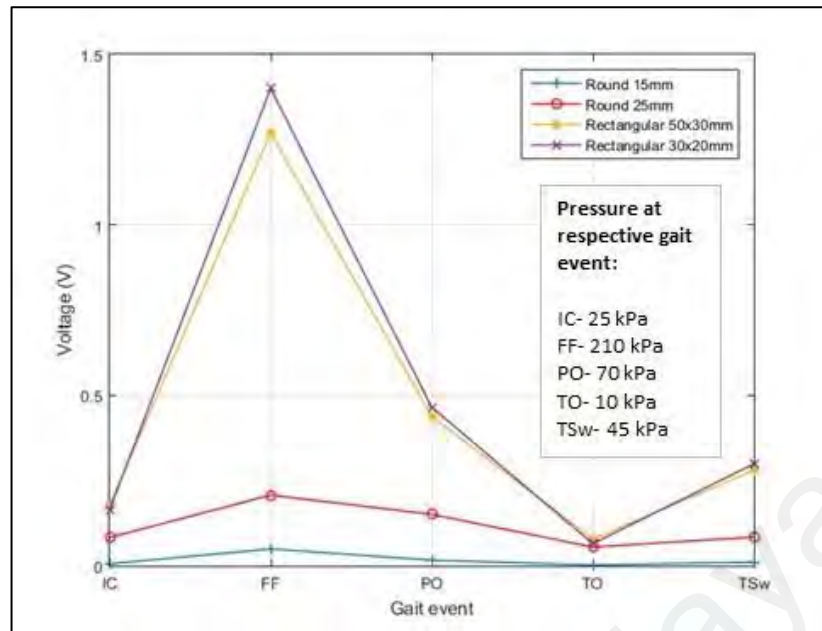


Figure 3.11: Results for simulation of different shape and size for the bicep femoris input.

Table 3.6: Tabulated results for voltage output (V) for different shapes and sizes for rectus femoris input.

Gait Phase	Pressure (kPa)	Round 15 mm	Round 25 mm	Rectangular 50x30	Rectangular 30x20
IC	90 kPa	0.022	0.083	0.641	0.591
FF	250 kPa	0.059	0.207	1.582	1.66
PO	180 kPa	0.043	0.151	1.153	1.194
TO	60 kPa	0.014	0.055	0.425	0.395
TS	100 kPa	0.024	0.084	0.643	0.663

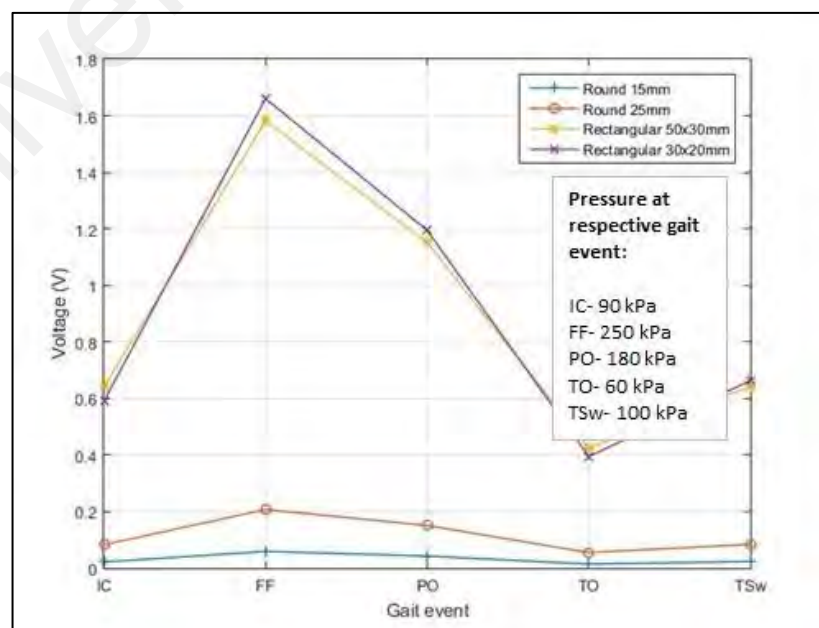


Figure 3.12: Results for simulation of different shape and size for rectus femoris input.

The findings from both studies (BF and RF input) suggested that the rectangular shape produced a higher amplitude voltage compared to the round shape. Comparing the piezo patch performance of the different shapes, it can be observed that during foot flat (produces the highest pressure to the muscle), the rectangular shape (size 50x30) produces ~6 times higher than the circle patch (diameter 25 mm). Figure 3.11 and Figure 3.12 also show that the voltage of both sizes of the rectangular shape patch is consistently giving higher output compared to the circular patch across the gait cycle. Furthermore, it can also be observed that the patch's size reduction of the circular patch gave a bigger impact to the piezo output voltage compared to the rectangular patch. The performance of the rectangular shape is more consistent even with a reduced size. From the findings, it can be deduced that a rectangular shape patch should be used. As for the size, since the impact of the size to the performance was not significant, the smaller patch was selected for this application. This was because with a number of smaller patches, the sensory system could better capture the force or pressure profile at different parts of the muscles.

Hence, a rectangular with smaller piezo sensors should be used in this in-socket sensory system. The piezofilm by Measurement Specialties, model FLDT 1-028K (Figure 3.13) that fits the desired criteria for this application was chosen.



Figure 3.13: Piezofilm sensor by Measurement Specialties (Measurement Specialties).

3.4.2 Mounting configuration method experiment

Table 3.7 presents the repeatability, linearity, and sensitivity of each tested configuration.

Table 3.7: Signal parameters of the mounting configuration experiment

Parameter	Input Force Type	CA		CE	
		Fit	Xtra	Fit	Xtra
Repeatability	Knock (MSE)	5.14E ⁻³	1.53E ⁻²	0.021	0.071
	Push (MSE)	1.09E ⁻⁵	1.17E ⁻⁵	3.2E ⁻⁵	1.85E ⁻⁵
Linearity	Knock (R2, p-value)	0.762, 1.66E ⁻¹³	0.476, 8.74E ⁻¹¹	0.372, 3.4E ⁻⁰⁸	0.544, 1.78E ⁻¹¹
	Push (R2, p-value)	0.11, 5.5E ⁻³	0.034, 0.257	0.031, 0.222	9.55E ⁻³ , 0.454
Sensitivity	Knock (mean±SD)	0.13 ± 0.012	0.13 ± 0.019	0.16 ± 0.036	0.14 ± 0.027
	Push (mean±SD)	3.15E-3 ± 8.39E ⁻⁴	1.95E-3 ± 2.99E ⁻⁴	4.76E-3 ± 8.57E ⁻⁴	4.32E-3 ± 9.56E ⁻⁴

The results showed that CA FIT configuration gives the least MSE value and highest R² value with the least p-value for both input types, which suggested that it had the most acceptable repeatability and linearity. In CA FIT configuration, the support was evenly distributed to the free end of the piezo sensor. Thus, the energy was also uniformly spread, which made the reading more consistent between the three points. On the other hand, CE FIT configuration gives the highest mean value of V/N that implied the highest sensitivity. Compared to the other configurations, CE FIT offered the smallest area of support to the free end of the sensor. The damping effect to the system was relatively small, thus, the energy lost due to the damping effect was also small. Hence, for the same amount of input force, CE FIT configuration causes the sensor to produce higher voltage.

Based on the findings of this exercise, the CA FIT mounting configuration was chosen to be adopted in the in-socket sensory system design. Although it did not give the best results for the sensitivity parameter, the advantage it had for repeatability and linearity outweighed the disadvantage because it is more important to ensure good performance of

the overall system. Figure 3.14 shows the CA FIT configuration that was adopted in the design.

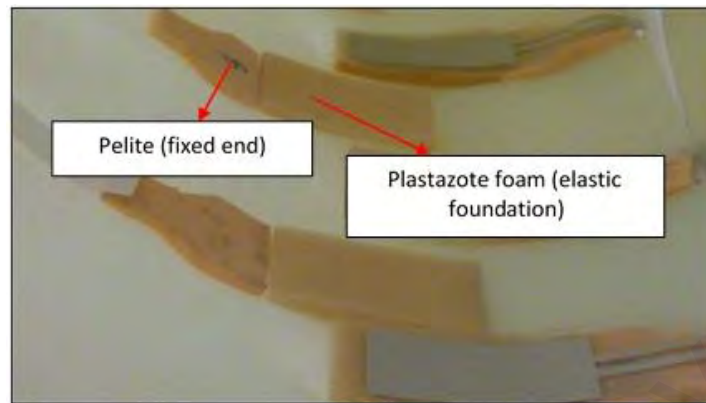


Figure 3.14: The mounting configuration adopted in the design.

3.4.3 Sensors placement orientation experiment

Table 3.8 shows the calculated value of the difference between MVC and the baseline average pressure for quadriceps and Table 3.9 are the results for the hamstring muscle group.

Table 3.8: Average pressure difference (kPa) of 5 trials for quadriceps muscle group

Box	Pressure (kPa)
1	12.03
2	18.4
3	11.20
4	5.07
5	9.74
6	18.40
7	9.99
8	5.12
9	4.72
10	5.17
11	10.00

Table 3.9: Average pressure difference of 5 trials (kPa) for hamstring muscle group

Box	A	B	C
Pressure (kPa)	8.60	8.09	6.45

Table 3.8 illustrates that Box 2 and 6 produced the highest average pressure of 18.41 kPa and 18.40 kPa, respectively, suggesting that these areas are the most active muscle in the quadriceps muscle, which is also known as the muscle belly. Whereas, Box 4 (5.07 kPa), 8 (5.12 kPa), 9 (4.72 kPa) and 10 (5.17 kPa) show the area with lowest average pressure readings. The rest of the locations produced moderate value. From the findings, it can be concluded that the active area of the quadriceps muscle of the amputee was located on the left and bottom area.

For the hamstring muscle group, the result in Table 3.9 shows that the area with high pressure readings was in the A and B box, which was located at the bottom area of the F-Socket sensor with the pressure of 8.60 kPa and 8.09 kPa, respectively.

Based on the results of this experiment, the placement of the piezo sensors was determined. A total of 15 piezo sensors were used in an array setting with 8 sensors placed on the anterior socket wall (quadriceps) and the other 7 were placed on the posterior area (hamstring). The sensors were arranged in a zig-zag orientation so that the deflection resulting from the muscle contraction by most of the identified area can be detected through the normal application of force onto the sensors (Figure 3.15). The fabricated socket and assembled prosthetic leg are shown in Figure 3.9.

The muscle assessment was a necessary process for the amputee because the area of one most active muscle area is different than of another amputee's. Therefore, to ensure that the sensors are in the right place, each user must undergo this process. However, it is just a one-time process, to be conducted before the socket fabrication.

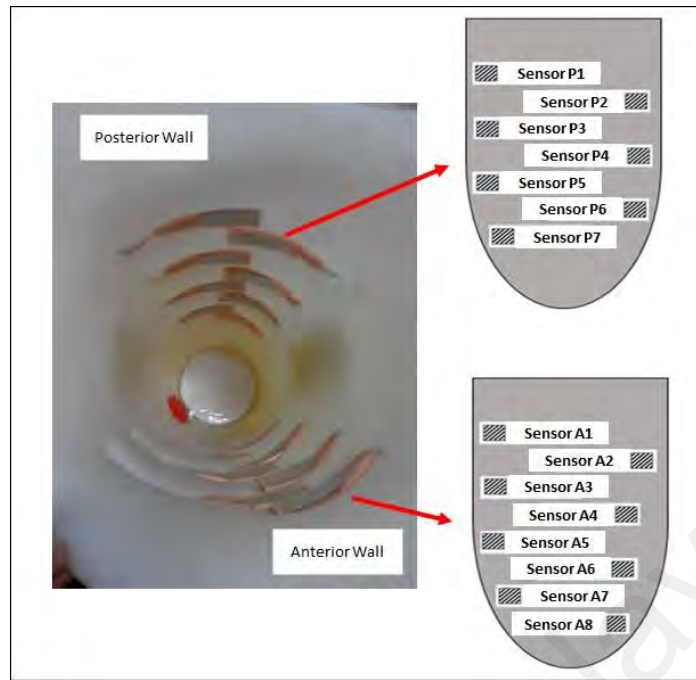


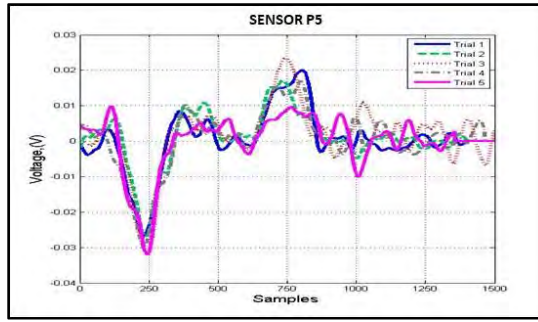
Figure 3.15: Piezo sensors placement for in-socket sensory system.

3.4.4 Results for consistency study of the sensors' output signal

Figure 3.16 shows an output signal from one piezo sensor (Sensor P5) and its corresponding correlation values, r , for 5 trials. To compare the performance of the individual sensors, the norm of the correlation matrix was calculated. Frobenius norm value was used to represent the strength of the correlation matrix of each sensor. The formula to calculate Frobenius norm of a $m \times n$ matrix is shown in Eq. (3.1). Since the maximum r -value is 1 which means the signals are similar to each other, the best norm value that the correlation can achieve is 5 (considering all r -values in the matrix was 1). Hence, in this study, the closer the norm value was to 5, the more consistent the sensor was.

$$\|A\|_F = \sqrt{\sum_{i=1}^m \left(\sum_{j=1}^n |A_{ij}|^2 \right)} \quad (3.1)$$

The calculated norm value of the correlation matrix and the minimum r -value in that matrix are presented in Table 3.10 for sensors located on the anterior part (Sensor A1 – Sensor A8) of the socket and Table 3.11 for the posterior part of the socket (Sensor P1- Sensor P7).



(a)

	1	2	3	4	5
1	1	0.88	0.88	0.89	0.84
2		1	0.88	0.89	0.86
3			1	0.87	0.77
4				1	0.83
5					1

(b)

Figure 3.16: Output signal and the correlation table of 5 trials, Sensor P5.

3.4.4.1 Quadriceps

All sensors produced high norm values ($\|A\|_F > 4.5$) and high correlation value for all 5 trials ($r > 0.8$) that suggested the output signal's pattern for all 5 trials were consistent with each other. The findings lead to a conclusion that all 8 sensors in the anterior area were working efficiently in the designated position and mounting configuration to detect pressure or force changes of the muscles while the patient was walking, regardless of the varying walking speed the amputee used in every trial.

Table 3.10: The minimum R-value in the correlation table and the norm value for Sensor A1- Sensor A8

SENSOR	MIN R-VALUE	NORM VALUE ($\ A\ _F$)
A1	0.915	4.82
A2	0.928	4.84
A3	0.884	4.72
A4	0.919	4.83
A5	0.916	4.80
A6	0.913	4.80
A7	0.913	4.81
A8	0.900	4.75

3.4.4.2 Hamstring

Table 3.11 tabulates the minimum R-value and the norm value for all posterior sensors (i.e. P1 to P7).

Table 3.11: The minimum R-value in the correlation table and the norm value for Sensor P1 - Sensor P7

SENSOR	MIN R-VALUE	NORM VALUE ($\ A\ _F$)
P1	0.700	4.28
P2	0.774	4.54
P3	0.762	4.44
P4	0.838	4.60
P5	0.773	4.45
P6	0.446	4.02
P7	0.718	4.14

The results revealed that except for Sensor P1, Sensor P6 and Sensor P7, other sensors gave good norm value, which is above 4.4. Sensor P1, P4 and P7 displayed low consistency value for most of the trials (lowest r-value is 0.446).

In Figure 3.15, Sensor P1 is the most top sensor, while Sensor P6 and P7 were located at the two most bottom locations of the hamstring sensors orientation. This implies to the conclusion that the most top sensor and the 2 most bottom ones did not perform very well in terms of signals consistency. This was probably because the contact between the stump and the sensors were not strong enough to generate a strong signal. The intermittent contact between the muscle and the sensors affected the consistency of the signal. Another reason could be that the top and the bottom muscle of this amputee subject was not strong enough to generate a consistent signal for every trial.

In order to work best as the in-socket sensory system to control the TF prosthetic leg powered knee, the pattern of the piezo sensors' output signals must be consistent for further processing; which is the classification phase. Thus, even if the pattern is a combination of shear and normal pressure, it was assumed to be the representative of the movement and would be valid for further processing.

The consistent output signals by the sensors implied the efficacy of the sensory system to be used as the control input for the powered prosthetic knee. As compared to the work done by El-Sayed et al. (2014), the resolution of the sensory system proposed in this work

was higher. The in-socket sensory-system proposed by El-Sayed utilized 3 piezo sensors with bigger size (Length×Width×Thickness: 61mm×31mm×0.51mm) to cover the anterior and posterior side of the socket. On the other hand, this work developed the in-socket sensory system with a total of 15 sensors with a smaller size (30mm×16mm×0.028mm). Hence, the resolution of the sensory system in this work is higher. Other than that, the sensors used in this work were thinner and more flexible because the material used was of PVDF-type instead of ceramic-type, which was used in El-Sayed's work.

Comparing the piezo-based sensory system with EMG-based, this proposed system has the advantage of providing the mechanical information (Ground reaction force (GRF)) that can eventually be used to derive the gait phase data, while EMG essentially only provides muscle activity. Furthermore, this proposed system enables easier donning process as the piezo sensor does not require tedious preparation, including electrode attachment on the skin before acquiring the data. However, EMG, which has been researched on for a longer time as a method to control active prosthetic, was proven to be able to produce reliable signals because it reads the electrical signal from the muscle. For the same reason, it has been successfully reported to detect the intention of the prosthetic's user (Wentink et al., 2014).

3.5 Summary

Based on the analysis conducted in this study, it was proven that the cantilever with elastic foundation CA FIT mounting configuration and zig-zag orientation yielded the best results in terms of repeatability, sensitivity and linearity. A socket with the instrumented in-socket sensory system was fabricated and tested on one unilateral subject and the consistency in the sensors' response was evaluated across multiple trials. The high norm value that was calculated for each sensor suggested that the in-socket sensory

system for TF prosthetic leg, which utilised piezo sensors could produce a consistent and reliable output signal with good sensitivity.

The findings of this study have been published in Journal 1 in the list of publication and a patent has been filed (PI Application Number: PI 2017702344) for the in-socket sensory system designed as illustrated in Figure 3.9. A certificate of patent filing application is attached in the Appendix A. Further trials are required to determine the signal performance in other locomotion settings.

University of Malaya

CHAPTER 4: ANALYSIS OF PIEZOELECTRIC-BASED IN-SOCKET SENSORY SYSTEM RESPONSE AS A GAIT DETECTION TOOL: A FEASIBILITY STUDY

4.1 Introduction

This study aims to test the feasibility of a piezoelectric-based in-socket sensory system as a gait detection tool. In order to do so, the relationship between the sensory system's responses and the kinematic and kinetic properties of the prosthetic leg during gait was studied.

4.2 Literature review

Gait analysis is a branch of study to analyse human locomotion. The outcome of gait analysis includes gait phase detection, human gait kinetics and kinematics parameters identification, and evaluation of human musculoskeletal functions. There are various approaches that were used in collecting gait data for the analysis. Among the popular methods is via camera system (Carse, Meadows, Bowers, & Rowe, 2013; Ganesan, Fong, Luximon, & Al-Jumaily, 2016; Jasni, Hamzaid, Mohd Syah, Chung, & Abu Osman, 2017; Pfister, West, Bronner, & Noah, 2014; Prakash, Mittal, Kumar, & Mittal, 2015; Ye, Yang, Stankovic, Stankovic, & Kerr, 2015). Camera or vision system typically is set up in the lab, in which the camera system is connected to a program that analyses the video captured by the camera. The gait parameters are retrieved from the video analysis. One of the gait analysis tool that use camera system is Vicon Motion Capture System (Vicon, UK). A study conducted by Jasni et al. (2017) which utilized Vicon Motion System to collect gait data from normal, TF and TT prosthetic users and orthosis users and analysed the parameters using a method called cyclogram to determine the gait disparity level of the groups as compared to normal group. Cyclogram can be defined as cyclic trajectories that combined any two of kinetic and kinematic parameters in one plot, without their respective time trajectory (Goswami, 1998). In the study, multiple cyclogram sets were

created for all four categories of the subjects; able-bodied, TF and TT prosthesis users, and orthosis users. The cyclograms of TF and TT prosthesis users and orthosis users were compared to the able-bodied cyclograms to evaluate their gait disparity. The closer the cyclograms are to the normal, the lesser the gait disparity is. Table 4.1 shows the percentage of closeness-to-normal-curve. From Table 4.1, it can be observed that TF prosthesis users obtained the lowest percentage, which indicates the gait performance of this group is the poorest in comparison to TT prosthesis and orthosis users.

Table 4.1: Percentage range of closeness to the normal curve

Subjects	No. of subjects	Percentage range
Orthosis	10	75–87%
TT prosthesis	10	73–81%
TF prosthesis	5	68–79%

Source: (Jasni et al., 2017)

The advantage of this system is in its precision and accuracy, because the data is collected in a controlled environment. However, it can also be a drawback in terms of its practicality and the ability to represent the real-life environment (walking on uneven surfaces, outdoor terrain, mountain climbing and others). Moreover, the allowable distance for data collection is very restricted.

In addition to the vision system, other method of gait analysis is by using sensors instrumented on the floor or also known as floor sensors (Agrawal, Thomassey, Cochrane, Lemort, & Koncar, 2017; Costilla-Reyes, Scully, & Ozanyan, 2015; LeMoyne, Kerr, Mastroianni, & Hessel, 2014; Muheidat & Tyrer, 2017; Serra, Croce, Peres, & Knittel, 2014) and wearable sensors (Levi J Hargrove, Simon, Lipschutz, Finucane, & Kuiken, 2013; L. J. Hargrove, Young, Simon, & et al., 2015; H. Huang et al., 2011; Novak et al., 2013; Takeda et al., 2009). These methods are usually used to retrieve parameters related to GRF, which could not be extracted using the vision system. Nonetheless, it carries the same drawback that the vision system possesses, which is its impracticality, failure to represent the real environment setup and restricted distance for data collection.

Wearable sensors method is becoming a favourite option recently for its advantage over the camera system and floor sensors approach. They are cheaper and are more practical to be adopted outside the laboratory setting with greater movement distance and are open to more natural setting (Pete B. Shull, Jirattigalachote, Hunt, Cutkosky, & Delp, 2014). Wearable sensors are sensors that are placed or attached on the subjects' body parts (waist, foot, and knee) to acquire gait parameters, such as the position, force and moment, acceleration and others.

Tao (2012) stated that there are three methods to perform gait analysis using wearable sensors, which are electromyography method, gait kinetics based method, and gait kinematics based method. One of the most favourable methods is using electromyography (EMG) sensor. EMG is a method of recording and evaluating the electrical activity produced by the skeletal muscle (Jamal, 2012). The movement of a human body is a coordination of muscles and the brain. When a human intends to move, the brain sends an excitation signal to the muscles through the Central Nervous System (CNS). The communication between the brain and the respected muscles creates electrical signal known as 'Motor Unit Action Potential' (MUAP) and when the activation continues, MUAP trains is produced. The EMG sensor captures this MUAP trains as its input signal can be used to identify muscles activity (Jamal, 2012). A number of studies had proposed the use of the EMG sensor to acquire data for gait analysis (Bogey & Barnes, 2017; S. W. Lee, Yi, Jung, & Bien, 2017; Ryu, Lee, & Kim, 2017). Although it is proven to be accurate, EMG method requires careful preparation on the skin. In some application, such as for the gait phase detection for active prosthesis control, this drawback limits the practicality of the whole system in which it complicates the donning process of the prosthetic device.

On the other hand, the other options of the wearable sensors are gait kinematics and kinetics-based method. Winter (1991) defined gait kinematics as '*the spatial movement*

of the body without considering the forces that cause movement'. The gait kinematics parameters include linear and angular displacements, velocities, and accelerations.

The accelerometer is one of the popular sensor used to retrieve the inertial acceleration of the leg (Goršič et al., 2014; Xu, Liu, Hu, & Zhang, 2016). Gyrometer or gyroscope is a device to measure the angular velocity of a mass. This device is also a favourite sensor in gait analysis (Cannan & Hu, 2013; P. B. Shull, Xu, Yu, & Zhu, 2017)

Kinetics, as defined by Winter (1991) is *'the analyses that investigate the forces, energies, and power of the body movement'*. Gait kinetics parameters are ground reaction forces, joint reaction forces, moments of forces, tendon forces, joint contact forces, power, work, and energies. The reaction forces can be defined as the resultant force exerting on or at any point in the skeletal system. The internal reaction force at any point is the resultant of all internal and external forces acting on or at that point at static, described in (4.1) or dynamic, expressed in (4.2), equilibrium state.

$$\Sigma F = 0 \quad (4.1)$$

$$\Sigma F = ma \quad (4.2)$$

Most of the literature on kinetics analysis proposed the use of shoe insoles to retrieve the ground reaction force of the leg (Du, Zhu, & Zhe, 2015; Giovanelli et al., 2014; Howell, Kobayashi, Hayes, Foreman, & Bamberg, 2013; Kanitthika & Chan, 2014). However, some research proposed the utilization of air pressure sensor (Ishikawa, Hayami, & Murakami, 2017) and strain gauges (Arami, Aminian, Forchelet, & Renaud, 2014).

The prosthetic leg control is one of the areas that applies gait analysis. The gait analysis method was applied to identify the activity, locomotion mode or gait phase that the amputee is currently on and feed the information to the controller of the prosthesis (Fey, Simon, Young, & Hargrove, 2014; Lawson, Varol, Huff, Erdemir, & Goldfarb, 2013; Shultz et al., 2016).

In this research, the feasibility of the in-socket sensory system, as proposed in chapter 3 and presented in an earlier study by the author (Jasni et al., 2016), in detecting

transfemoral amputee gait was investigated. The in-socket sensory system consisted of 15 piezoelectric sensors, which were placed on the TF socket inner wall. One unilateral TF amputee subject participated in this experiment. Data from the sensory system and the ground reaction force data from the force plates were collected and analysed to investigate the feasibility of the proposed sensory system detecting walking gait.

4.3 Mathematical modelling of the relationship between the in-socket sensory system and forces on the stump

This section presents the derivation of the mathematical relationship between the piezoelectric sensors and the input forces.

4.3.1 Piezoelectric as a dynamic force sensor

Piezoelectric is a device that has an electromechanical feature that can convert electrical to mechanical energy and vice versa. The electromechanical attribute can be described mathematically by using the constitutive equations. The general expression of the constitutive equation (Moheimani & Fleming, 2006) is:

$$\varepsilon_i = S_{ij}^E \sigma_j + d_{mi} E_m \quad (4.3)$$

$$D_m = d_{mi} \sigma_i + \xi_{ik}^{\sigma} E_k \quad (4.4)$$

where i and j is a number from 1 to 6, while m and k is a number from 1 to 3, respectively.

The number represents the axis of interest and it can be illustrated in Figure 4.1. The definition of each term in ((4.3) to (4.6) are presented in Table 4.2.

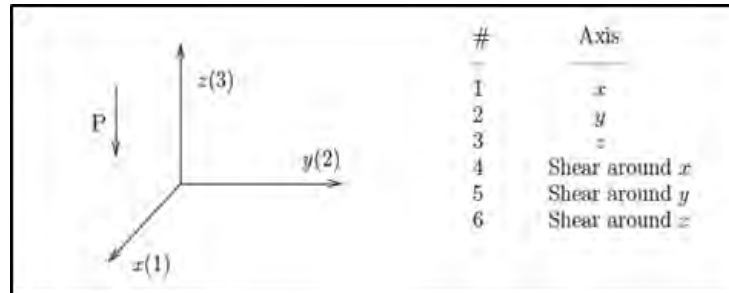


Figure 4.1: Illustration of axis assignation (Moheimani & Fleming, 2006)

Table 4.2: Definition of abbreviation in equations (1)-(8)

Term	Definition (<i>unit</i>)
ε	Strain vector (<i>m/m</i>)
\mathbf{S}	Matrix of compliance coefficients (<i>m²/N</i>)
σ	Stress vector (<i>N/m²</i>)
\mathbf{d}	Matrix of piezoelectric strain constants (<i>m/V</i>)
\mathbf{E}	Vector of applied electric field (<i>V/m</i>)
\mathbf{D}	Vector of electric displacement (<i>C/m²</i>)
ξ	Permittivity (<i>F/m</i>)
u	Strain (<i>m</i>)
t_p	Thickness of the piezo (<i>m</i>)
f	Force (<i>N</i>)
A_p	Surface area of the piezo
v	Applied voltage (<i>v</i>)
q	Charge (<i>C</i>)
Y_3^E	Short-circuit elastic moduli constant in 3-direction

For force sensor application, the state of piezo is focused only in 3-direction and if,

$S_{33} = \frac{1}{Y_3^E}$ (Leo, 2007). Thus, the equations can be written as:

$$\varepsilon_3 = \frac{1}{Y_3^E} \sigma_3 + d_{33} E_3 \quad (4.5)$$

$$D_3 = d_{33} \sigma_3 + \xi_{33}^{\sigma} E_3 \quad (4.6)$$

To derive the relationship among force, displacement, voltage and charge, we assume strain and applied electric field is uniform across the piezo thickness, while pressure and electric displacement is uniform over the piezo surface area:

$$\varepsilon_3 = \frac{u_3}{t_p}, \quad \sigma_3 = \frac{f}{A_p}, \quad E_3 = \frac{v}{t_p}, \quad D_3 = \frac{q}{A_p}, \quad k_p^E = \frac{Y_3^E A_p}{t_p} \quad (4.7)$$

Converting it to equation (4.8) and (4.9), and assume short circuit boundary condition, where $v = 0$ becomes:

$$u_3 = \frac{1}{k_p^E} f \quad (4.8)$$

$$q = d_{33} f \quad (4.9)$$

If the piezo sensor is modelled as a mass, m , with time-dependent applied force, $f(t)$ as illustrated in Figure 4.2, equation (4.10) and (4.11) can be written as:

$$u(t) = \frac{1}{k_p E} [f(t) - m\ddot{u}(t)] \quad (4.10)$$

$$q(t) = d_{33} [f(t) - m\ddot{u}(t)] \quad (4.11)$$

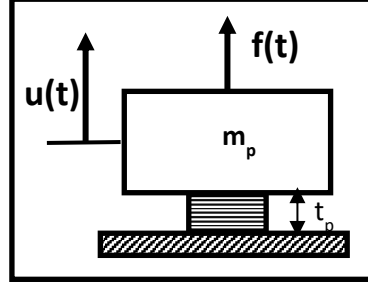


Figure 4.2: Free body diagram for piezo as dynamic force sensor

And the output voltage of the sensor can be written as:

$$v(t) = \frac{q(t)}{C_p} = \frac{d_{33}}{C_p} [f(t) - m\ddot{u}(t)] \quad (4.12)$$

where C_p is the piezo capacitance.

Re-writing the equations in a second order differential equation and transform it to Laplace representation, the transfer function to describe the relationship between strain (u), charge (q), and output voltage (v) to the input force (f) in the frequency domain can be represented by:

$$\begin{aligned} \frac{U(s)}{F(s)} &= \frac{1}{k_p E + m_p s^2} \\ \frac{Q(s)}{F(s)} &= \frac{k_p E d_{33}}{k_p E + m_p s^2} \\ \frac{V(s)}{F(s)} &= \frac{k_p E d_{33}}{C_p} \end{aligned} \quad (4.13)$$

4.3.2 Input force

The proposition of this study is there are 3 components of force that causes strain to the piezo sensor (F_{piezo}). They are the resultant mechanical force of the leg movement (F_r), the force produced by the ‘bulging’ movement of the respected muscles while

contracting (F_{muscle}) and interface stump-socket force (F_{socket}). Mathematically, it can be represented by:

$$\hat{F}_{piezo} = \hat{F}_r + \hat{F}_{muscle} + \hat{F}_{socket} \quad (4.14)$$

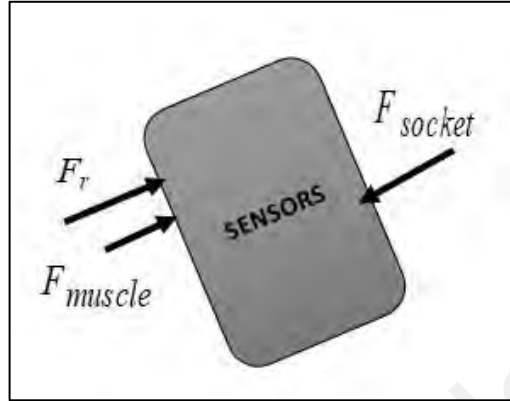


Figure 4.3: Example of free body diagram of the forces acting on one anterior sensor. Note: F_r could be in either direction depending on the body/leg position and gait phase

4.3.2.1 Reaction force from the ground

To derive the equation of F_R , the stump is modelled as a mass connected with three-bar linkages. The joints involved are the ankle, knee, and the socket joint. Meanwhile, the links represent the foot (from the ankle joint to the toe), shank (from the knee joint to the ankle joint), and thigh-socket (from the socket joint to the knee joint). The model of the leg and each link are illustrated in Figure 4.4 and Figure 4.5 below.

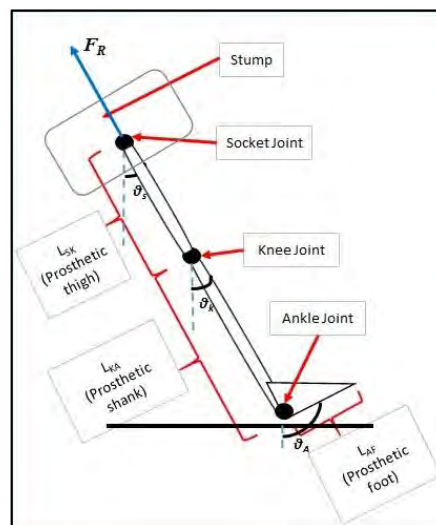


Figure 4.4: Leg model.

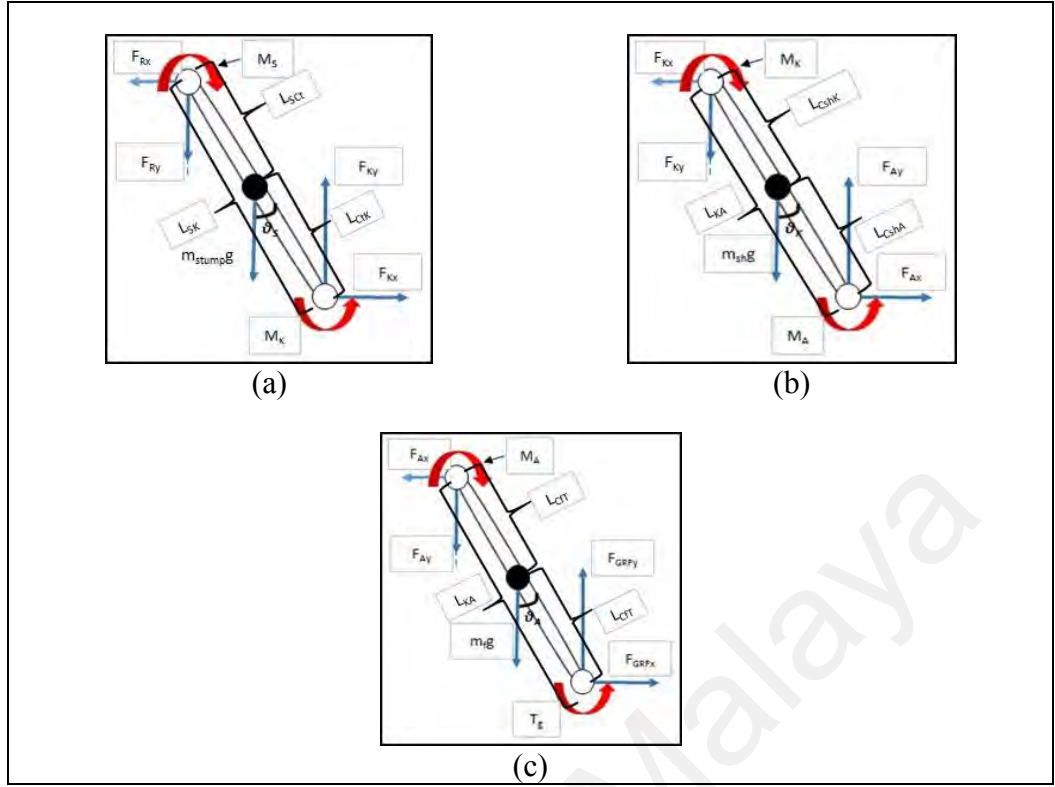


Figure 4.5: Diagram of leg model links. (a) thigh-socket link, (b) shank link, and (c) foot link.

Based on Newton's second law, the summation of the forces acting on a mass is equal to the product of mass and acceleration of the body (equation (4.2)). Thus, the displacement ($x(t)$, and $y(t)$), velocity ($\dot{x}(t)$, and $\dot{y}(t)$) and acceleration ($\ddot{x}(t)$, and $\ddot{y}(t)$) for the center of mass (COM) for all links were derived. Then, using equation (3), the reaction force of each joint was calculated. The derived F_R expression is:

$$\begin{aligned}
 \sum F_x &= m_{stump} \ddot{x}_{stump} \\
 F_{Rx} &= F_{GRFx} - \begin{bmatrix} m_f + m_{sh} + m_{st} \\ 0 \end{bmatrix} \begin{bmatrix} \ddot{x}_{st} & \ddot{y}_{st} \end{bmatrix} - \\
 &\quad \begin{bmatrix} m_f L_{SK} \cos \theta_S + m_{sh} L_{SK} \cos \theta_S + m_t L_{SCt} \cos \theta_S \\ m_f L_{KA} \cos \theta_K + m_{sh} L_{KCh} \cos \theta_K \\ m_f L_{ACf} \cos \theta_A \end{bmatrix} \begin{bmatrix} \ddot{\theta}_S & \ddot{\theta}_K & \ddot{\theta}_A \end{bmatrix} + \\
 &\quad \begin{bmatrix} m_f L_{SK} \sin \theta_S + m_{sh} L_{SK} \sin \theta_S + m_t L_{SCt} \sin \theta_S \\ m_f L_{KA} \sin \theta_K + m_{sh} L_{KCh} \sin \theta_K \\ m_f L_{ACf} \sin \theta_A \end{bmatrix} \begin{bmatrix} \dot{\theta}_S^2 & \dot{\theta}_K^2 & \dot{\theta}_A^2 \end{bmatrix}
 \end{aligned} \tag{4.15}$$

$$\begin{aligned}
\Sigma F_y &= m_{stump} \ddot{y}_{stump} \\
F_{Ry} &= F_{GRFy} - \begin{bmatrix} m_f \\ m_{sh} \\ m_{st} \end{bmatrix} g - \begin{bmatrix} 0 \\ m_f + m_{sh} + m_{st} \end{bmatrix} \begin{bmatrix} \ddot{x}_s & \ddot{y}_s \end{bmatrix} - \\
&\quad \begin{bmatrix} m_f L_{SK} \sin \theta_S + m_S L_{SK} \sin \theta_S + m_t L_{SCt} \sin \theta_S \\ m_f L_{KA} \sin \theta_K + m_S L_{KCSH} \sin \theta_K \\ m_f L_{ACf} \sin \theta_A \end{bmatrix} \begin{bmatrix} \ddot{\theta}_S & \ddot{\theta}_K & \ddot{\theta}_A \end{bmatrix} \\
&\quad - \begin{bmatrix} m_f L_{SK} \cos \theta_S + m_{sh} L_{SK} \cos \theta_S + m_t L_{SCt} \cos \theta_S \\ m_f L_{KA} \cos \theta_K + m_S L_{KCSH} \cos \theta_K \\ m_f L_{ACf} \cos \theta_A \end{bmatrix} \begin{bmatrix} \dot{\theta}_S^2 & \dot{\theta}_K^2 & \dot{\theta}_A^2 \end{bmatrix}
\end{aligned} \tag{4.16}$$

In this case, F_R is assumed to be at the centre of the stump as illustrated in Figure 4.6. Therefore, the magnitude of the F_R at different points of the socket might not be the same. In this application, the exact amplitude of F_r in Equation (4.14) position on the stump was modelled to be the function of F_R with respect to the radius from the centre to the socket wall. Therefore, F_r can be written as:

$$F_r = F_R(r) \tag{4.17}$$

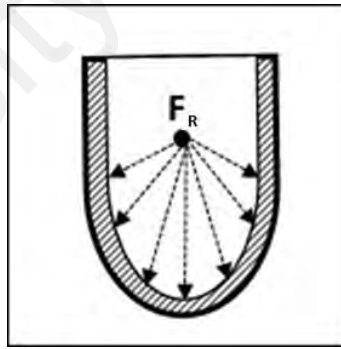


Figure 4.6: F_R to the wall of the socket.

Thus, equation (4.14) that describes the input force to the piezo sensor can be re-written as:

$$\hat{F}_{piezo} = \hat{F}_R(r) + \hat{F}_{muscle} + \hat{F}_{socket} \tag{4.18}$$

4.4 Experiment methodology

An experiment was designed and conducted to gather the signal responses from the in-socket sensory system during amputee gait in order to investigate the feasibility of the

proposed in-socket sensory system to detect gait phases. This section explains the details of the experiment.

4.4.1 Subject and prosthetic leg

One healthy male, transfemoral amputee participated in this study. The description of the subject is detailed in Table 4.3. The subject provided his written and informed consent. Approval for the experimental procedure was obtained from the Medical Research Ethics Committee of University of Malaya Medical Centre (the ethics approval letter is attached in the Appendix).

Table 4.3: Description of the subject

Age	36 years old
Height	174.5 cm
Weight	80.5 kg
Criteria	<ul style="list-style-type: none"> • Unilateral amputation (left leg) due to trauma • Type K3-amputee (based on US Health Care Financing Administration's, HCFA classification) • Has been wearing prosthesis for 17 years • Current prosthetic leg used is mechanical knee-joint and single-axis foot

The prosthetic leg used in this experiment is owned by University Malaya. The socket used was polypropylene quadrilateral type and was custom-made to perfectly fit the subject. The sensors were instrumented to the socket following the configuration described in F. Jasni (2016). Since the piezo sensors used in this study were the unimorph type, the response polarity was dependent on the method of mounting the sensor (negative surface upward or downward). For this study, all 15 sensors were mounted with a negative surface facing upward (Figure 4.7) to ensure uniformity in the polarity of the response.

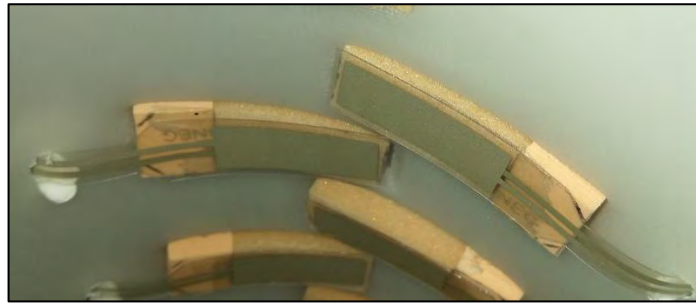


Figure 4.7: Sensor mounting. The negative side is facing upward.

Figure 4.8 illustrates the relationship between the strain and the response (i.e. voltage) of the sensor when it is mounted with this configuration.

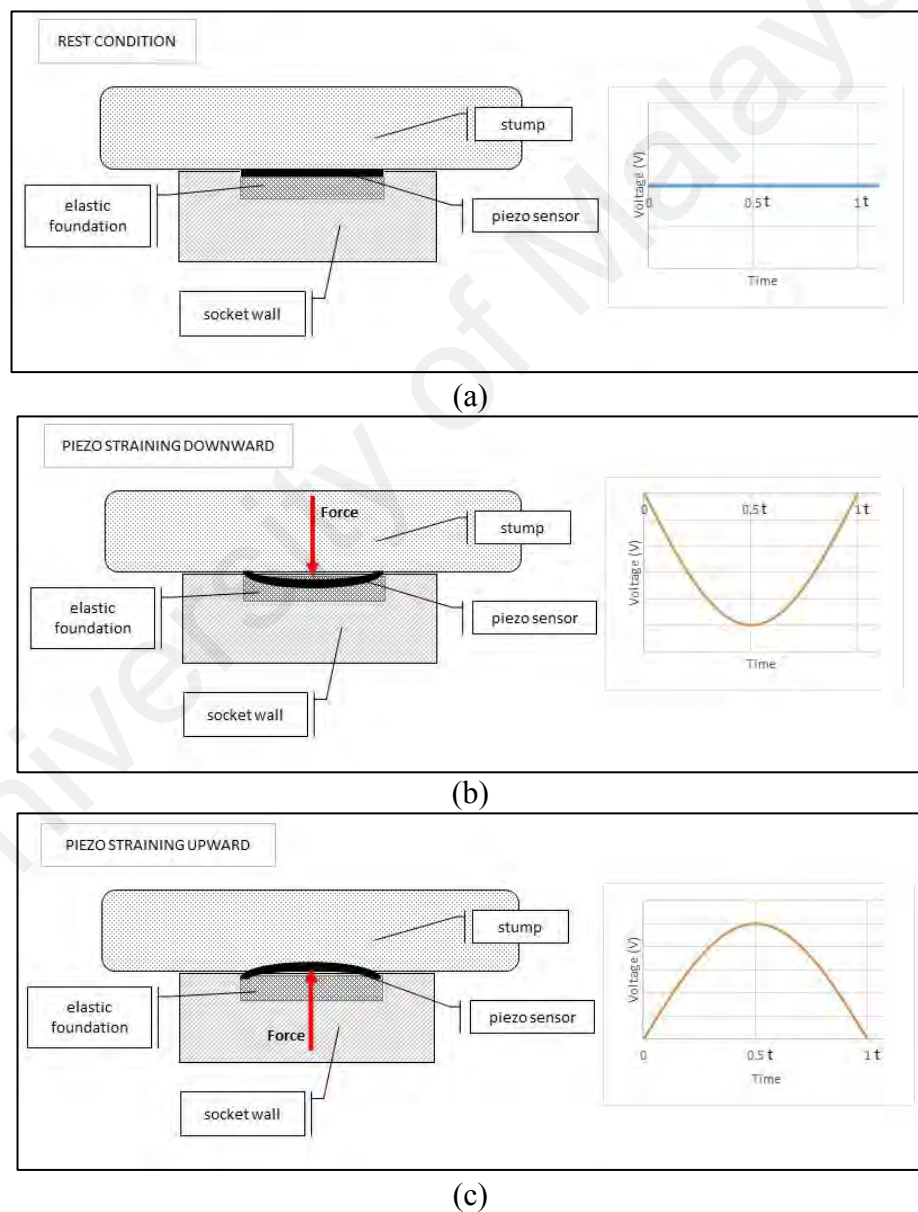


Figure 4.8: Sensor response with respect to the sensor's strain. (a) rest condition, (b) strain downward, and (c) strain upward.

In order to calibrate the sensors, the response during the quiet standing activity was recorded for all sensors. Figure 4.9 shows the response of all sensors for quiet standing. It can be seen that the range of the response is within -0.02 to +0.02V.

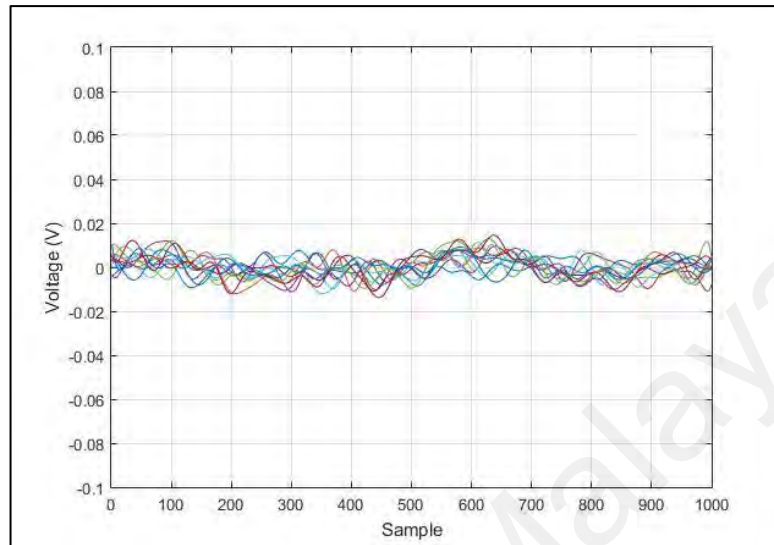


Figure 4.9: Sensors response for quiet standing for all 15 sensors

The hydraulic knee joint and Solid Ankle Cushion Heel (SACH) foot was used by the amputee (3R60 EBS Pro, Ottobock, US). Figure 4.10 shows the complete set of the prosthetic leg used for the experiment. Prior to the experiment, the subject was given time to practice walking with the provided prosthetic leg to allow for familiarisation and to ensure that the captured data was as close as possible to his normal gait.

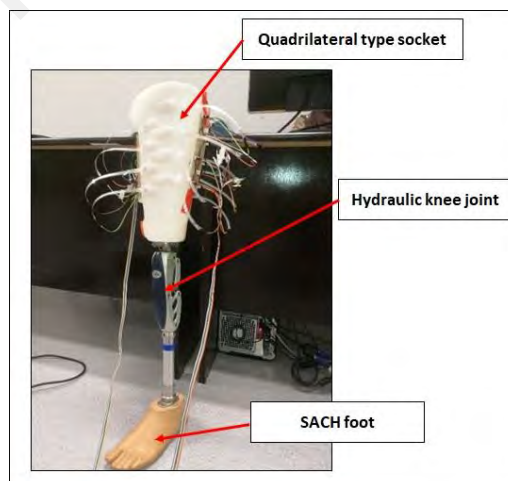


Figure 4.10: Prosthetic leg used in this experiment.

4.4.2 Lab setup

The experiment was conducted in the motion system lab in University of Malaya, which was equipped with two force plates to capture the subject's GRF data. The

sampling rate of both force plates was set to 1 kHz. A motion analysis software (VICON Nexus version 1.8.5) was used to process the force plate data. The lab setup is shown in Figure 4.11.

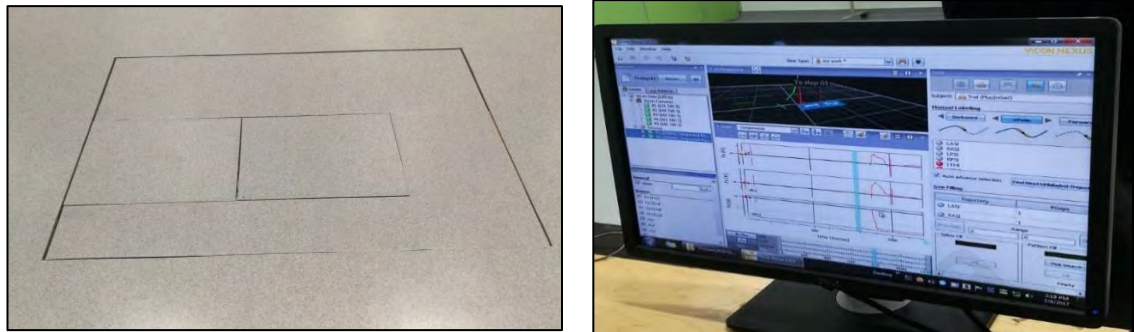


Figure 4.11: VICON Motion system. Left: Force plates, Right: VICON Nexus software GUI.

4.4.3 In-socket sensory system data acquisition and signal processing

Since piezoelectric sensor could detect a wide frequency range, thus, signal conditioning process was required to ensure only significant range of signal was captured. The output signal from the sensors was first pre-processed, amplified, and low-pass filtered before it was sent to the DAQ card for analogue-digital conversion. Each sensor was connected to an active low pass filter circuit with a voltage gain of 11 and the cut-off frequency of 800 Hz. The circuit diagram of the active low pass filter circuit is illustrated in Figure 4.12.

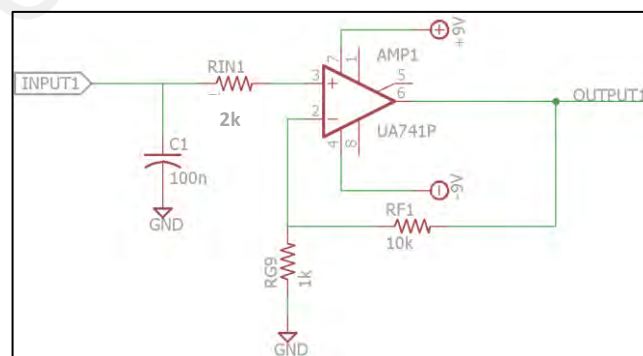


Figure 4.12: Active low pass filter circuit diagram.

Next, the processed analogue signal was sent to DAQ Card (NI 9221, National Instrument, USA) for digital-analogue conversion and to be viewed and recorded using LabVIEW software, version 2014 (National Instrument, USA). Two similar DAQ Card unit's models (specification is described in Table 3.4) were used to acquire the signals

from all 15 sensors. Signals from the anterior sensors (A1-A8) were connected to the first DAQ Card module, while the posterior sensors (P1-P7) were wired to the second module via two 3 meters-long ribbon cables (one for the anterior and another for posterior). Both modules were connected to the computer via a four-slot USB chassis (NI cDAQ-9174, National Instruments, USA). The DAQ Card modules were set to acquire data for every 0.001 s (sampling rate 1 kHz).

In order to get a smoother signal, the acquired data was again band-pass filtered in the LabVIEW software by sixth-order Butterworth Infinite Impulse Response (IIR) filter with a passing frequency of 1 to 20 Hz based on the findings of the work done by Prendergast, Helm and Duda (2005) which reported that the muscle's activity signal fall in the low frequency range.

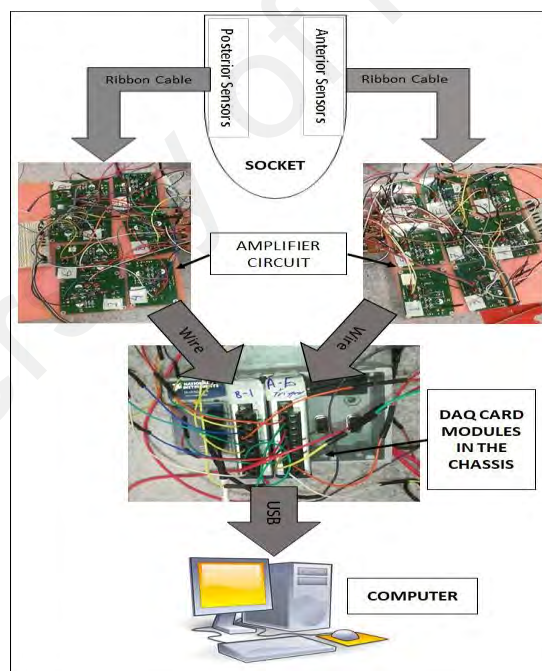


Figure 4.13: Data acquisition setup from sensors to computer

4.4.4 Experimental procedure

This experiment was divided into two routines. The first one is called the single stride walking routine and the second one is the continuous walking routine. During the single stride walking routine, data from the sensor and the force plates were collected

simultaneously. Thus, the relationship between the force and the sensors' response can be observed. On the other hand, the continuous walking routine was to collect a natural continuous walking data. Only sensory data was collected in this routine.

The rationale for having separate routines was to eliminate the need for long wire to be used to connect the sensors to the signal conditioning circuit, which was stationed near the DAQ card unit. Pre-investigation had been made which determined that the optimum length of the cable to reduce noise caused by the cable is 3 m. Hence, the first routine enabled the comparison between sensory system response and GRF data to be made with only single stride, while the second routine enabled the investigation of the sensory system behaviour for continuous natural walking.

4.4.4.1 Single stride routine

The objective of this routine was to collect data from the sensory system and GRF simultaneously. Thus, the subject was asked to walk for only one stride over the force plates. The starting point was set outside of the first force plate where the subject stood quietly. Data recording was started for both systems (sensory and GRF). One force sensor was used as the trigger switch. It was placed on the second force plate and wired to the DAQ card module that was used to collect the sensory data. The trigger sensor was knocked and set the beeping sound. When the subject heard the beeping sound, the walking starts with the prosthetic leg first. The prosthetic leg stepped on the first force plate, followed by the intact leg stepped on the second force plate. Then, the prosthetic leg also stepped on the second force plate and the triggering switch was triggered once again to mark the second heel strike. Data recording was stopped thereafter. The trials were repeated 10 times.

The first trigger switch was used to synchronize the starting point of the routine for both systems. Since the switch was located on the force plate, when the sensor was knocked, the force plate also detected some response. Thus, data for both systems could

be cropped from that point onwards. The illustration of the synchronization method is presented in Figure 4.14. The point where the first force plate data started to raise was marked as the first heel strike. Meanwhile, the point where there are abrupt changes in the force plate 2 was considered as the second heel strike point. This was validated by a video recording. Figure 4.15 shows the process. The data for GRF and sensory data for single stride (from the first heel strike to the second heel strike) was cropped accordingly for all 10 trials and the mean and standard deviation was calculated.

Before the data recording was started, the subject was given some time to practice and determine the suitable distance for him to start and end the routine, so that the step can be regarded as his normal step. However, it is noted that the stride performed by the subject was actually a start-up stride and the pattern might not be the same with the on-going strides. But, since the aim is to analyse the pattern of the sensors response with respect to the GRF curve, which was recorded during the start-up stride as well, thus, the procedure is assumed to be acceptable.

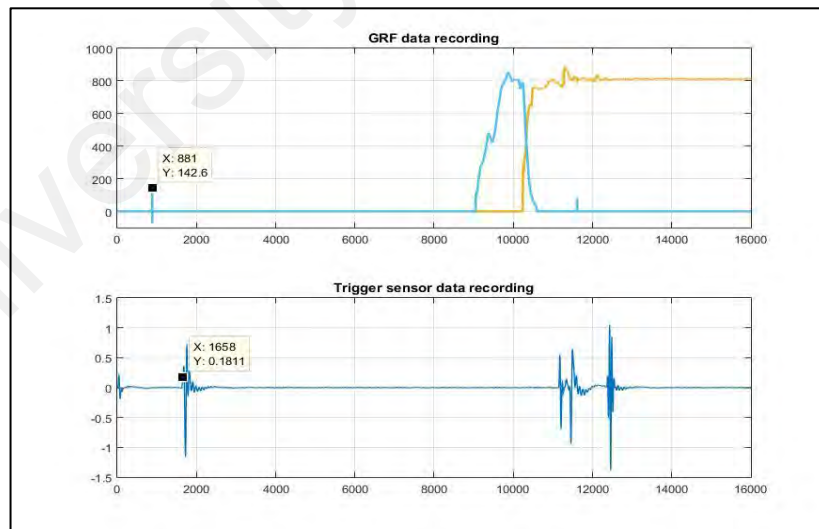


Figure 4.14: Data synchronization method. Top: The data for GRF. Bottom: Trigger sensor data. It can be seen that force plate was knocked at X=881 after the recording started and the trigger sensor was activated 1658 samples after recording started.

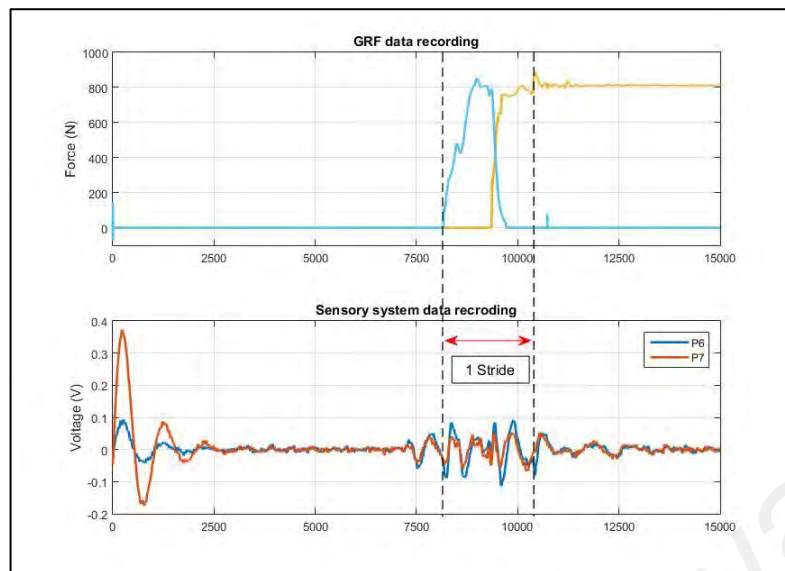


Figure 4.15: Illustration of how the 1st and 2nd heel strike was identified.

4.4.4.2 Continuous walking routine

The subject was then asked to walk at a self-selected normal walking speed. At first, the subject was asked to stand quietly on the starting line. Data recording was started. One start switch was used as the indicator of the starting point of the procedure. Thus, during the data analysis, the signals that were captured before the switch was triggered could be cropped out.

To start the procedure, the start switch was triggered, at the same time, a 3 seconds timer was set. After the 3 seconds is up, beeping sound was released. When the subject heard the beep sound, the subject started to walk following the path (Figure 4.16) that has been set with his self-selected walking speed until the finishing line and stopped walking. The circle path was used in this experiment to compensate the limitation of the length of the wire. However, it was assumed that the subject's steps are similar to the steps when he walks in a straight line due to the big ratio of the path circumference to the stride length (18.85:1). The trigger switch was pressed again to mark the end of the walking routine. Data recording was stopped immediately upon completion of the amputee gait. Five trials were performed with an average of nine complete continuous strides were performed in each trial. However, only six strides were taken omitting the first two steps and the final step, so only on-going strides were included in the analysis.

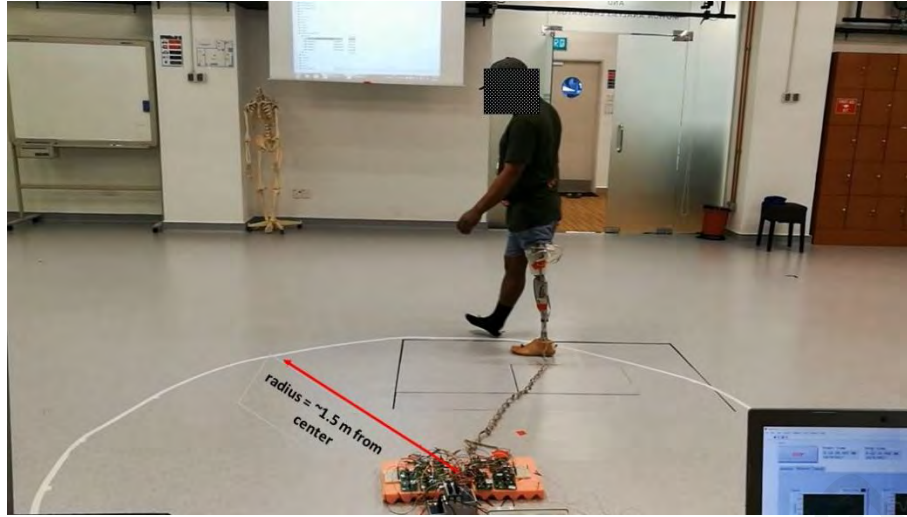


Figure 4.16: Illustration of the walking path for the experiment. Circular path with ~1.5 m radius measured from the centre.

To mark the gait events during the gait, a video throughout the trial was recorded and analysed using Kinovea program to confirm and adjust the gait phase's identification. Data for single stride was cropped accordingly. The mean and standard deviation of 30 complete gait cycles (5 trials \times 6 strides/trial) for each sensor were calculated. Data from both routines were normalized to 100% gait cycle.

The significant sensors for both routines were identified based on the response of the sensor during the respective gait phase. Two criteria that the sensor must possess to be significant are; 1) at least one slope sign change, and 2) at least one peak with amplitude $-0.02V > \text{Peak}$, or $\text{Peak} > 0.02V$, during the respective phase. $0.02V$ is chosen because it is outside the quite standing voltage range stated in Section 4.4.3. The findings are presented in the next section.

4.5 Results

Based on the video analysis and by analysing the average GRF curve, the average gait phase percentage distribution was determined. Table 4.4 shows the gait phase distribution for both walking types.

Table 4.4: Gait phase percentage for both walking types.

Gait phase	Single stride walking	Continuous walking
IC	0%	0%
LR (DS1)	0 – 23%	0 – 19%
MSt (SS)	23 – 35%	19 – 33%
TSt (SS)	35 – 46%	33 – 48%
PSw (DS2)	46 – 65%	48 – 62%
Sw	65 – 100%	62 – 100%

IC=Initial contact, LR=Loading response, DS1=Double support 1, MSt=Mid-stance, SS=Single support, TSt=Terminal stance, PSw=Pre-swing, Sw=Swing.

4.5.1 Single stride walking

Figure 4.17 and Figure 4.18 shows the mean response and standard deviation for all anterior sensors, A1 to A8, in which A1 was the top most and A8 was the bottom most sensor. The corresponding vertical GRF (GRV) and anterior-posterior GRF (AP GRF) were also presented in the figures. The response behaviour is corresponding to the strain pattern of the piezo sensor as illustrated in **Figure 4.8**.

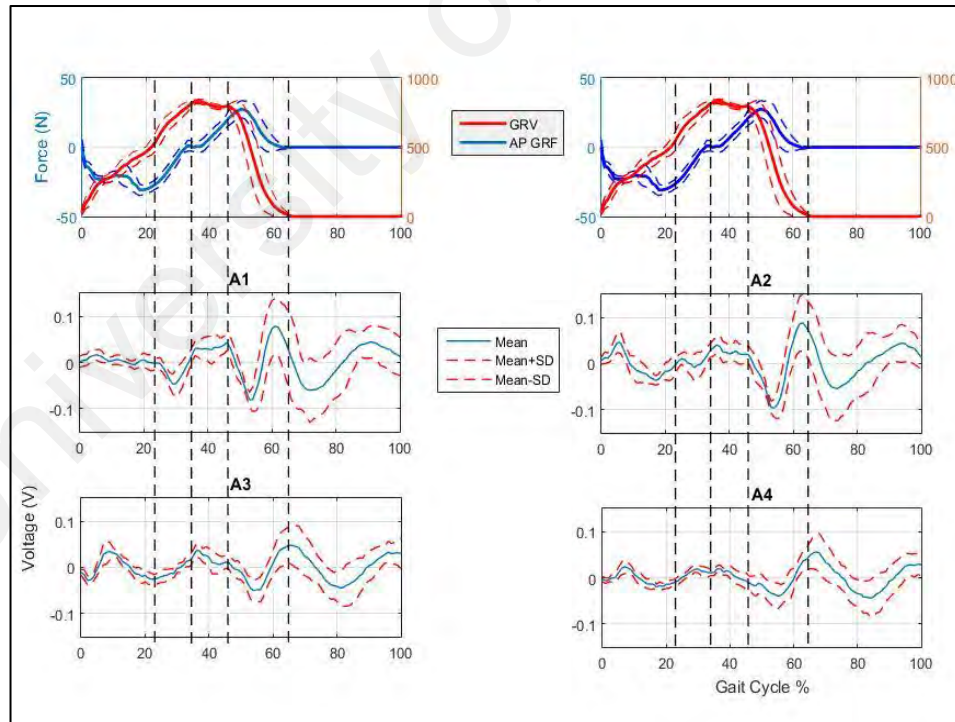


Figure 4.17: Anterior sensors responses for single stride walking for Sensor A1 to A4 with respect to the GRV and AP GRF. The vertical dashed line represents the separator of gait phases.

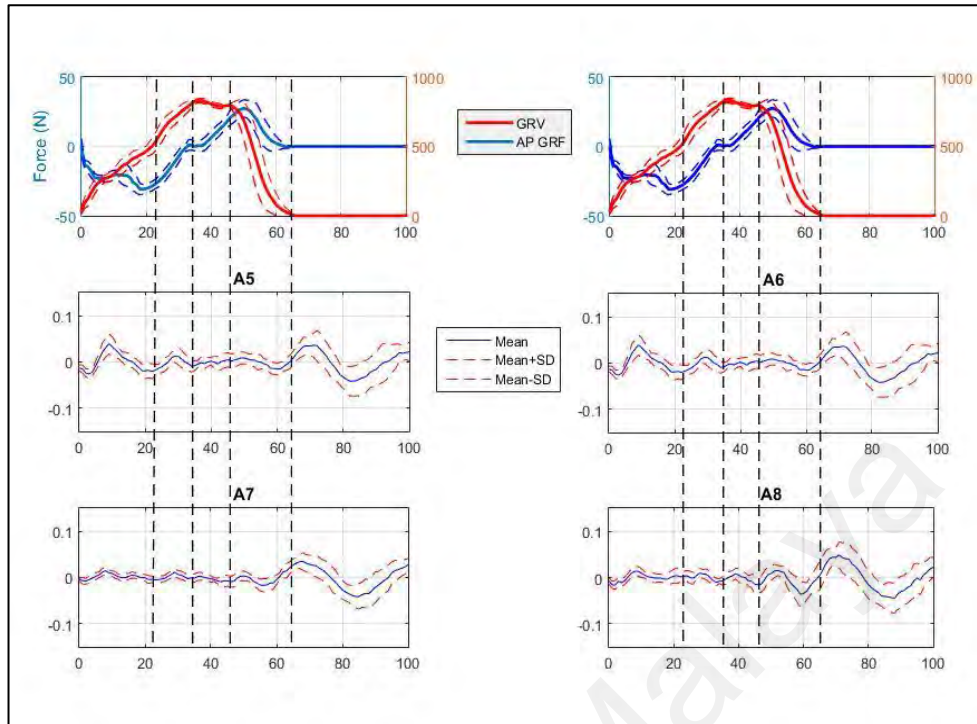


Figure 4.18: Anterior sensors responses for single stride walking for Sensor A5-A8 with respect to the GRV and AP GRF. The vertical dashed line represents the separator of gait phases.

From the plots, it can be seen that all sensors showed good consistency, especially in the stance phase. The deviation was quite high during the swing phase. In terms of amplitude, sensor A1, A2 and A3 (the top 3 sensors) showed the highest intensity compared to the others.

During the first section of the gait cycle (0-23%), sensors A3, A4, A5 and A6 showed a significant response compared to other anterior sensors. This period is the first double support and weight acceptance phase, which is also known as the LR phase.

For the second section (23%-35%) of the gait cycle, which is the first half of the single support phase (MSt), two main patterns were observed. Sensors A1 to A4 showed upward quadratic curve, meanwhile, sensors A5 to A8 displayed a downward quadratic curve. Sensors A1, A2, A5 and A6 showed a prominent pattern compared to the others.

As for the TSt phase (35-46%), which is the second half of the single support phase, not much activity was detected by all sensors, except for sensor A8, which displayed a

small downward curve and sensors A3 and A4 showed a gradual decrease back to zero line.

During the second double support phase (PSw phase), sensors A1, A2 and A8 showed a more outstanding behaviour compared to the other sensors. However, A8 behaved differently from A1 and A2 in which the curve looks like the opposite of the A1 and A2 curve.

Finally, for Sw phase, all sensors behaved almost the same with more intensity seen at A1-A4 compared to the other 4 sensors located on the bottom part.

Figure 4.19 and Figure 4.20 shows the mean response for all posterior sensors, P1 to P7. The standard deviation for all posterior sensors shows that the response signals are consistent across 10 trials, even though a bigger variation was observed during the swing phase. The middle sensors, P4 and P5, were the sensors with the highest amplitude.

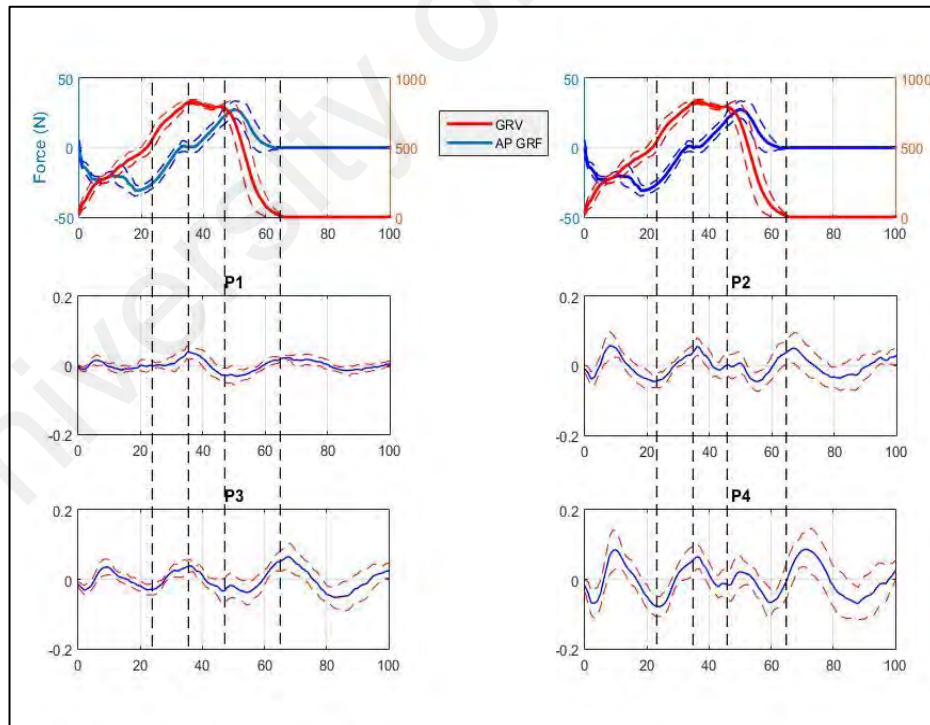


Figure 4.19: Posterior sensors response for single stride walking for Sensor P1 to P4 with respect to the GRV and AP GRF. The vertical dashed line represents the separator of gait phases.

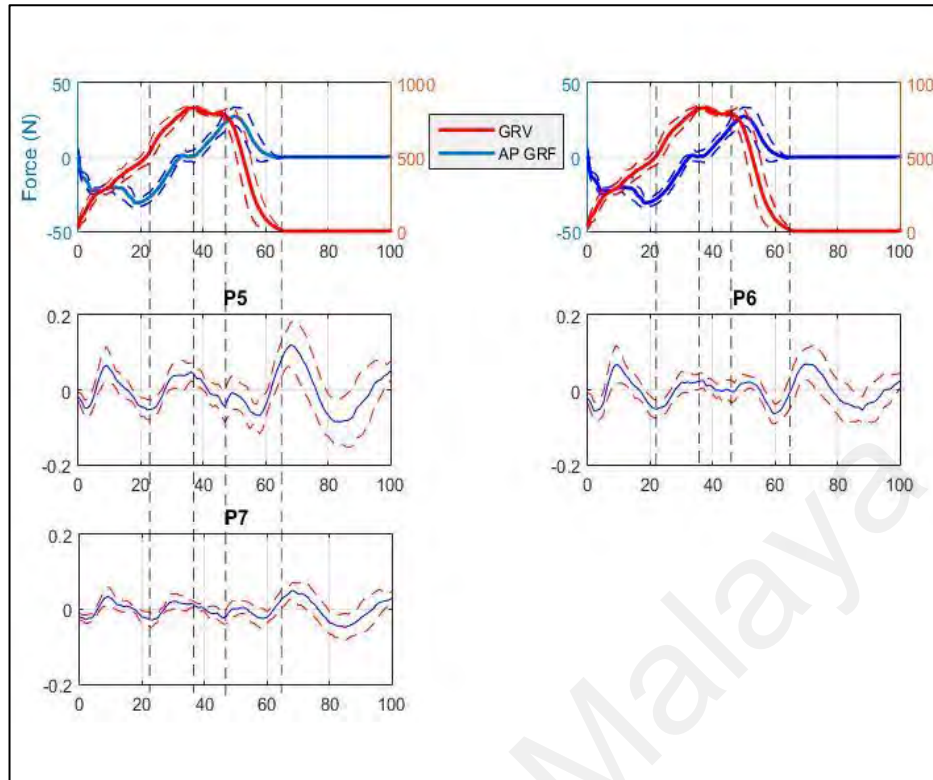


Figure 4.20: Posterior sensors response for single stride walking for Sensor P5 to P7 with respect to the GRV and AP GRF. The vertical dashed line represents the separator of gait phases.

During the first double support period (LR phase), almost all posterior sensors were responsive, except for sensor P1. The pattern displayed was almost the same for all sensors. In the single support phase (MSt and TSt phase), 23-46% of the gait cycle, a prominent response can be seen in the P1-P5 sensors. The next phase is the PSw phase, or the second double support, sensors P2, P4, P5 and P6 showed a significant response. Finally, during Sw phase, it was observed that all posterior sensors behaved the same but with different intensity. Higher amplitude was detected in the middle posterior sensors, which were P3, P4 and P5.

4.5.2 Continuous walking

Figure 4.21 displays the plots for all anterior response signal for the continuous walking routine with its respective standard deviation. Overall, it could be deduced that the consistency for all sensors was good, especially for the even numbered sensors, A2, A4, A6 and A8.

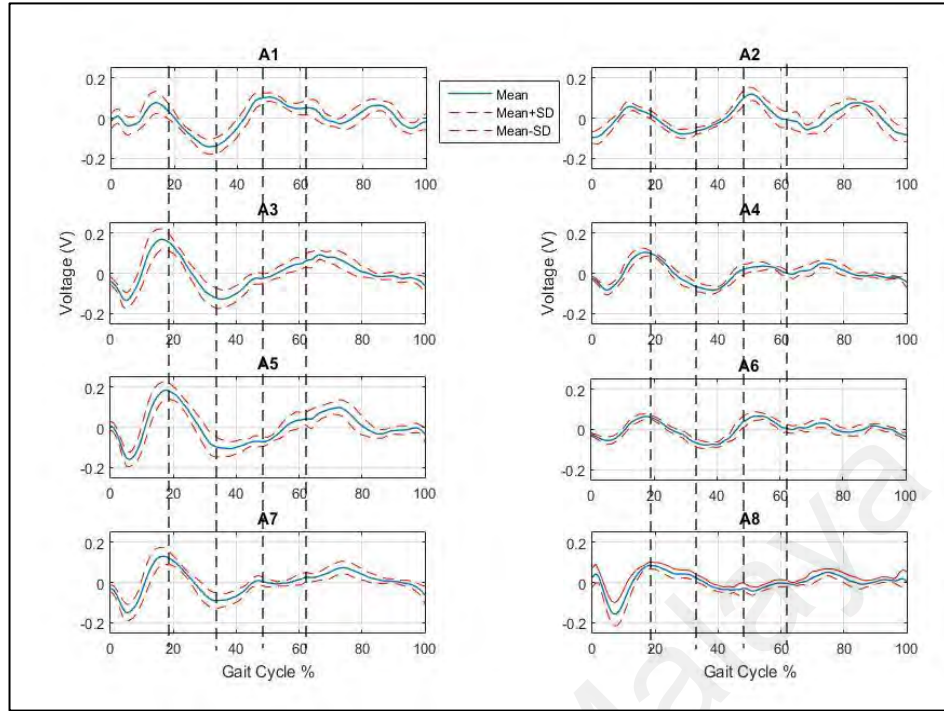


Figure 4.21: Anterior sensors response for continuous walking. The vertical dashed lines represent the separator of gait phases.

For the LR phase, all sensors showed almost the same pattern, however, sensors A3, A5 and A7 showed a higher intensity. As for the single support phase (MSt and TSt), all sensors, except sensor A8 displayed the same pattern, but higher amplitudes were found at sensors A1 and A3. During PSw phase, only slight activity was detected in the anterior sensors' response. Meanwhile, during Sw phase, the significant pattern was observed at sensors A1, A2 and A5 responses. Nevertheless, sensor A5 response pattern was the opposite to the curve showed by sensors A1 and A2.

The response for all posterior sensors for the continuous walking routine is illustrated in Figure 4.22. Small standard deviation for all sensors, except for Sensor P3, suggested that the response for the sensors were consistent across multiple trials.

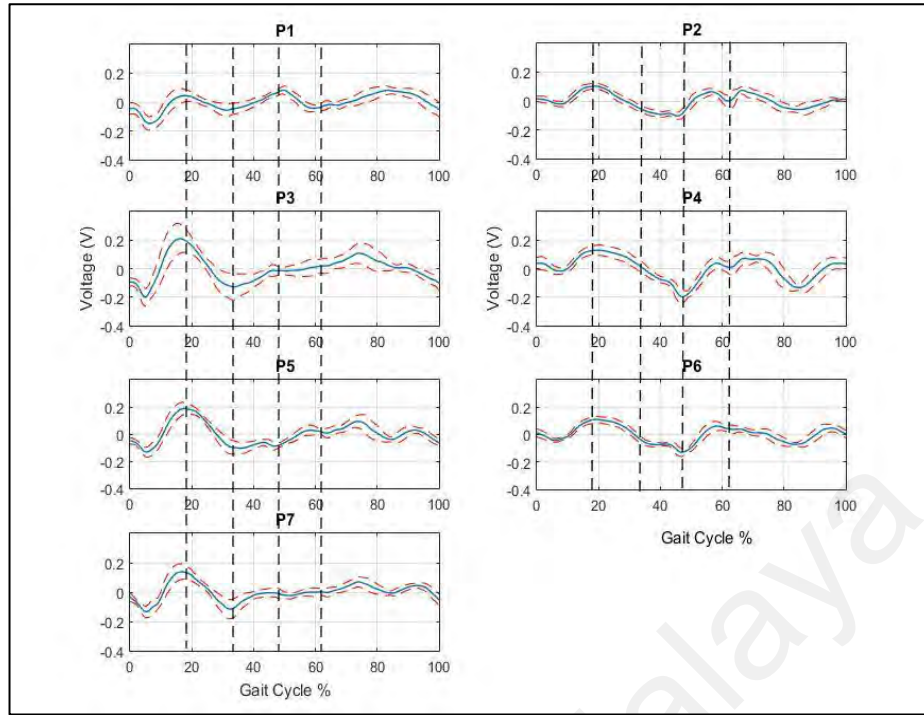


Figure 4.22: Posterior sensors response for continuous walking. The vertical dashed lines represent the separator for gait phases.

During LR phase, all sensors responded quite similarly, but higher amplitude was detected in the P3, P5 and P7 sensors. For MSt and TSt phase (single support phase), sensors P3, P5 and P7 displayed a prominent behaviour compared to the others. As for PSw phase, sensor P1 shows a gradual decrease, while sensor P2, P4, P5 and P6 showed increment in the value. The rest of the sensor showed no response (stagnant at zero line). Lastly, in Sw phase, P4, P5, P6 and P7 displayed the same response and the highest intensity can be seen in the P4 response.

4.5.3 Continuous walking vs single stride walking

Figure 4.23 to Figure 4.26 and Figure 4.27 to Figure 4.30 illustrate the comparison of continuous walking and single stride walking response for all anterior and posterior sensors, respectively. Three main observations were noted. First, the amplitude of the single stride walking response was smaller than the continuous walking for almost all sensors. Second, the response pattern of most of the sensors showed similarity for both types of walking, but, shifted in the time domain. For instance, for sensor P2, the positive peak for single stride walking occurred at ~10% of the gait cycle, but for continuous

walking, it happened at $\sim 20\%$ of the gait cycle. Finally, for continuous walking some particular phases had larger signal standard deviation. Nonetheless, the standard deviation is still within the acceptable range (i.e. SD calculated for all sensors fall within the $\pm 1\text{SD}$ from the mean in its normal distribution, and the highest SD calculated was 3 times smaller in magnitude to compare to the signal magnitude) suggests that the responses were still consistent across multiple trials.

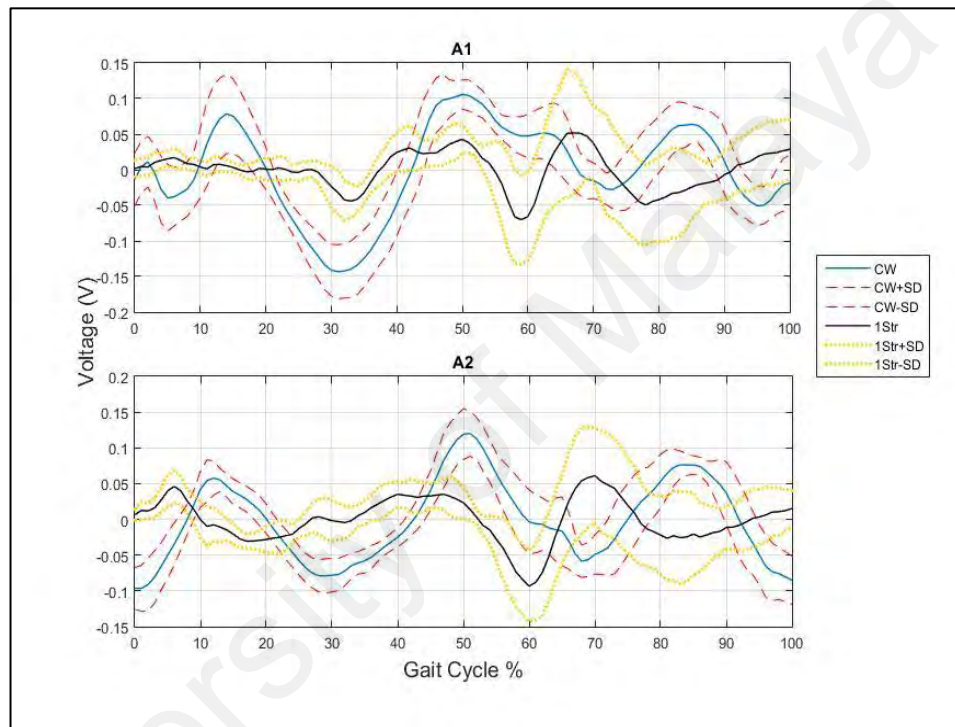


Figure 4.23: Anterior sensors response for continuous walking and single stride walking for Sensor A1 and A2.

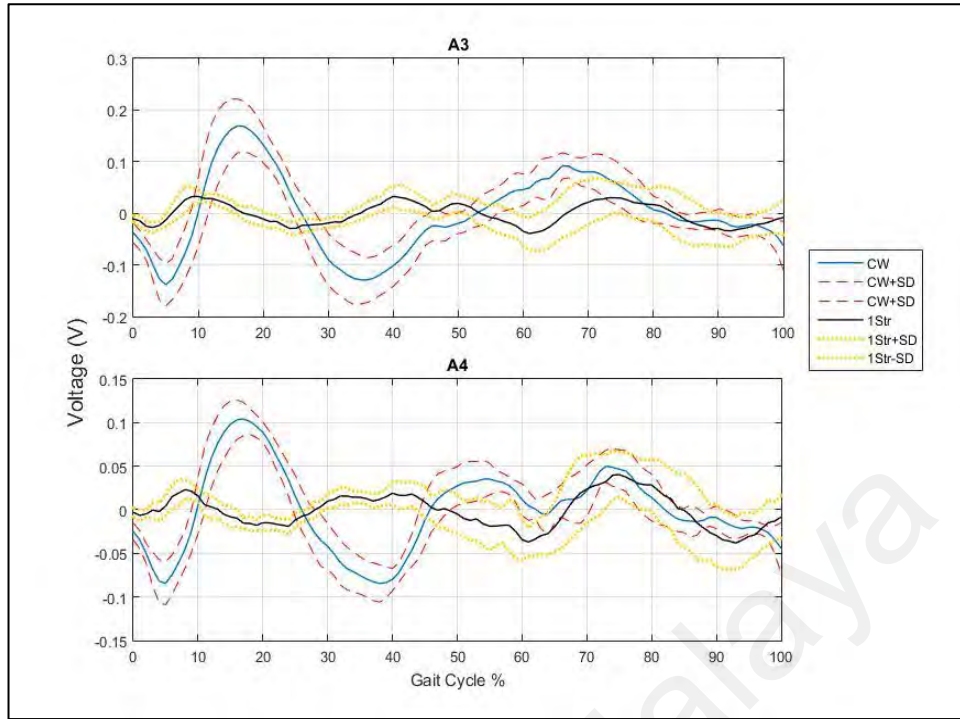


Figure 4.24: Anterior sensors response for continuous walking and single stride walking for Sensor A3 and A4.

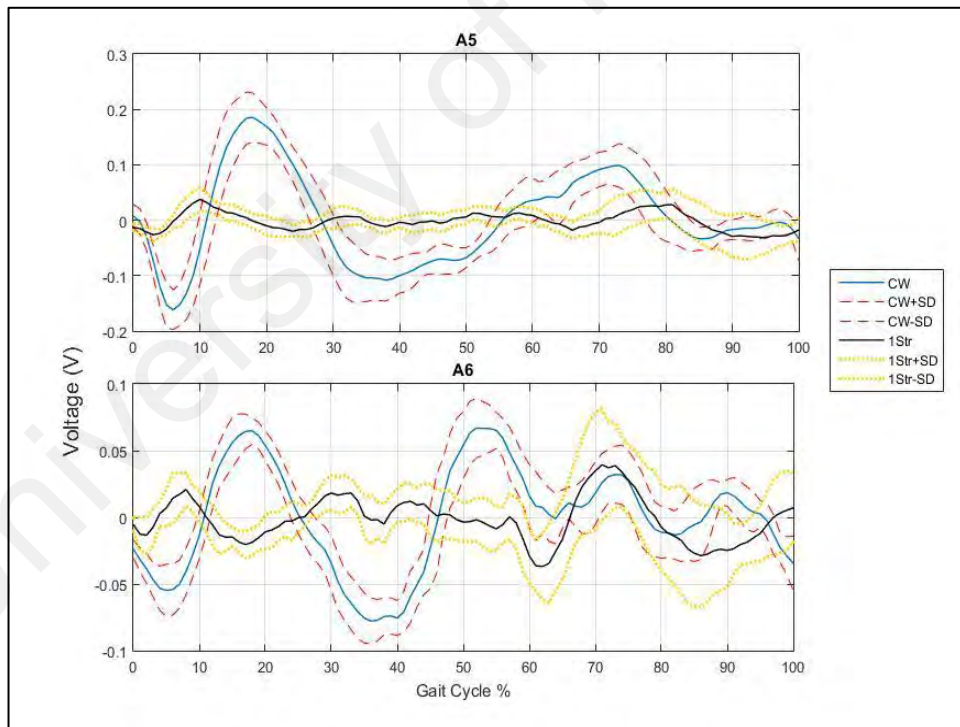


Figure 4.25: Anterior sensors response for continuous walking and single stride walking for Sensor A5 and A6.

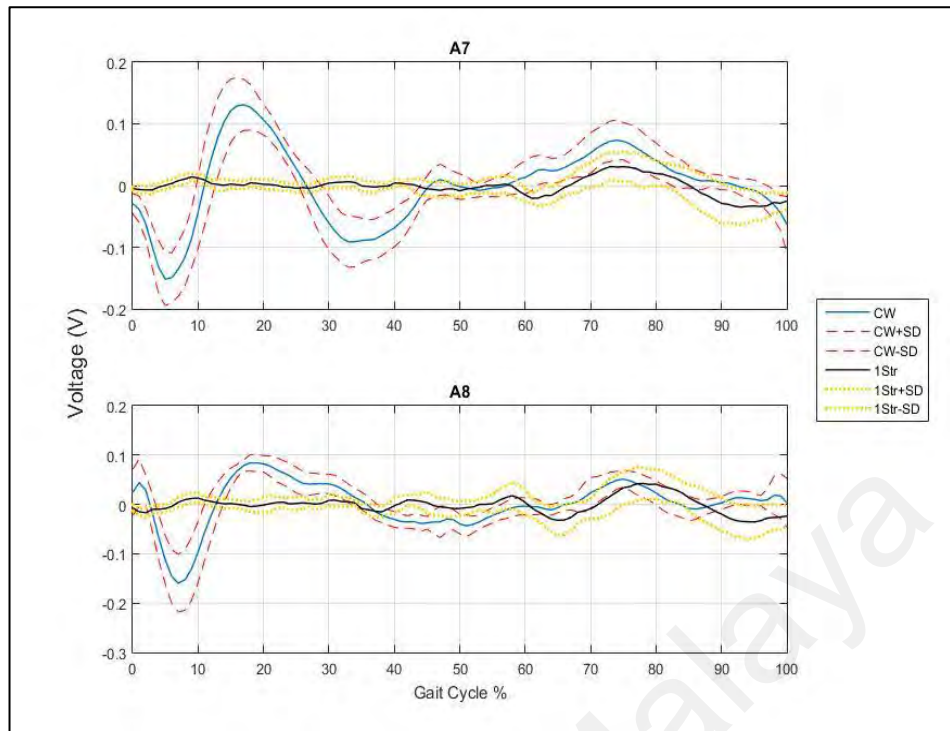


Figure 4.26: Anterior sensors response for continuous walking and single stride walking for Sensor A7 and A8.

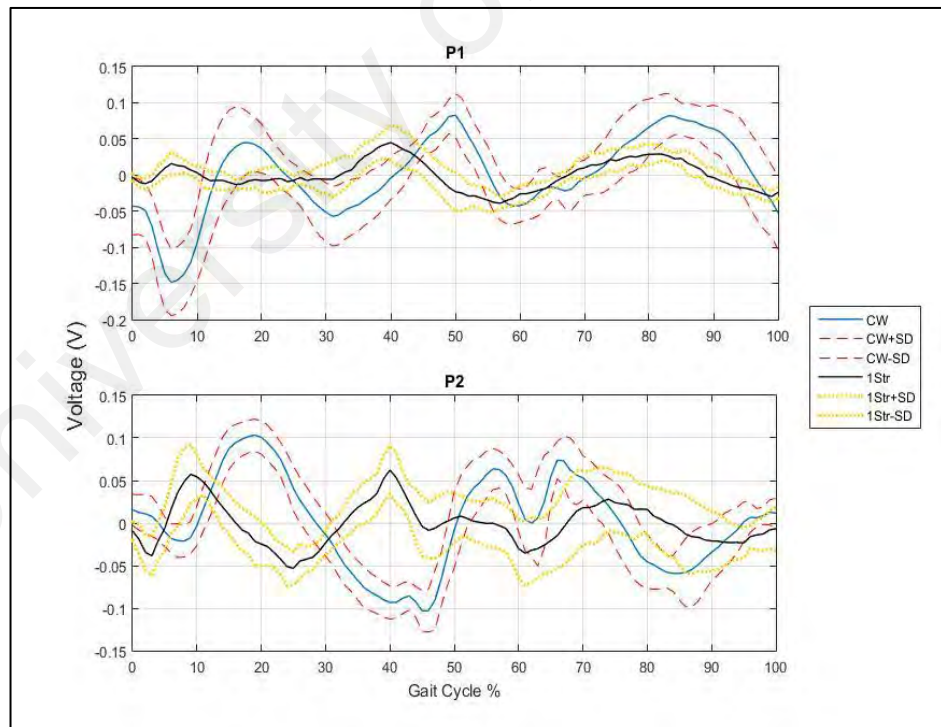


Figure 4.27: Posterior sensors response for continuous walking and single stride walking for Sensor P1 and P2.

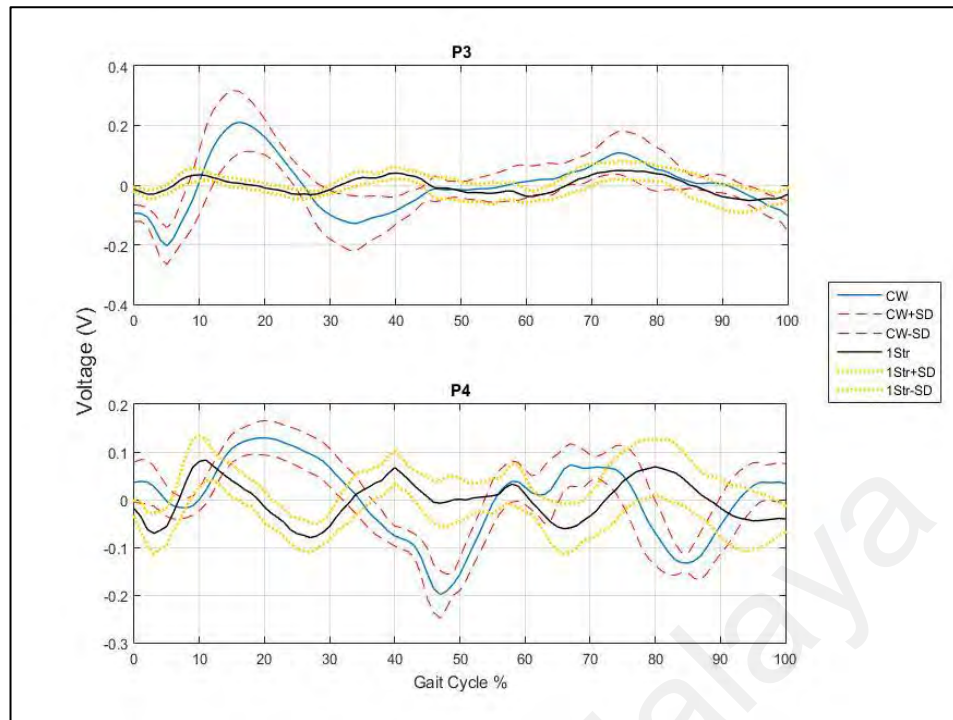


Figure 4.28: Posterior sensors response for continuous walking and single stride walking for Sensor P3 and P4.

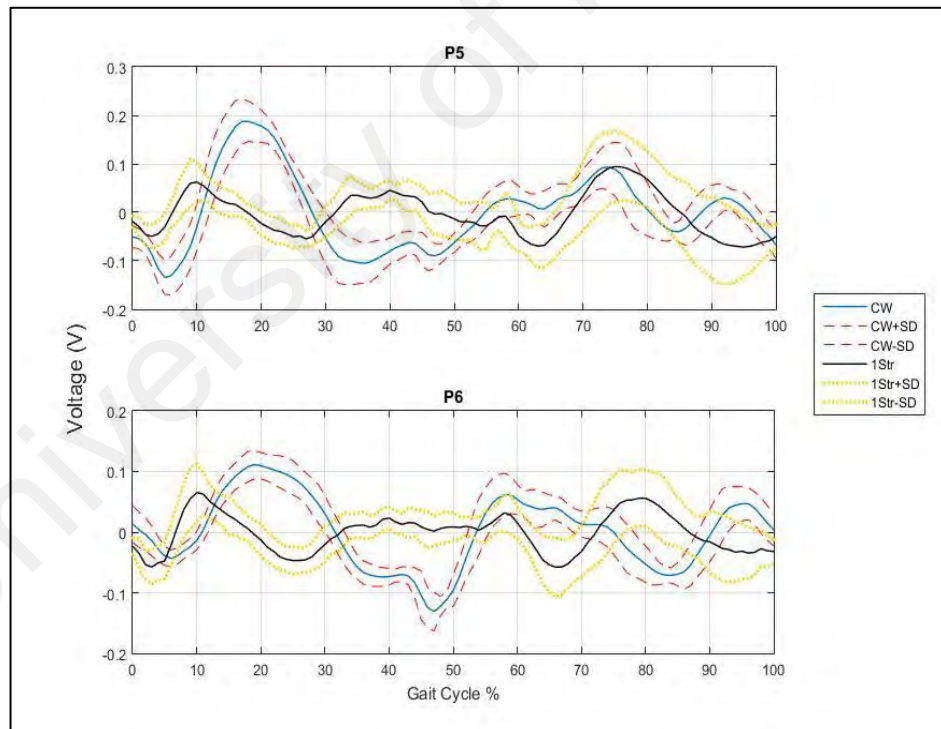


Figure 4.29: Posterior sensors response for continuous walking and single stride walking for Sensor P5 and P6.

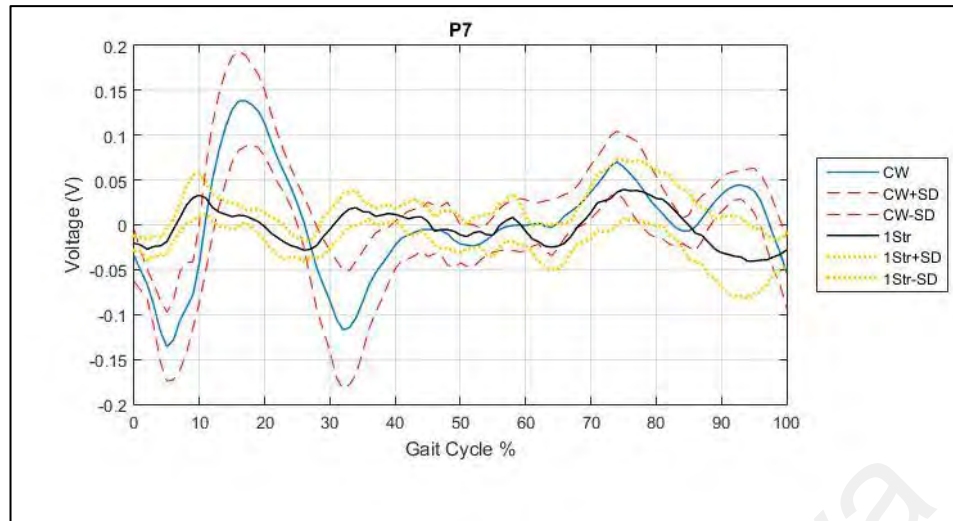


Figure 4.30: Posterior sensors response for continuous walking and single stride walking for Sensor P7.

4.6 Discussion

The findings of this study suggested that in-socket sensory system was able to detect the gait phases of a transfemoral amputee. Table 4.5 summarises the significant sensors for single stride and continuous walking routines in the respective gait phases.

Table 4.5: Summary of the significant sensor during respective gait phase and transition from phase to phase.

Gait Phase	Anterior Sensors								Posterior sensors						
	A1	A2	A3	A4	A5	A6	A7	A8	P1	P2	P3	P4	P5	P6	P7
LR															
LR->MSt															
MSt															
MSt->TSt															
TSt															
TSt->PSw															
PSw															
PSw->Sw															
Sw															

Blue boxes = single stride walking, Pink boxes = Continuous walking.

From the table, almost all gait phases and the transitions from one phase to the next phase could be detected based on the activity of the sensors for both walking types. The

activity of the sensors was seen to be more active during LR, the transition from LR and MSt, the transition from MSt to TSt, and Sw phase for both walking types. LR is the period where weight acceptance event takes place. Therefore, it might explain the high intensity of the force change detected by the piezo during this phase. As for the transition from LR to MSt, it was the starting point of a single support phase in the gait. Thus, the body weight distribution which was supported by two feet was transferred to the one foot during single support, hence, explains the activity in most of the sensors. Next is the transition from MSt to TSt. This can be explained by the push off event that started to take place during this time. Finally, the high sensors' activity during Sw period is caused by the high intensity of the quadricep and hamstring muscles to move the leg forward (Bonnetfoley-Mazure & Armand, 2015).

Less activity was detected during the MSt and TSt phase, especially for the continuous walking. This might be due to the minimal muscles' activity during this period (Cerqueira, Yamaguti, Mochizuki, Amadio, & Serrão, 2013; Wentink, Prinsen, Rietman, & Veltink, 2013). However, this can still be compensated by the ability of the sensory system to detect the transition between MSt to TSt. During PSw period, more sensors were triggered for single stride walking compared to the continuous walking. It was probably due to the stopping action after the swing phase for single stride walking. Thus, the force profile was different between single stride and continuous walking. This finding suggests that the sensory system can also be used to detect gait termination.

The possible factor for the difference between the sensors' response for the single stride walking and the continuous walking was due to the speed and momentum during the walking motion. For the continuous walking, the subject walked at a higher speed than the single stride walking. Thus, higher amplitude was detected for continuous walking due to the momentum effect. The difference on the walking speed from one step to another might also contribute to the higher standard deviation in some phases of the

continuous walking. The difference between the two walking types led to the assumption that the in-socket sensory system can also detect the difference in the walking type or speed by the amputee. However, more studies have to be planned and conducted to further verify this new hypothesis.

4.7 Summary

The following observations are derived from this study:

1. The proposed piezoelectric based in-socket sensory system was proved to be feasible for TF gait phase detection in one subject.
2. This sensory system could be used to characterise single stride and continuous walking, based on the different response observed for each walking type in one subject.
3. The findings also suggested that the proposed sensory system might be used to recognise gait termination.

In this study, the analysis was conducted with the aim to prove the concept that piezo-based in-socket sensory system can be used to characterise the gait phases. The phases were determined via the force profile that is relatively portrayed by the sensors' response. The quantitative analysis of the sensors' response and the amount of force applied to the sensors were not performed in this study. Thus, in future, an in-depth study to investigate the relationship of the resultant input force (from muscle, GRF and interface pressure/force) and the sensor's response in terms of the direction and amplitude of the force should be conducted.

CHAPTER 5: CLASSIFICATION OF SENSORY SYSTEM RESPONSE USING STATISTICAL PATTERN RECOGNITION METHOD FOR TRANSFEMORAL AMPUTEE GAIT DETECTION

5.1 Introduction

This study presents the development of pattern recognition algorithm to classify the gait phases using the response of the in-socket sensory system for two selected walking speeds (i.e. 1.0km/h and 2.0km/h). An experiment was performed to collect data and develop the classifier model. An analysis was conducted to determine the optimal parameters of the classifier; the classifier type, window size, and training dataset that resulted in the highest accuracy rate for both speeds. The performance of the selected classifier model was tested with the datasets from different sessions to evaluate its generality. Finally, optimization method was performed with the aim to reduce the number of sensors without affecting the classifier performance.

5.2 Literature review

Gait phase detection is one of the gait analysis branches and it is a process of identifying the gait phases of the subject while performing locomotion. It is usually done by analysing the gait parameters, such as joints angle, velocity, moment and power, ground reaction force (GRF) data and others. The application of gait phase detection study can be seen in sports (Alahakone, Senanayake, & Senanayake, 2010), rehabilitation treatment (Patterson, Delahunt, Sweeney, & Caulfield, 2014; Salarian et al., 2004), powered walking assistive device control (Crea, Cipriani, Donati, Carrozza, & Vitiello, 2015; Maqbool et al., 2017; Mazumder, Kundu, Lenka, & Bhaumik, 2017; Plauché, Villarreal, & Gregg, 2016) and others.

Accurate identification of the gait phase/event is very crucial in powering the prosthetic leg system. This is because the information on the gait phase/event is used to

control the actuator that acts as the joint replacement of the prosthetic leg. Thus, the stability and safety of the user depend on the efficiency of the gait phase/event identification. For example, a robotic leg prosthesis developed by a group of researchers from Vanderbilt University, USA used multiple mechanical sensors, absolute joint decoders, load cells and six-axis IMU units to extract data to detect the gait phase of the prosthetic leg. The gait detection process is conducted in the main controller unit, which then communicates with the servo controller unit to actuate the servo motors that was designed to replace knee and ankle joint of the leg based on the gait phase detection information (Lawson et al., 2014).

Pattern recognition method is commonly used as a tool to identify the gait phases based on the pattern of the output signal from the sensor/s when performing gait. Basically, a complete gait detection process consists of a few components, such as sensory system and its data acquisition, signal conditioning, and finally classification. Figure 5.1 summarises the gait detection process.

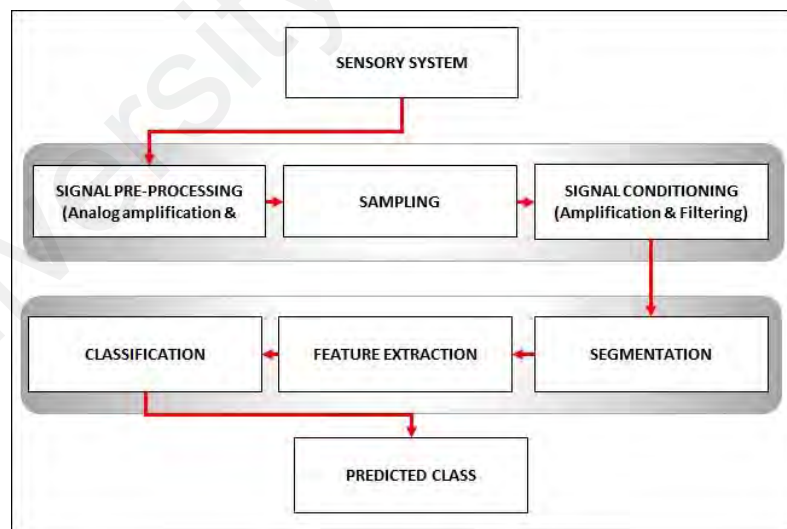


Figure 5.1: Illustration of the gait detection process.

The first component is the sensory system and its data acquisition. There are many types of sensory system adopted in a powered prosthetic leg system in acquiring data for the gait detection process. Most researchers proposed the use of electromyography (EMG) device as the sensory system (S. W. Lee et al., 2017; Ryu et al., 2017; Young,

Simon, Fey, & Hargrove, 2013). EMG reads the electrical signal of the muscle during muscle activation. Although EMG was proved to be accurate because it probes directly to the muscle, it has one unavoidable drawback, which it requires careful preparation of the skin to ensure the accuracy of the data (Jamal, 2012). Thus, it complicates the prosthesis' donning process and makes it impractical for everyday use. Other alternative for the sensory system proposed in the literature to detect intention is mechanical sensor, such as encoders, axial load cells, IMU and gyroscopes to get the kinetics and kinematics pattern from the user (Ishikawa et al., 2017; Simon et al., 2014; Young & Hargrove, 2016; Young, Simon, Fey, & Hargrove, 2014). This type of sensory system provides comprehensive information from the prosthetic leg as it utilizes many sensors that are located at every important joints and links of the prosthesis, which would require careful maintenance and calibration process.

Second, the signal conditioning process. Most of the sensory system signal needs to be conditioned to remove noise before it can be used for analysis. Some require the signal to be processed twice before it can be analysed, which is before the data acquisition and once again after the data acquisition. The first time is to process the output signal directly from the hardware (sensor/s) before it is sampled and go through the A/D conversion process. For instance, the amplitude of the sEMG signal is usually very small to be processed, thus, it has to be amplified before it is sent to the DAQ unit for sampling (Ryu et al., 2017; Xi, Tang, Miran, & Luo, 2017). The second one is meant to reduce the noise caused by the sampling process.

Finally, the classification phase, which consists of data segmentation, feature extraction and classification. Physiological signals, such as electromyogram (EMG), electrocardiogram (ECG) and others, and some response signal from the mechanical sensors usually fall into a non-stationary signal, which means that the statistical properties of the signal are not the same. Therefore, it requires segmentation process, that is to break

the signals into small segments so that the assumption that the signal of the segmented portion is stationary. In general, the methods of the segmentation for the non-stationary signal can be categorised into fixed-sized and adaptive segmentation.

Fixed-size segmentation, the signals are partitioned into multiple segments that are equal in size (Bao & Intille, 2004; Ravi, Dandekar, Mysore, & Littman, 2005; Xu et al., 2016). Meanwhile, in adaptive segmentation, the signals are divided into different parts that are unequal in size, based on their statistical properties (Azami, Hassanpour, Escudero, & Sanei, 2015; Ragnerius & Widelund, 2016; Sanei, 2013).

Feature extraction on the other hand is the process of retrieving properties, such as the statistical properties of the segmented signal. Various methods for feature extraction are found in the literature. Those methods are categorised into 3 main types. They are time domain features, frequency domain features, and time-frequency features.

Time-domain features (Geethanjali & Ray, 2014) implies features which are extracted in time domain. The process is simple and easy to implement. This is because the features can be directly extracted from the sensor's raw signal. The example of time-domain features are Zero Crossing, Mean Absolute Value, Slope Sign Change, Variance and Standard Deviation, Root Mean Square, Waveform Length and Histogram.

Frequency-domain features (Al-Angari, Kanitz, Tarantino, & Cipriani, 2016; Bao & Intille, 2004) is where the raw signals are Fourier-transformed to make it accessible in frequency domain. The frequency-domain enables the access to the power spectrum density of the signals. Nonetheless, this type of feature extraction method is rarely used for motion recognition. It is more common in muscle fatigue and motor unit recruitment analysis (Nazmi et al., 2016). Examples of the frequency-domain feature are mean and median frequency, power spectrum ratio and energy.

Time-Frequency features (Duan et al., 2016; Kakoty, Saikia, & Hazarika, 2013) are the features that combine the time and frequency information. One of the advantages is it can provide more non-stationary information by characterising the frequency parameters depending on the time location (Nazmi et al., 2016). One of the most common Time-Frequency features is Wavelet Packet Transform (WPT).

The features that have been extracted from the signals are represented in the feature vector. The next process is feeding the feature vector to the classifier for pattern mapping. Basically, the role of the classifier is to categorise the classes based on the features information provided in the feature vector so that the classes can be applied in the control algorithm for the controller to decide the next move. There are various types of classifier model that can be adopted. Among the popular approaches are Support Vector Machine (Chinas, Lopez, Vazquez, Osorio, & Lefranc, 2015; Naik, Kumar, & Jayadeva, 2010), k-Nearest Neighbour (Ishikawa et al., 2017), Decision Tree (Geethanjali & Ray, 2014), Artificial Neural Network (Delis et al., 2009; Fei et al., 2015), Fuzzy Logic (Khezri & Jahed, 2011), Linear Discriminant Analysis (Englehart & Hudgins, 2003), and Bayes Classifier (Sanchis, Juan, & Vidal, 2012).

This article presents the pattern recognition algorithm development and analysis based on the in-socket sensory system response signal described in the Chapter 3. 15 piezoelectric sensors were instrumented on the socket of the TF prosthetic leg and data were collected for walking activity. The classification algorithm was developed to classify the data into gait phases. The analysis was done to determine the best classification parameters (classifier type, window size and dataset to be used) to check the performance of the classifier across the different walking speed data and data collected from a different session. The findings are presented and discussed.

5.3 Material and methodology

This section describes the material and methodology used in this study.

5.3.1 Data collection

5.3.1.1 Subject and material

The sensory data during gait was collected from one subject, which is the same subject recruited for the previous experiment and the details about this subject can be found in section 4.4.1. As for the prosthetic leg, this study used a different quadrilateral socket from the one used in the previous experiment described in section 4.4.1. The reason for changing the socket was the previous socket was no longer fit the subject due to weight gain. Thus, a new socket was fabricated and piezo sensors were instrumented on the socket wall following the configuration summarised in F. Jasni (2017) and replicated the old socket sensors placement as much as possible. The same signal conditioning circuit that has been described in section 4.4.3 was adopted for this experiment. However, for data acquisition method, the sampling rate of 500 Hz was used in this experiment. This is due to the observation that, 500Hz sampling rate was sufficient to acquire information from the sensors.

5.3.1.2 Experiment procedure

For this experiment, the subject walked on a treadmill (Schiller MTM-1500, USA) with two speed setting. The first speed was set at 1.0 km/h, which was regarded as the normal walking speed. The second speed was 2.0 km/h as the fast walking speed. These speed settings were selected by the subject as the normal and fast walking speed.

Two force sensors (Round Force-Sensitive Resistor, Interlink Electronics, USA) were placed on the heel and toe of the foot to identify the heel strike and toe off of the prosthetic leg. Other than that, force sensors were also placed on top of the START, STOP, INCREASE and DECREASE button on the treadmill controller. Hence, when these buttons are pressed, the sensory data acquisition will also capture the signal.

The routine started with the subject performed quiet standing on the treadmill. Data recording was started from the ‘quiet standing’ phase. The START button was pressed and the treadmill was activated. The treadmill speed was increased by pressing the INCREASE button until the speed reached 1.0 km/h. The subject was allowed to walk with the selected speed for approximately 15 seconds. Then, the treadmill’s speed was increased again until it reached 2.0 km/h and the subject walked with this speed for 10 seconds. Then, the speed was decreased until the normal walking speed of 1.0 km/h. The subject walked with this speed for another ~15 seconds before the STOP button was pressed. The process was illustrated in Figure 5.2. Data recording was stopped after the treadmill and the subject was static. Data were collected from the two experiment sessions and ten trials were performed for every session. Each session was separated with a week gap.

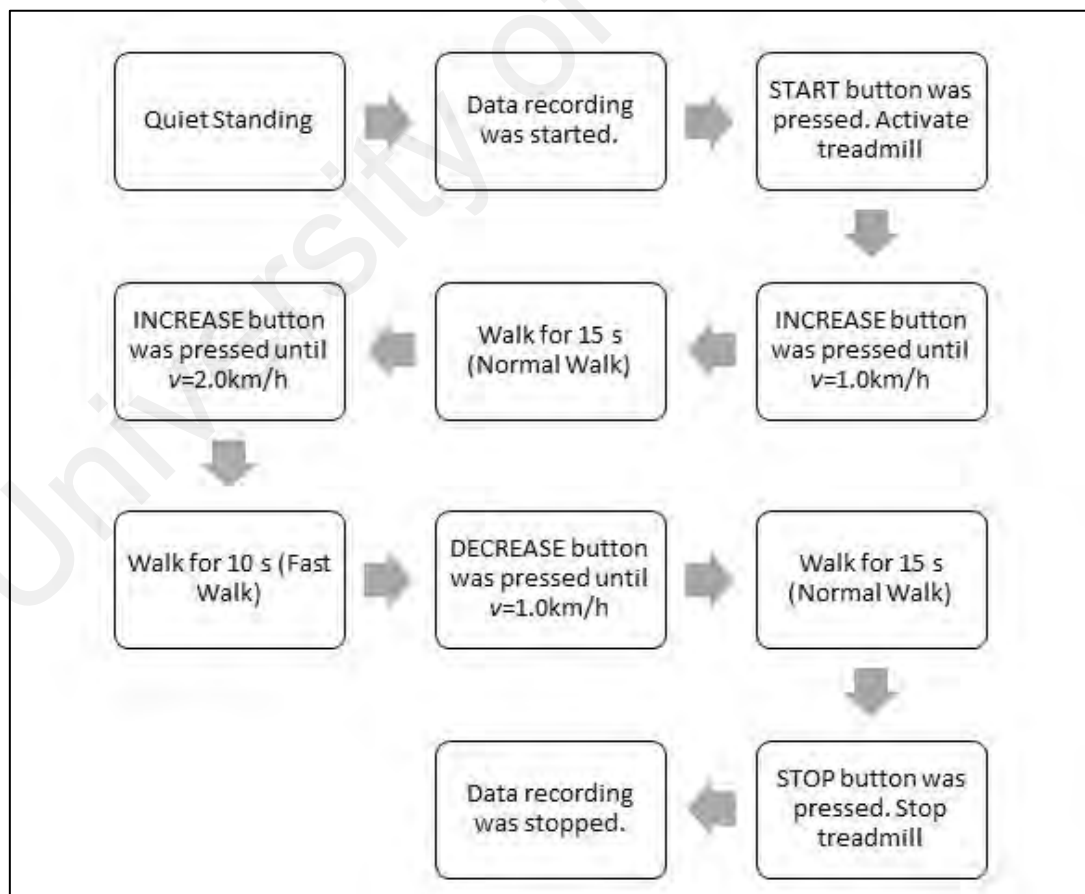


Figure 5.2: Flowchart of the experimental procedure.

Using the signal of the START, STOP, INCREASE and DECREASE buttons, the data from the single trial were segmented into 4 segments of speed transition 1 (from start to normal walk speed), normal walking, transition 2 (from normal walk speed to fast walk speed), fast walking and transition 3 (from fast walking to minimum speed before stopping (illustrated in Figure 5.4). For each trial, 6 normal-walk gait cycles from 20 gait cycles and 6 fast-walk gait cycles from 10 gait cycles were extracted. The six most similar cycles, in terms of time taken to complete one stride were chosen for normal walk and fast walk data, therefore all selected cycles can be assumed to have the equal step length, since the speed is already fixed (i.e. 1km/h). Therefore, 60 sets of data for normal and fast walking were extracted in one session. Fifty sets were used for classifier training purposes and the other 10 sets were used for testing purposes.



Figure 5.3: Experiment using treadmill to collect walking data.

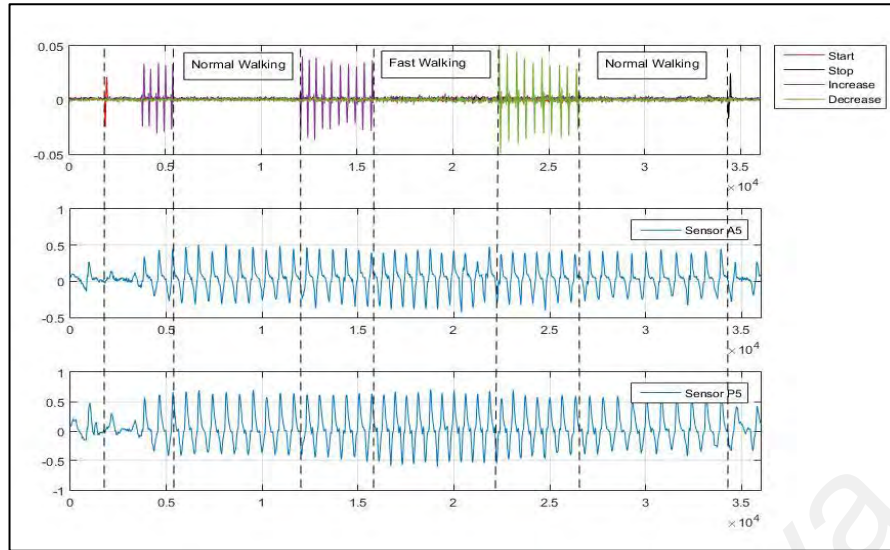


Figure 5.4: The segmentation process of the data that has been collected.

5.3.2 Feature extraction

In this study, five time-domain feature extraction methods were adopted. The advantage of the time-domain features is on its easy implementation because the features can be directly extracted from the raw sensor signal. The features selected for this study are:

1. Zero crossing (ZC)

ZC is a feature that describes how many times the signal cross zero within the selected window size. The expression to describe ZC is:

$$ZC = (\{x_n > 0 \text{ AND } x_{n+1} < 0\} \text{ OR } \{x_n < 0 \text{ AND } x_{n+1} > 0\}) \text{ AND } (|x_n - x_{n+1}| \geq \text{threshold}) \quad (5.1)$$

A threshold is used in the calculation with the purpose of abstaining the background noise. In this study, the threshold value set is 0.015V, based on the observation made earlier that the signal for quiet standing is less than that.

2. Slope sign change (SSC)

This feature is a count of the signal's slope changing sign within the window size. For the same reason with ZC, a threshold is added to eliminate the background noise, and threshold value set was 0.015V. The SSC count increased by one if:

$$SSC = \{x_n > x_{n-1} \text{ AND } x_n > x_{n+1}\} \text{ OR } \{x_n < x_{n-1} \text{ AND } x_n < x_{n+1}\} \\ \text{AND } [(|x_n - x_{n-1}| \geq \text{threshold}) \text{ OR } (|x_n - x_{n+1}| \geq \text{threshold})] \quad (5.2)$$

3. Peak (PK)

This feature retrieves the values of positive or negative peak/s found in the signal within the window size.

4. Wavelength length (WL)

Waveform length (WL) is the summation of the waveform's length over the window size. The mathematical expression for WL is:

$$WL = \sum_{n=1}^{N-1} |x_{n+1} - x_n| \quad (5.3)$$

5. Root mean square (RMS)

RMS is the measurement of the square root of the mean of the squared value of all components within the time frame.

$$RMS = \sqrt{\frac{1}{N} \sum_{n=1}^N x_n^2} \quad (5.4)$$

These 5 features were extracted from the sensors' signal for 3 different windows sizes. Literature proved that the optimal time delay for MPC prosthesis control is 100 ms (Farrell & Weir, 2007). Therefore, 3 window sizes, 25 ms, 50 ms, and 100 ms were chosen to analyse the effect of classification accuracy to the varying window size. Features were extracted from the signals of 15 sensors, for normal walk routine, fast walk routine and also combination of normal and fast walk routine. The feature vectors for all 3 windows sizes and 3 dataset were constructed, which finally resulted in 9 feature vectors. They are:

1. 3 feature vectors using normal walking speed data set but with different window size – NW25, NW50 and NW100
2. 3 feature vectors using fast walking speed data set but with different window size – FW25, FW50 and FW100

3. 3 feature vectors using both normal and fast walking speed data set but with different window size- COMB25, COMB50 and COMB100.

The size of each feature vector matrix is $n \times m$, where the value of n depends on the number of windows ($numwin$) needed to represent the signal. And m was determined based on the number of sensors and number of features. In this study, 15 sensors were utilized and 5 featured were extracted, therefore, $m=75$. The formula to calculate n and $numwin$ are:

$$numwin = \frac{signalTotalLength - wininc}{winsize} + 1 \quad (5.5)$$

$$\begin{aligned} \text{where, } wininc &= \text{window increment} \\ winsize &= \text{window size} \\ n &= numwin \times totaltrials \end{aligned} \quad (5.6)$$

5.3.3 Classifier

In order to choose the suitable classifier model to be adopted, the feature vectors developed were trained with 6 different classifier models. The classifiers are Complex Tree, Linear Support Vector Machine (SVM), Quadratic SVM, Cubic SVM, Bagged Tree, and Subspace Discriminant. The last two classifiers fall into ensemble type classifier (classification method that try to mimic human being nature of seeking multiple opinions before making a decision (Lior, 2009)).

The classification algorithm was trained to classify 4 classes of gait phases. They are LR, MSt and TSt, PSw, and SW. ‘Classification Learner’ apps by MATLAB was used to train the classifier. The cross-validation method (with k-fold=5) was used to evaluate the performance of the classifier model. Top two classifier that yielded the highest accuracy rate were chosen and the model was built using the Classification Learner apps.

5.3.4 Off-line Testing method

The final aim of this section was to decide the best classifier model, including the decision on the classifier type, the window size, and training data set. Thus, a few test methods have been designed.

First, the performance of the shortlisted classifier models was evaluated using 10 trials of normal and fast walk fresh data (i.e. data that was not used for training). The accuracy rate between the true class and the predicted class from the classifier model was calculated and plotted. To calculate the classification rate, the expression below was used:

$$\text{Classification \%} = \frac{TN + TP}{P + N} \times 100 \quad (5.7)$$

where, TN = true negative. Predicted negative, and its negative
 TP = true positive. Predicted positive, and its positive
 P = total number of positive elements
 N = total number of negative elements

The ANOVA single factor analysis was conducted on the classification accuracy with the varying parameters (i.e. window size and training data set) for both normal walking and fast walking tests. The p-value was recorded.

Other than the classification rate, the processing time taken to complete the classification task was also recorded and tabulated. The average of the classification rate and processing time of each classifier model for all 3 test data sets were calculated and plotted.

The second test was to evaluate the generality of the chosen classifier across the different session. Thus, a fresh data from the different session was used to evaluate the classifier performance. The classification rate was tabulated and plotted in the next section.

5.3.5 Reduction of number of sensors

In this section, the adopted method to reduce the number of sensors is described. In order to do so, the Sequential Backward Selection (SBS) algorithm was utilized. SBS is

one of the feature selection algorithm that starts with a full set of the feature vector and removes one feature at a time in which, the removal does not decrease the performance of the classifier or increasing the classification rate by its absence (Chandrashekar & Sahin, 2014).

5.4 Results

The results for training, and test performance of the classifiers were presented in this section. The performance after the optimization of the classifier's features was also presented in this section.

5.4.1 Training performance

Table 5.1 shows the classification rate of 6 different classifiers using 3 different window sizes and 3 different training datasets. Figure 5.5 shows the average classification percentage for each classifier.

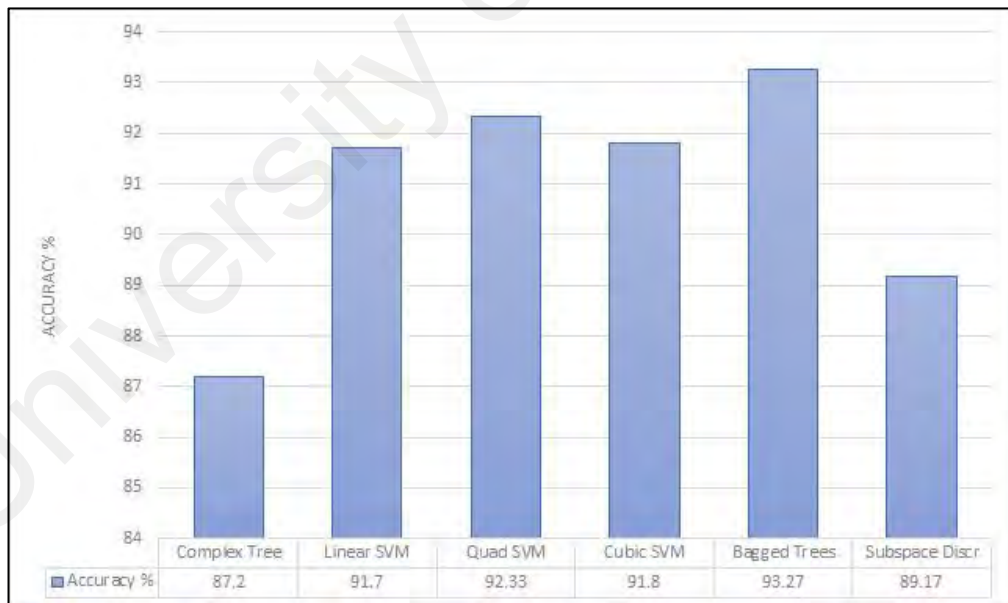


Figure 5.5: The average training accuracy percentage for different classifiers.

Table 5.1: Accuracy rate (%) for 6 classifiers with different training data set and window sizes.

		NW	FW	Combined	Average
Complex tree	100 ms	90.8	87	85	87.2
	50 ms	89.6	88.6	83.9	
	25 ms	89.7	86.3	83.8	
Linear SVM	100 ms	94	93.8	91	91.7
	50 ms	92.8	91.8	89.8	
	25 ms	91.8	89.8	90.6	
Quad SVM	100 ms	94.1	94.5	92.6	92.3
	50 ms	93	92.6	91.4	
	25 ms	92.2	89.9	91	
Cubic SVM	100 ms	95	94	91.2	91.8
	50 ms	92.4	92.5	90.7	
	25 ms	91	89.4	90	
Bagged Trees	100 ms	95.6	94.8	93.4	93.3
	50 ms	94	92.6	91.8	
	25 ms	93.6	91.7	91.9	
Subspace discriminant	100 ms	94.2	93.5	89.5	89.2
	50 ms	89.8	89.1	85	
	25 ms	89.4	87.9	84.1	

Note: NW = Normal Walk Dataset, FW = Fast Walk Dataset.



Figure 5.6: The confusion matrix for Bagged Trees classifier. Class 1=LR, Class 2=MSt, Class 3=TSt, Class 4=PSw and Class 5=Sw.

From the bar chart (Figure 5.5), it can be observed that the Bagged Trees classifier yielded the classification rate of 93.27%, which put it as the best classifier among the others. Therefore, Bagged Trees classifier was selected to be used for off-line testing.

Figure 5.6 shows the confusion matrix for the Bagged Trees classifier. Class 1 and Class 5, which represent LR and SW phase, respectively, showed the highest accuracy. This is consistent with the findings in Section 4.6 that the sensors are more active in these phases. Class 2, 3 and 4 that represent MSt, TSt and PSw showed a lower percentage since fewer sensors' activity was monitored. However, the percentage (>85%) indicates that the phases are still recognisable by the classification algorithm probably by the transition from one phase to another that triggered more sensors' activity.

5.4.2 Test performance

The test performance for two different analysis were presented in this section. The first analysis was to test the performance of the classifier for normal and fast walking test and its effect to the varying classifier parameters. The second analysis was to evaluate the selected classifier model in classifying test data from different sessions.

5.4.2.1 Normal vs Fast walking test

Table 5.2 and Figure 5.7 shows the average accuracy rate and the p-value calculated for the variations (i.e. window size and training dataset) of BT classifier for different window sizes (25 ms, 50 ms, and 100 ms) and training dataset (NW dataset, FW dataset, and combined dataset) for normal walking test, while Table 5.3 and Figure 5.8 are for fast walking test. The figures stated in both tables are the average value for accuracy rate and its standard deviation yielded for 10 trials of normal walking and 10 trials of fast walking test data.

Table 5.2: Accuracy rate (%) and p-value for Normal Walking test using BT classifier.

	25 ms	50 ms	100 ms	p-value	Average
NW Dataset	88.54±3.84	88.55±8.78	89.73±5.73	5.17E-11	88.94±0.559
FW Dataset	81.04±6.22	86.55±3.91	76.97±9.11	3.35E-06	81.52±3.926
Combined Dataset	78.45±6.85	63.05±16.91	90.19±8.41	4.35E-17	77.23±11.11
p-value	9.99E-10	3.56E-20	4.03E-08		

Note: NW = Normal Walk Dataset, FW = Fast Walk Dataset.

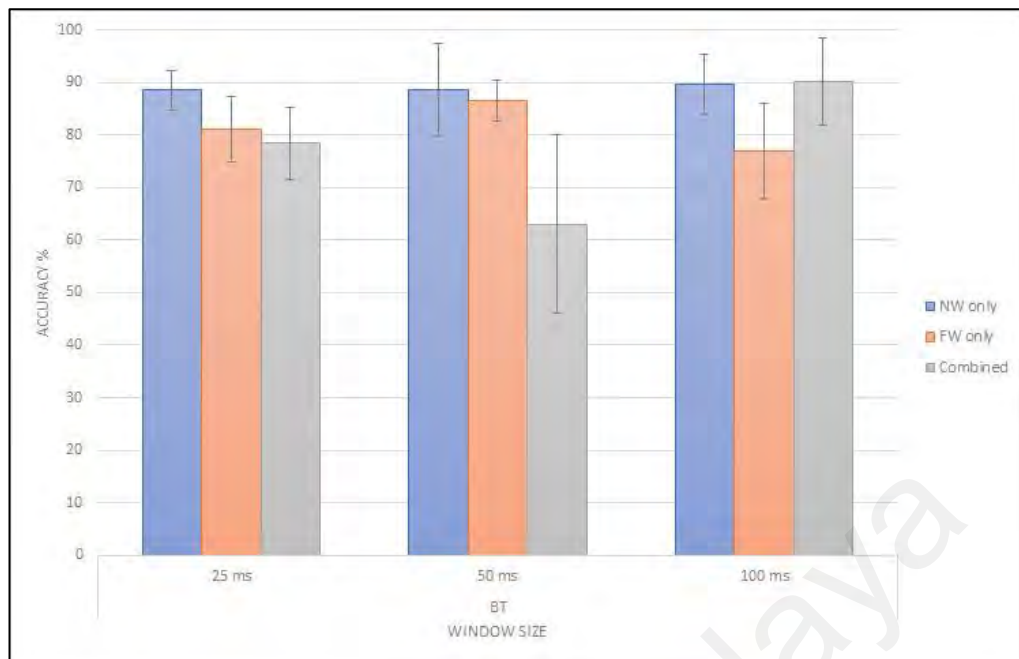


Figure 5.7: Average accuracy rate for 10 trials of normal walking test using BT classifier that was trained with different window size and training dataset.

Table 5.3: Accuracy rate (%) and p-value for Fast Walking test using BT classifier.

	25 ms	50 ms	100 ms	p-value	Average
NW Dataset	81.18±4.74	75.31±3.94	89.41±4.25	7.27E-05	81.97±5.783
FW Dataset	87.49±3.07	88.42±3.69	84.57±6.73	0.199	86.83±1.64
Combined Dataset	87.49±3.44	88.8±8.73	82.07±5.84	0.025	86.12±2.913
p-value	0.007	1.18E-06	0.053		

Note: NW = Normal Walk Dataset, FW = Fast Walk Dataset.

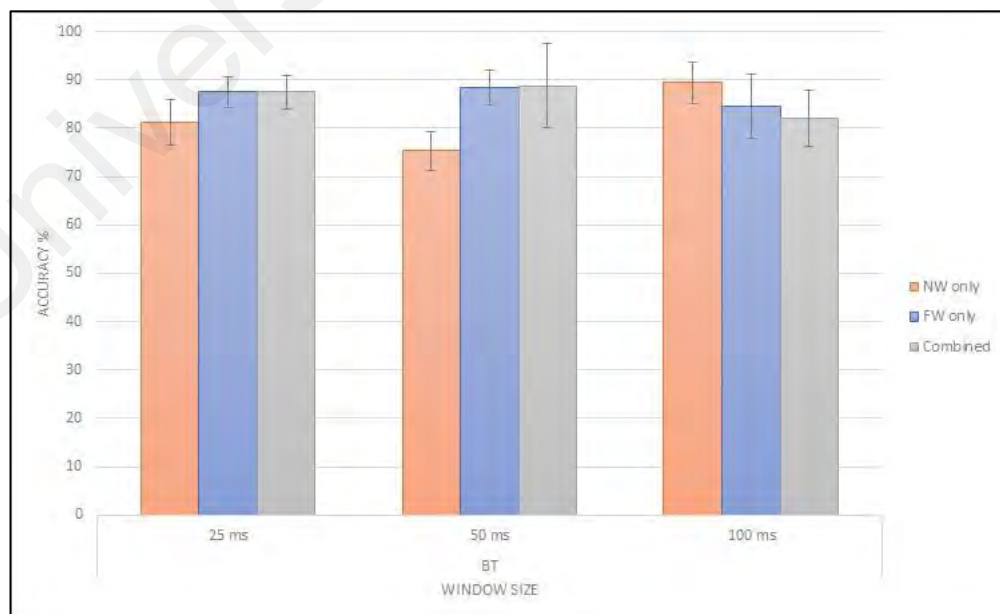


Figure 5.8: Average accuracy rate for 10 trials of fast walking test using BT classifier that was trained with different window size and training dataset.

From the tables, it can be observed that the combination of the combined feature vector and a window size of 100 ms resulted in the highest accuracy rate for the normal walking test with a mean \pm SD value of 89.73 \pm 5.73. It can also be deduced that, the changes in window size and training data set did significantly affected the accuracy of normal walking test ($p<0.05$). However, the performance of NW feature vector is more consistent for all three window sizes. The mean \pm SD calculated for NW feature vector for all three window sizes is 88.94 \pm 0.559.

On the other hand, for the fast walking test, the NW feature vector and a window size of 100 ms yielded the highest accuracy, 89.41 \pm 4.25. However, in average, FW feature vector-based classifier outperformed the rest with a mean \pm SD of 86.83 \pm 1.64. The changes in window size gave affect the classifier performance significantly for NW and combined feature vectors ($p<0.05$), but not for FW feature vector ($p>0.05$) which indicates that the changes in window size did not significantly affect the performance of the classifier trained with FW dataset.

The findings suggest that for an individual test, the respective training set still yielded the best results even with a different window size. Furthermore, training the classifier with a combined NW and FW feature vector does not show any improvements to the classifier performance for both tests.

(a) ***Window size analysis***

Figure 5.9 illustrates the performance of the classifier with respect to the different window size. The blue and red bar represents the mean accuracy percentage for multiple trials (10 trials for normal walking test and 10 trials for fast walking test). The final column (grey colour) in each section illustrates the mean of the accuracy percentage for both normal and fast walking tests and its standard deviation.

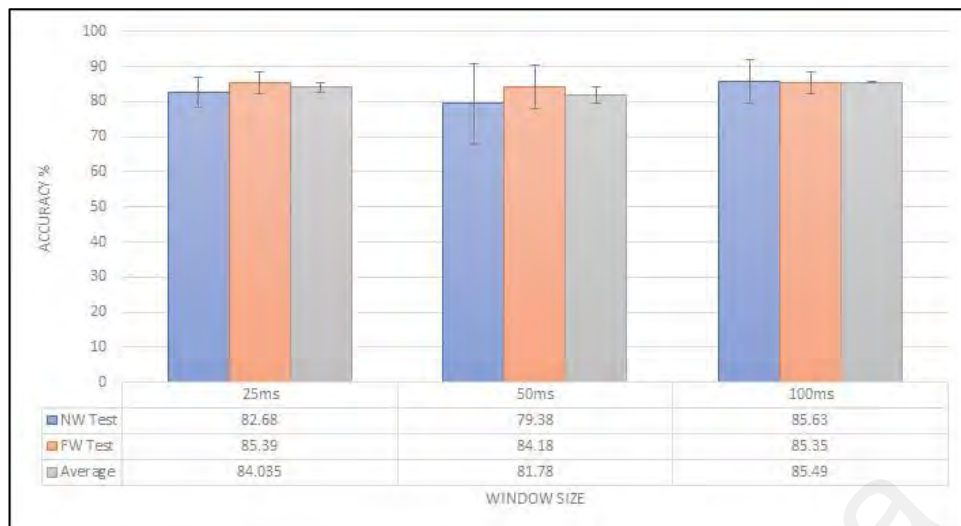


Figure 5.9: The average accuracy rate for 25 ms, 50 ms, and 100 ms in normal and fast walking test.

The window size 100 ms shows the highest accuracy percentage and a small standard deviation (85.49 ± 0.14). Meanwhile, Figure 5.10 illustrates the time taken for a complete testing process for a 1.434 s testing data using different window size. It shows that the window size of 100 ms yielded the smallest processing time compared to the 25 ms and 50 ms.

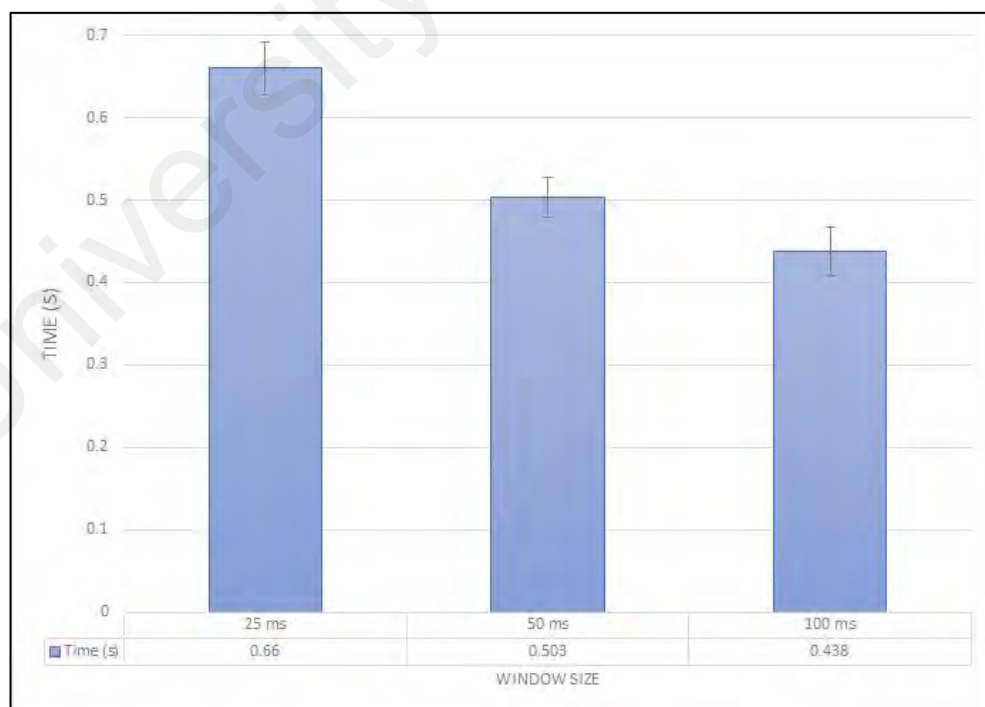


Figure 5.10: The average computing time for BT classifier with 25, 50 and 100 ms window size to classify a 1.434 s long testing data.

Thus, it can be deduced that the window size of 100 ms is the best to be used in this application. The window size selected is still within the range of the acceptable delay time for prosthesis controller, which was studied by Farrel and Weir (2007). The findings from this study indicate that the optimal controller delay is approximately between 100 ms for fast movement and 125 ms for slower movement (Farrell & Weir, 2007).

(b) *Training feature vector analysis*

Figure 5.11 shows the performance of the classifier for normal and fast walking test with varying dataset used to develop the algorithm.



Figure 5.11: The average accuracy rate for NW dataset, FW dataset and Combined dataset in normal and walking test.

It can be observed that NW dataset outperformed the other two by yielding the highest accuracy rate (mean \pm SD=87.89 \pm 0.085). Although the standard deviation is not the lowest among the other three, the variation was acceptable (i.e. within the \pm 1SD of its normal distribution).

The findings suggest that the NW dataset is the optimal dataset to be used in order for the classifier to be used in a larger range walking speed setting. However, in this analysis, only 2 speeds ranging from 1.0 km/h to 2.0 km/h were considered. The speed was chosen based on the subject's self-preference. The 1.0 km/h is considered as the normal walking

phase, and 2.0 km/h as the fast walking speed. Thus, the inferences made from the findings are bound to this limitation.

5.4.2.2 Between sessions analysis

Table 5.4 shows the average accuracy rate of the selected classifier (BT with 100 ms window size and NW dataset) for test data from the same session (dataset used for training) and different session.

Table 5.4: The classification accuracy for different sessions.

	Classification accuracy (%)
Session 1	88.94
Session 2	87.71
Average	88.32

The mean \pm SD calculated is 88.32 \pm 0.615, which shows high accuracy and consistency between the sessions. Thus, it can be deduced that the in-socket sensory system is feasible to be used to detect gait phases even though the socket is already removed from the stump and re-worn, the classifier performance is still good.

5.4.3 Reduced number of sensors performance

Based on the results of the SBS feature selection method, Sensor P1 was eliminated and new feature vector was developed. The BT classifier model with 100 ms window size, trained with new feature vector was built and tested on the same test data. The result indicated that eliminating sensor P1 from the feature vector did not significantly affect the classifier performance in gait phase detection for walking motion, in fact, some increment in the accuracy rate was detected. The accuracy rate of the optimized classifier was 0.17% higher than the original classifier. Therefore, it can be deduced that the proximal sensor on the posterior side can be removed as it will not affect the performance of the classifier in the gait phase identification.

5.5 Discussion

In this study, analyses were performed to select the classifier, window size and training data set that could yield the highest classification accuracy in detecting the five gait phases, namely; Loading Response (LR), Midstance (MSt), Terminal Stance (TSt), Pre-swing (PSw) and Swing (Sw). Findings show that the Ensemble Bagged Trees yielded the highest accuracy, which is 93.3%. This is in agreement with study conducted by (Dietterich, 2000) which claimed that ensemble type classifier is better than single classifier in three aspects, namely; statistical, computational, and representational.

As for the window size, findings show that 100ms performed best in yielding the highest accuracy. This means, the algorithm will classify the signal for every 0.1s and determine which gait phase that the signal indicates. The findings might be related to the fact that the muscle contracts in a very slow rate (i.e. less than 20 Hz) which was proven by Prendergast et al. (2005). Thus, the significant change in force profile, which was captured by the piezoelectric sensors can only be better interpreted by the signals in a wider window segment. A test was performed to classify a 1.438s long data, consist a complete stride, and the time taken to complete the classification is 0.438s, which is the lowest among the other two options. Assuming the processing time is divided equally to the five gait phases, each gait phase will consume ~ 0.09 s to be classified, which is still lower than the optimal controller delay time deduced by Farrell and Weir (2007), in which 100ms for fast movement and 125ms for slow movement.

Performance of the classifier using the normal walking data as the training data is the best as compared to classifier which was trained with fast walking and combined walking dataset. The results suggested that, the normal walking data is more flexible to be used to classify different speed (i.e. 1km/h and 2km/h) walking gait phases. However, tests for more speed setting should be tested in the future to investigate the range of that training dataset validity.

The performance of in-socket sensory system-based classifier is 8.13% lower than the impedance-based sensory system in CYBERLEGS (Ambrozic et al., 2014), which the average classification accuracy calculated for steady-state gait was 96.45%. Meanwhile, the classification accuracy is 8.68% lower than the neuro-mechanical fusion sensory system proposed by Huang et al. (2011). To compare the results obtained from a study that utilized sEMG sensors on the residual limb only (H. Huang et al., 2009), the classifier proposed by this study performed better, by 2.65% in classifying the level walking gait phases. Table 5.5 summarizes the difference between the proposed in-socket sensory system in this study, and the results from other studies.

Table 5.5: Summary of the performance comparison between the proposed in-socket sensory system classifier and other studies.

	Sensory system type	Average classification accuracy %	Difference from the proposed in-socket sensory system
(Jasni et al., 2016)	In-Socket sensory system	88.32	
(Ambrozic et al., 2014)	Prosthetic-device oriented	96.45	-8.13
(H. Huang et al., 2009)	User's-biological-input oriented	85.67	+2.65
(H. Huang et al., 2011)	Neuro-mechanical fusion	97	-8.68

Note: - sign represents the classification accuracy is less than the respective study's percentage, and + sign represents the classification accuracy is greater than the respective study's percentage.

The findings show that the in-socket sensory system performance is comparable to the EMG-based classifier (H. Huang et al., 2009), but lower than the sensory system that integrated the mechanical sensors (Ambrozic et al., 2014; H. Huang et al., 2011) in it. It can be deduced from this results that the multiple sensors used, which were placed on multiple positions (i.e. joints, foot, and residual limb) of the prosthetic device as described in Ambrozic et al. (2014) and H. Huang et al. (2011), improved the performance of the classifier in gait detection due to the richer information provided. The information extracted from only the residual limb by EMG and piezo-based in-socket sensory system is not sufficient to optimize the classifier performance. However, it is believed the performance of piezo-based in-socket sensory system can be improved by investigating

methods to extrapolate the sensory response's signal to other meaningful information, such as the GRF information. In addition, this study only considered the time-domain features in developing the classifier model. Extending the options to frequency-domain and time-frequency domain might reduce the classification error.

5.6 Summary

This study analysed the optimal parameters for pattern recognition algorithm using data from the piezo-based in-socket sensory system in detecting the gait phase for TF amputee. Findings showed that the ensemble-type BT classifier, which was trained with feature vector extracted from NW signal with a window size of 100 ms performed best in classifying the gait phases.

However, this study is bound to the limitations that only one subject was used for the data collection and the effect of variability of feature extraction methods are not evaluated in this study. In addition, the algorithm developed was tested on a speed range of 1.0 km/h to 2.0 km/h only. Hence, future work is needed to evaluate the effects of the classifier with wider range of walking speed. Besides, further study to investigate the optimal feature extraction methods (i.e. frequency domain, time-domain frequency domain) should also be conducted.

CHAPTER 6: CONCLUSIONS AND RECOMMENDATIONS

In this chapter, the summary of the findings on the analyses that have been reported in the earlier chapters is presented. The limitations of this study and recommendation for future research are also stated in this chapter.

6.1 Summary of the findings

This study was conducted based on three objectives. Therefore, the summary of the findings is discussed with respect to the objectives outlined.

1. To configure and analyse the piezoelectric-based in-socket sensory system for transfemoral prosthetic leg's application.

Findings in Chapter 3 have proven that a PVDF-based piezoelectric sensor with rectangular shape should be used as the sensors based on the results of the simulation studies. In addition, the findings from the bench-experiment led to the conclusion that the CA FIT cantilever with elastic foundation mounting configuration and zig-zag orientation should be adopted in instrumenting the piezo sensors to the socket. It is also proven from Chapter 3 that the piezo-based in-socket sensory system for TF prosthetic leg could produce a consistent and reliable output signal with good sensitivity based on the signal consistency analysis conducted using the instrumented socket for one unilateral amputee.

Hence, the in-socket sensory system for TF prosthetic leg has been successfully configured and proved to be reliable in producing consistent signal during gait.

2. To analyse the proposed sensory system's response and investigate its feasibility as a gait detection tool.

The study described in Chapter 4 aimed to achieve this objective. Based on the findings, it is proven that the sensors' response highly corresponds to the gait phases while walking. Hence, it can be concluded that the proposed in-socket sensory system can be used to detect gait phases. Other than that, it is also proven that the sensory system can

be used to detect the different walking types based on the findings that there was a significant difference in the response for the different types of walking motion (single stride walking and continuous walking).

3. To develop the gait phase classification algorithm using the sensory system response and evaluate the classifier performance.

A classifier model that used the data from the proposed sensory system to detect gait phases has been successfully developed. Analyses have been performed to determine the classifier parameters and it can be concluded that the classifier, which was trained with features extracted from the normal walking data using the window size of 100 ms performed best in classifying the signal for walking ranging from 1.0 km/h to 2.0 km/h. It is also proven that the sensory system works best with a minimum of 14 sensors based on the results obtained from the SBS feature selection method.

Summarizing the findings obtained in all three studies, it can be concluded that the main contributions of this study are:

1. The study offered a research platform for utilization of the piezo-based in-socket sensory system in TF prosthetic leg. To date, this research work is the first that proposed the utilization of the piezo sensors' signal located inside the TF socket to perform gait detection.
2. This study provided a guideline to design the piezo-based in-socket sensory system for TF prosthesis gait detection. Some key points that need to be highlighted are:
 - a. The placement of the sensors is user-dependent. Thus, MVC evaluation (described in section 3.3.3) has to be performed on individual user so that the active muscle area can be identified, and sensors are placed on the active area.

This is only needed once for each user. The same placement can be used for the same user if the socket must be changed.

- b. Since the sensors' placement is user-dependent, hence, the classification algorithm is also user-dependent. Thus, training data has to be collected from each user. It is a common practice for a new prosthetic user that he/she has to undergo training with the physicians/certified prosthesis officer to ensure he/she is confident enough to use the prosthetic. Therefore, it is suggested that the training data collection process can also be done during the training sessions. Hence, the optimal classifier parameter, the walking speed range that can be detected by the classifier can be identified.

6.2 Limitations of the study

The results and findings reported in this study are restricted to the limitations below:

1. This study is limited to the efficacy investigation of the piezo-based in-socket sensory system in detecting gait phases for TF prosthetic leg. Hence, the implementation of the proposed sensory system in powered knee prosthetic leg control setting was not discussed in this study.
2. Only one subject was recruited throughout the study. The same subject was used in determining the position of the sensors by performing MVP experiment and consistency study described in Chapter 3, data collection to analyse the sensors' response, explained in Chapter 4, data collection for gait phase's classification process described in Chapter 5. The rationale of using only one subject is because this study focusses on configuring the piezo-based in-socket sensory system and developing the gait detection algorithm using the proposed sensory response. It is proven in the literature that the variance in muscle activity and the interface pressure among TF amputees are relatively high than the normal person. Study

conducted by Wentink et al. (Wentink, Prinsen, et al., 2013) proved that the variation ratio of the lower limb muscles' activity including quadriceps and hamstring is very high. Meanwhile, work by Hong and Mun (2005) proved that the variation of the pressure measurement between two TF subjects were quite big. Therefore, it can be deduced that different subject will require different configuration and gait detection algorithm. Thus, recruitment of only one subject is deemed sufficient at this stage.

3. This study does not discuss the force profile or pressure profile of the stump-socket quantitatively. The relative force/pressure profile obtained via the piezo sensors were analysed with the intention to study its feasibility to be used as a gait detection tool. Therefore, the quantitative measurement of the force/pressure was neglected in this study.
4. All the findings and deductions made in this study was obtained by analysing the data that was collected using the prosthetic leg components described in section 4.4.1. Varying the components might yield a different outcome. This study did not analyse the variation in the outcome caused by varying the prosthetic components.

6.3 Future recommendations

In order to tackle the limitations of this study, the recommendations below are suggested:

1. The generality of the proposed sensory system and its classification algorithm should be tested with more TF amputees with different stump length. Thus, the varying parameters such as the resolution of the sensory system, classifier parameters and others can be optimised.
2. Optimization study on improving the accuracy of the classifier in detecting gait should be conducted. The effect of using different feature extraction method (i.e.

frequency domain and time-frequency domain) is not tested in this study, thus, it is good to conduct the study with the aim to increase the classification accuracy.

3. Study on optimizing the number of sensors should be done. In this study, only SBS feature selection method was tested to reduce the number of sensors. Other optimization methods should be utilized and compare the classification accuracy with the accuracy achieved by this study.
4. The study on intention recognition (gait initiation and gait termination) using the proposed sensory system should be conducted. This study offered a platform on gait classification using the sensory system's response signal, thus, it can be foreseen that gait intention detection can also be implemented.
5. Future works to study other locomotion mode and activity such as stairs climbing, sit-to-stand and stand-to-sit, running, jumping and others should be done.
6. Study on the life-span and long-term performance of the proposed in-socket sensory system should be conducted in terms of sensors sensitivity and classifier algorithm. From this, estimation on the maintenance schedule (i.e. how often the sensory system needs to be changed) can be made. In addition, investigation on the performance of the sensory system with changing stump (i.e. thinner/less volume) should also be conducted.
7. Investigation on the correlation between the sensory system's response and the variation of the prosthetic components used should be done.
8. Integration and implementation of the proposed piezo-based in-socket sensory system into the powered-knee prosthetic leg control system. The real-time efficiency of the prosthetic leg controller, which used the proposed sensory system as the feedback should be evaluated.

REFERENCES

- Adams, T. P., Brillhart, B. A., Bushek, D. J., & Kroll, K. (2001). Piezoelectric film transducer for cochlear prosthetic: Google Patents.
- Agrawal, T. K., Thomassey, S., Cochrane, C., Lemort, G., & Koncar, V. (2017). Low-Cost Intelligent Carpet System for Footstep Detection. *IEEE Sensors Journal*, 17(13), 4239-4247.
- Al-Angari, H. M., Kanitz, G., Tarantino, S., & Cipriani, C. (2016). Distance and mutual information methods for EMG feature and channel subset selection for classification of hand movements. *Biomedical Signal Processing and Control*, 27, 24-31.
- Alahakone, A. U., Senanayake, S. M. N. A., & Senanayake, C. M. (2010, 6-9 Dec. 2010). *Smart wearable device for real time gait event detection during running*. Paper presented at the 2010 IEEE Asia Pacific Conference on Circuits and Systems.
- Ambrozic, L., Gorsic, M., Geeroms, J., Flynn, L., Lova, R. M., Kamnik, R., Munih, M., & Vitiello, N. (2014). CYBERLEGs: A User-Oriented Robotic Transfemoral Prosthesis with Whole-Body Awareness Control. *IEEE Robotics & Automation Magazine*, 21(4), 82-93.
- Andrysek, J., Liang, T., & Steinnagel, B. (2009). Evaluation of a Prosthetic Swing-Phase Controller With Electrical Power Generation. *IEEE Transactions on Neural Systems and Rehabilitation Engineering*, 17(4), 390-396.
- Arami, A., Aminian, K., Forchelet, D., & Renaud, P. (2014, 22-24 Oct. 2014). *Implantable and wearable measurement system for smart knee prosthesis*. Paper presented at the 2014 IEEE Biomedical Circuits and Systems Conference (BioCAS) Proceedings.
- Arami, A., Simoncini, M., Atasoy, O., Ali, S., Hasenkamp, W., Bertsch, A., Meurville, E., Tanner, S., Renaud, P., Dehollain, C., Farine, P. A., Jolles, B. M., Aminian, K., & Ryser, P. (2013). Instrumented Knee Prosthesis for Force and Kinematics Measurements. *IEEE Transactions on Automation Science and Engineering*, 10(3), 615-624.
- Azami, H., Hassanpour, H., Escudero, J., & Sanei, S. (2015). An intelligent approach for variable size segmentation of non-stationary signals. *Journal of Advanced Research*, 6(5), 687-698.
- Bai, O., Kelly, G., Fei, D. Y., Murphy, D., Fox, J., Burkhardt, B., Lovegreen, W., & Soars, J. (2015, 1-4 Nov. 2015). *A wireless, smart EEG system for volitional control of lower-limb prosthesis*. Paper presented at the TENCON 2015 - 2015 IEEE Region 10 Conference.
- Bao, L., & Intille, S. S. (2004). Activity Recognition from User-Annotated Acceleration Data. In A. Ferscha & F. Mattern (Eds.), *Pervasive Computing: Second International Conference, PERVASIVE 2004, Linz/Vienna, Austria, April 21-23, 2004. Proceedings* (pp. 1-17). Berlin, Heidelberg: Springer Berlin Heidelberg.

- Bogey, R. A., & Barnes, L. A. (2017). An EMG-to-Force Processing Approach for Estimating in Vivo Hip Muscle Forces in Normal Human Walking. *IEEE Transactions on Neural Systems and Rehabilitation Engineering*, 25(8), 1172-1179.
- Bonnefoy-Mazure, A., & Armand, S. (2015). Normal gait. In F. Canavese & J. Deslandes (Eds.), *Orthopedic Management of Children with Cerebral Palsy: A comprehensive Approach* (pp. 199-214). New York, USA: Nova Science Publishers, Inc.
- Búa-Núñez, I., Posada-Román, J. E., Rubio-Serrano, J., & Garcia-Souto, J. A. (2014). Instrumentation System for Location of Partial Discharges Using Acoustic Detection With Piezoelectric Transducers and Optical Fiber Sensors. *IEEE Transactions on Instrumentation and Measurement*, 63(5), 1002-1013.
- Buckley, J. G., De Asha, A. R., Johnson, L., & Beggs, C. B. (2013). Understanding adaptive gait in lower-limb amputees: insights from multivariate analyses. *J Neuroeng Rehabil*, 10(98).
- Campanella, H., Camargo, C. J., Garcia, J. L., Daza, A., Urquiza, R., & Esteve, J. (2012). Thin-Film Piezoelectric MEMS Transducer Suitable for Middle-Ear Audio Prostheses. *Journal of Microelectromechanical Systems*, 21(6), 1452-1463.
- Cannan, J., & Hu, H. (2013, 9-11 Sept. 2013). *Feasibility of Using Gyro and EMG Fusion as a Multi-position Computer Interface for Amputees*. Paper presented at the 2013 Fourth International Conference on Emerging Security Technologies.
- Carse, B., Meadows, B., Bowers, R., & Rowe, P. (2013). Affordable clinical gait analysis: An assessment of the marker tracking accuracy of a new low-cost optical 3D motion analysis system. *Physiotherapy*, 99(4), 347-351.
- Cerqueira, A. S. O. d., Yamaguti, E. Y., Mochizuki, L., Amadio, A. C., & Serrão, J. C. (2013). Ground reaction force and electromyographic activity of transfemoral amputee gait: a case series. *Revista Brasileira de Cineantropometria e Desempenho Humano*, 15(1).
- Chandrashekar, G., & Sahin, F. (2014). A survey on feature selection methods. *Computers & Electrical Engineering*, 40(1), 16-28.
- Chinas, P., Lopez, I., Vazquez, J. A., Osorio, R., & Lefranc, G. (2015). SVM and ANN Application to Multivariate Pattern Recognition Using Scatter Data. *Latin America Transactions, IEEE (Revista IEEE America Latina)*, 13(5), 1633-1639.
- Choi, J., Duan, X., Li, H., Wang, T. D., & Oldham, K. R. (2017). Multi-Photon Vertical Cross-Sectional Imaging With a Dynamically-Balanced Thin-Film PZT z-Axis Microactuator. *Journal of Microelectromechanical Systems*, 26(5), 1018-1029.
- Costilla-Reyes, O., Scully, P., & Ozanyan, K. B. (2015, 1-4 Nov. 2015). *Temporal pattern recognition for gait analysis applications using an "intelligent carpet" system*. Paper presented at the 2015 IEEE SENSORS.

- Cotton, D. P. J., Chappell, P. H., Cranny, A., White, N. M., & Beeby, S. P. (2007). A Novel Thick-Film Piezoelectric Slip Sensor for a Prosthetic Hand. *IEEE Sensors Journal*, 7(5), 752-761.
- Crea, S., Cipriani, C., Donati, M., Carrozza, M. C., & Vitiello, N. (2015). Providing Time-Discrete Gait Information by Wearable Feedback Apparatus for Lower-Limb Amputees: Usability and Functional Validation. *IEEE Transactions on Neural Systems and Rehabilitation Engineering*, 23(2), 250-257.
- Creighton, F. X., Guan, X. Y., Park, S., Kymissis, I., Nakajima, H. H., & Olson, E. S. (2016). An Intracochlear Pressure Sensor as a Microphone for a Fully Implantable Cochlear Implant. *Otology & Neurotology*, 37(10), 1596-1600.
- Dante, A., Bacurau, R. M., Spengler, A. W., Ferreira, E. C., & Dias, J. A. S. (2016). A Temperature-Independent Interrogation Technique for FBG Sensors Using Monolithic Multilayer Piezoelectric Actuators. *IEEE Transactions on Instrumentation and Measurement*, 65(11), 2476-2484.
- Dedić, R., & Dindo, H. (2011, 27-29 Oct. 2011). *SmartLeg: An intelligent active robotic prosthesis for lower-limb amputees*. Paper presented at the 2011 XXIII International Symposium on Information, Communication and Automation Technologies.
- Delis, A. L., de Carvalho, J. L. A., Borges, G. A., de Siqueira Rodrigues, S., dos Santos, I., & da Rocha, A. F. (2009, 3-6 Sept. 2009). *Fusion of electromyographic signals with proprioceptive sensor data in myoelectric pattern recognition for control of active transfemoral leg prostheses*. Paper presented at the Annual International Conference of the IEEE Engineering in Medicine and Biology Society, 2009. EMBC 2009. , Minnesota, USA.
- Dietterich, T. G. (2000). *Ensemble methods in machine learning*. Paper presented at the International workshop on multiple classifier systems.
- Dong, W., Xiao, L., Hu, W., Zhu, C., Huang, Y., & Yin, Z. (2017). Wearable human-machine interface based on PVDF piezoelectric sensor. *Transactions of the Institute of Measurement and Control*, 39(4), 398-403.
- Du, L., Zhu, X., & Zhe, J. (2015). An Inductive Sensor for Real-Time Measurement of Plantar Normal and Shear Forces Distribution. *IEEE Transactions on Biomedical Engineering*, 62(5), 1316-1323.
- Duan, F., Dai, L., Chang, W., Chen, Z., Zhu, C., & Li, W. (2016). sEMG-Based Identification of Hand Motion Commands Using Wavelet Neural Network Combined With Discrete Wavelet Transform. *IEEE Transactions on Industrial Electronics*, 63(3), 1923-1934.
- El-Sayed, A. M., Hamzaid, N. A., & Abu Osman, N. A. (2014). Piezoelectric Bimorph's Characteristics as in-Socket Sensor for Transfemoral Amputees *Sensors*, 2014(14).

- El-Sayed, A. M., Hamzaid, N. A., & Osman, N. A. A. (2014). Piezoelectric Bimorphs' Characteristics as In-Socket Sensors for Transfemoral Amputees. *Sensors*, 14(12), 23724.
- El-Sayed, A. M., Hamzaid, N. A., Tan, K. Y. S., & Abu Osman, N. A. (2014). Detection of Prosthetic Knee Movement Phases via In-Socket Sensors: A Feasibility Study. *The Scientific World Journal*.
- El-Sayed, A. M., Hamzaid, N. A., Tan, K. Y. S., & Abu Osman, N. A. (2015). Detection of Prosthetic Knee Movement Phases via In-Socket Sensors: A Feasibility Study. *The Scientific World Journal*, 2015, 13.
- Englehart, K., & Hudgins, B. (2003). A robust, real-time control scheme for multifunction myoelectric control. *IEEE Transactions on Biomedical Engineering*, 50(7), 848-854.
- Eshraghi, A., Abu Osman, N. A., Gholizadeh, H., Ali, S., Saevarsson, S. K., & Wan Abas, W. A. (2013). An experimental study of the interface pressure profile during level walking of a new suspension system for lower limb amputees. *Clin Biomech (Bristol, Avon)*, 28(1), 55-60.
- Farnsworth, B. D., Talyor, D. M., Triolo, R. J., & Young, D. J. (2009, 21-25 June 2009). *Wireless in vivo EMG sensor for intelligent prosthetic control*. Paper presented at the International Solid-State Sensors, Actuators and Microsystems Conference, 2009 (TRANSDUCERS 2009). , Colorado,USA.
- Farooq, M., & Sazonov, E. (2017). Segmentation and Characterization of Chewing Bouts by Monitoring Temporalis Muscle Using Smart Glasses With Piezoelectric Sensor. *Ieee Journal of Biomedical and Health Informatics*, 21(6), 1495-1503.
- Farrell, T. R., & Weir, R. F. (2007). The Optimal Controller Delay for Myoelectric Prostheses. *IEEE Transactions on Neural Systems and Rehabilitation Engineering*, 15(1), 111-118.
- Fei, W., Tenglong, Y., Chenxi, L., Yuanke, Z., Yifan, W., & Jian, L. (2015, 8-12 June 2015). *Prediction of lower limb joint angle using sEMG based on GA-GRNN*. Paper presented at the 2015 IEEE International Conference on Cyber Technology in Automation, Control, and Intelligent Systems (CYBER).
- Fey, N. P., Simon, A. M., Young, A. J., & Hargrove, L. J. (2014). Controlling Knee Swing Initiation and Ankle Plantarflexion With an Active Prosthesis on Level and Inclined Surfaces at Variable Walking Speeds. *IEEE Journal of Translational Engineering in Health and Medicine*, 2, 1-12.
- Fite, K., Mitchell, J., Sup, F., & Goldfarb, M. (2007, 13-15 June 2007). *Design and Control of an Electrically Powered Knee Prosthesis*. Paper presented at the 2007 IEEE 10th International Conference on Rehabilitation Robotics.
- Fitzsimmons, N. A., Lebedev, M. A., Peikon, I. D., & Nicolelis, M. A. L. (2009). Extracting Kinematic Parameters for Monkey Bipedal Walking from Cortical Neuronal Ensemble Activity. *Frontiers in Integrative Neuroscience*, 3, 3.

- Fuhr, T., Quintern, J., Riener, R., & Schmidt, G. (2008). Walking with WALK! *IEEE Engineering in Medicine and Biology Magazine*, 27(1), 38-48.
- Ganesan, B., Fong, K., Luximon, A., & Al-Jumaily, A. (2016). Kinetic and kinematic analysis of gait pattern of 13 year old children with unilateral genu valgum. *European review for medical and pharmacological sciences*, 20(15), 3168.
- Geethanjali, P., & Ray, K. K. (2014). EMG based man-machine interaction—A pattern recognition research platform. *Robotics and Autonomous Systems*, 62(2014), 864-870.
- Gere, J. M. (2004). *Mechanics of material* (Sixth ed.). USA: Brooks/Cole-Thomson Learning.
- Giovanelli, D., Giovanelli, N., Taboga, P., Barjuei, E. S., Boscariol, P., Vidoni, R., Gasparetto, A., & Lazzer, S. (2014, 15-17 Oct. 2014). *A mechatronic system mounted on insole for analyzing human gait*. Paper presented at the 2014 Second RSI/ISM International Conference on Robotics and Mechatronics (ICRoM).
- Goršič, M., Kamnik, R., Ambrožič, L., Vitiello, N., Lefeber, D., Pasquini, G., & Munih, M. (2014). Online Phase Detection Using Wearable Sensors for Walking with a Robotic Prosthesis. *Sensors*, 14(2), 2776.
- Goswami, A. (1998). A new gait parameterization technique by means of cyclogram moments: Application to human slope walking. *Gait & Posture*, 8, 15-36.
- Gregg, R. D., & Sensinger, J. W. (2014). Towards Biomimetic Virtual Constraint Control of a Powered Prosthetic Leg. *Ieee Transactions on Control Systems Technology*, 22(1), 246-254.
- Hardaker, P. A., Passow, B. N., & Elizondo, D. (2013a, 9-11 Sept. 2013). *State detection from electromyographic signals towards the control of prosthetic limbs*. Paper presented at the 2013 13th UK Workshop on Computational Intelligence (UKCI).
- Hardaker, P. A., Passow, B. N., & Elizondo, D. (2013b, 9-11 Sept. 2013). *State detection from electromyographic signals towards the control of prosthetic limbs*. Paper presented at the 13th UK Workshop on Computational Intelligence (UKCI).
- Hargrove, L. J., Simon, A. M., Lipschutz, R., Finucane, S. B., & Kuiken, T. A. (2013). Non-weight-bearing neural control of a powered transfemoral prosthesis. *J Neuroeng Rehabil*, 10(62).
- Hargrove, L. J., Young, A. J., Simon, A. M., & et al. (2015). Intuitive control of a powered prosthetic leg during ambulation: A randomized clinical trial. *JAMA*, 313(22), 2244-2252.
- Hofmann, D., Jiang, N., Vujaklija, I., & Farina, D. (2016). Bayesian Filtering of Surface EMG for Accurate Simultaneous and Proportional Prosthetic Control. *IEEE Transactions on Neural Systems and Rehabilitation Engineering*, 24(12), 1333-1341.

- Hong, J. H., & Mun, M. S. (2005). Relationship between socket pressure and EMG of two muscles in trans-femoral stumps during gait. *Prosthet Orthot Int*, 29(1), 59-72.
- Howell, A. M., Kobayashi, T., Hayes, H. A., Foreman, K. B., & Bamberg, S. J. M. (2013). Kinetic Gait Analysis Using a Low-Cost Insole. *IEEE Transactions on Biomedical Engineering*, 60(12), 3284-3290.
- Hu, H., Hu, Y., Chen, C., & Wang, J. (2008). A system of two piezoelectric transducers and a storage circuit for wireless energy transmission through a thin metal wall. *IEEE transactions on Ultrasonics, Ferroelectrics, and Frequency Control*, 55(10), 2312-2319.
- Huang, A., Ono, Y., & Ieee. (2016). *Estimation of Wrist Flexion Angle from Muscle Thickness Changes Measured by a Flexible Ultrasonic Sensor*. New York: Ieee.
- Huang, H., Kuiken, T. A., & Lipschutz, R. D. (2009). A Strategy for Identifying Locomotion Modes Using Surface Electromyography. *IEEE Transactions on Biomedical Engineering*, 56(1), 65-73.
- Huang, H., Zhang, F., Hargrove, L. J., Dou, Z., Rogers, D. R., & Englehart, K. B. (2011). Continuous Locomotion-Mode Identification for Prosthetic Legs Based on Neuromuscular-Mechanical Fusion. *IEEE Transactions on Biomedical Engineering*, 58(10), 2867-2875.
- Huang, Q., Yang, D. P., Jiang, L., Zhang, H. J., Liu, H., & Kotani, K. (2017). A Novel Unsupervised Adaptive Learning Method for Long-Term Electromyography (EMG) Pattern Recognition. *Sensors*, 17(6), 28.
- Huang, Z.-X., Zhang, X.-D., & Li, Y.-N. (2012, 20-24 Aug. 2012). *Design of a grasp force adaptive control system with tactile and slip perception*. Paper presented at the 2012 IEEE International Conference on Automation Science and Engineering (CASE), Seoul, Korea.
- Huang, Z. X., Zhang, X. D., & Li, Y. N. (2012, 20-24 Aug. 2012). *Design of a grasp force adaptive control system with tactile and slip perception*. Paper presented at the 2012 IEEE International Conference on Automation Science and Engineering (CASE).
- Hudgins, B., Parker, P., & Scott, R. N. (1991a, 31 Oct-3 Nov 1991). *The Recognition Of Myoelectric Patterns For Prosthetic Limb Control*. Paper presented at the Proceedings of the Annual International Conference of the IEEE Engineering in Medicine and Biology Society.
- Hudgins, B., Parker, P., & Scott, R. N. (1991b, 31 Oct-3 Nov 1991). *The Recognition Of Myoelectric Patterns For Prosthetic Limb Control*. Paper presented at the Engineering in Medicine and Biology Society, 1991. Vol.13: 1991., Proceedings of the Annual International Conference of the IEEE.
- Inoue, K., Wada, T., Harada, R., & Tachiwana, S. (2013, 24-26 June 2013). *Novel knee joint mechanism of transfemoral prosthesis for stair ascent*. Paper presented at the 2013 IEEE 13th International Conference on Rehabilitation Robotics (ICORR).

- Ishikawa, T., Hayami, H., & Murakami, T. (2017, 21-23 Nov. 2017). *Comprehensive evaluation of human activity classification based on inertia measurement unit with air pressure sensor*. Paper presented at the 2017 24th International Conference on Mechatronics and Machine Vision in Practice (M2VIP).
- Jamal, M. Z. (2012). Signal Acquisition Using Surface EMG and Circuit Design Considerations for Robotic Prosthesis. In G. R. Naik (Ed.), *Computational Intelligence in Electromyography Analysis - A Perspective on Current Applications and Future Challenges* (pp. 427-448): InTech.
- Jasni, F., Hamzaid, N. A., Mohd Syah, N. E., Chung, T. Y., & Abu Osman, N. A. (2017). Analysis of Interrelationships among Voluntary and Prosthetic Leg Joint Parameters Using Cyclograms. *Frontiers in Neuroscience*, 11(230).
- Jasni, F., Hamzaid, N. A., Muthalif, A. G. A., Zakaria, Z., Shasmin, H. N., & Ng, S. C. (2016). In-Socket Sensory System for Transfemoral Amputees Using Piezoelectric Sensors: An Efficacy Study. *IEEE/ASME Transactions on Mechatronics*, 21(5), 2466-2476.
- Johansson, J. L., Sherrill, D. M., Riley, P. O., Bonato, P., & Herr, H. (2005). A clinical comparison of variable-damping and mechanically passive prosthetic knee devices. *American journal of physical medicine & rehabilitation*, 84(8), 563-575.
- Joshi, D., & Hahn, M. E. (2016). Terrain and Direction Classification of Locomotion Transitions Using Neuromuscular and Mechanical Input. *Ann Biomed Eng*, 44(4), 1275-1284.
- Kakoty, N. M., Saikia, A., & Hazarika, S. M. (2013). Exploring a family of wavelet transforms for EMG-based grasp recognition. *Signal, Image and Video Processing*, 9(3), 553-559.
- Kanitthika, K., & Chan, K. S. (2014, 22-25 June 2014). *Pressure sensor positions on insole used for walking analysis*. Paper presented at the The 18th IEEE International Symposium on Consumer Electronics (ISCE 2014).
- Kapti, A. O., & Muhurcu, G. (2014). Wearable acceleration sensor application in unilateral trans-tibial amputation prostheses. *Biocybernetics and Biomedical Engineering*, 34(1), 53-62.
- Kapti, A. O., & Yucenur, M. S. (2006). Design and control of an active artificial knee joint. *Mechanism and Machine Theory*, 41(12), 1477-1485.
- Kaufman, K. R., Levine, J. A., Brey, R. H., Iverson, B. K., McCrady, S. K., Padgett, D. J., & Joyner, M. J. (2007). Gait and balance of transfemoral amputees using passive mechanical and microprocessor-controlled prosthetic knees. *Gait & Posture*, 26(4), 489-493.
- Kebin, Y., Qining, W., & Long, W. (2015). Fuzzy-Logic-Based Terrain Identification with Multisensor Fusion for Transtibial Amputees. *IEEE/ASME Transactions on Mechatronics*, 20(2), 618-630.

- Khademi, G., Mohammadi, H., Simon, D., & Hardin, E. C. (2015, 22-24 Oct. 2015). *Evolutionary optimization of user intent recognition for transfemoral amputees*. Paper presented at the 2015 IEEE Biomedical Circuits and Systems Conference (BioCAS).
- Khezri, M., & Jahed, M. (2011). A Neuro-Fuzzy Inference System for sEMG-Based Identification of Hand Motion Commands. *IEEE Transactions on Industrial Electronics*, 58(5), 1952-1960.
- Krajewski, A. S., Magniez, K., Helmer, R. J. N., & Schrank, V. (2013). Piezoelectric Force Response of Novel 2D Textile Based PVDF Sensors. *IEEE Sensors Journal*, 13(12), 4743-4748.
- Krausz, N. E., Lenzi, T., & Hargrove, L. J. (2015). Depth Sensing for Improved Control of Lower Limb Prostheses. *IEEE Transactions on Biomedical Engineering*, 62(11), 2576-2587.
- Krut, S., Coste, C. A., & Chablot, P. (2011). Secure microprocessor-controlled prosthetic leg for elderly amputees: Preliminary results. *Applied Bionics and Biomechanics*, 8(3-4), 385-398.
- Lacour, S. P., Graz, I., Cotton, D., Bauer, S., & Wagner, S. (2011, Aug. 30 2011-Sept. 3 2011). *Elastic components for prosthetic skin*. Paper presented at the 2011 Annual International Conference of the IEEE Engineering in Medicine and Biology Society.
- Lawson, B. E., Mitchell, J., Truex, D., Shultz, A., Ledoux, E., & Goldfarb, M. (2014). A Robotic Leg Prosthesis: Design, Control, and Implementation. *IEEE Robotics & Automation Magazine*, 21(4), 70-81.
- Lawson, B. E., Varol, H. A., Huff, A., Erdemir, E., & Goldfarb, M. (2013). Control of Stair Ascent and Descent With a Powered Transfemoral Prosthesis. *IEEE Transactions on Neural Systems and Rehabilitation Engineering*, 21(3), 466-473.
- Lee, S. H., & Kim, J. Y. (2017). Walking algorithm for a robotic transfemoral prosthesis capable of walking pattern recognition and posture stabilization. *Advanced Robotics*, 31(18), 965-989.
- Lee, S. W., Yi, T., Jung, J. W., & Bien, Z. (2017). Design of a Gait Phase Recognition System That Can Cope With EMG Electrode Location Variation. *IEEE Transactions on Automation Science and Engineering*, 14(3), 1429-1439.
- LeMoyne, R., Kerr, W., Mastroianni, T., & Hessel, A. (2014, 3-6 Dec. 2014). *Implementation of Machine Learning for Classifying Hemiplegic Gait Disparity through Use of a Force Plate*. Paper presented at the 2014 13th International Conference on Machine Learning and Applications.
- Leo, D. J. (2007). *Engineering analysis of smart material systems*. USA: John Wiley & Sons, Inc.
- Level Four. (2017). 4 basic components of prosthetic leg Retrieved from <http://www.level4oandp.com/blog/post/4-basic-components-of-prosthetic-legs>

- Leysieffer, H., Hortmann, G., & Baumann, J. (1994). Electromechanical transducer for implantable hearing aids: Google Patents.
- Li, P., Jin, F., & Yang, J. (2013). A piezoelectric energy harvester with increased bandwidth based on beam flexural vibrations in perpendicular directions. *IEEE transactions on Ultrasonics, Ferroelectrics, and Frequency Control*, 60(10), 2214-2218.
- Lin, Y. Y., Wu, H. T., Hsu, C. A., Huang, P. C., Huang, Y. H., & Lo, Y. L. (2017). Sleep Apnea Detection Based on Thoracic and Abdominal Movement Signals of Wearable Piezoelectric Bands. *Ieee Journal of Biomedical and Health Informatics*, 21(6), 1533-1545.
- Lior, R. (2009). *Pattern Classification Using Ensemble Methods*: World Scientific Publishing Company.
- Liu, H., Xia, Y., Chen, T., Yang, Z., Liu, W., Wang, P., & Sun, L. (2017). Study of a Hybrid Generator Based on Triboelectric and Electromagnetic Mechanisms. *IEEE Sensors Journal*, 17(12), 3853-3860.
- Liu, Z. J., Lin, W., Geng, Y. L., & Yang, P. (2017). Intent Pattern Recognition of Lower-limb Motion Based on Mechanical Sensors. *Ieee-Caa Journal of Automatica Sinica*, 4(4), 651-660.
- Lorenzelli, L., Sordo, G., Bagolini, A., & Resta, G. (2017, 6-9 Sept. 2017). *Socketmaster: Integrated Sensors System for the Optimised Design of Prosthetic Socket for above Knee Amputees*. Paper presented at the 2017 New Generation of CAS (NGCAS).
- Ma, X., Ma, C. L., Huang, J., Zhang, P., Xu, J., & He, J. P. (2017). Decoding Lower Limb Muscle Activity and Kinematics from Cortical Neural Spike Trains during Monkey Performing Stand and Squat Movements. *Frontiers in Neuroscience*, 11, 16.
- Maqbool, H. F., Husman, M. A. B., Awad, M. I., Abouhossein, A., Iqbal, N., & Dehghani-Sanij, A. A. (2017). A Real-Time Gait Event Detection for Lower Limb Prosthesis Control and Evaluation. *IEEE Transactions on Neural Systems and Rehabilitation Engineering*, 25(9), 1500-1509.
- Martin, J., Pollock, A., & Hettinger, J. (2010). Microprocessor lower limb prosthetics: Review of current state of the art. *Journal of Prosthetics and Orthotics*, 22(3).
- Mashal, F., Shafique, M., & Khan, Z. H. (2015, 19-20 Dec. 2015). *Towards a low cost Brain-computer Interface for real time control of a 2 DOF robotic arm*. Paper presented at the 2015 International Conference on Emerging Technologies (ICET).
- Mazumder, O., Kundu, A., Lenka, P., & Bhaumik, S. (2017). Design of speed adaptive myoelectric active ankle prosthesis. *Electronics Letters*, 53(23), 1508-1510.
- McMullen, D. P., Hotson, G., Katyal, K. D., Wester, B. A., Fifer, M. S., McGee, T. G., Harris, A., Johannes, M. S., Vogelstein, R. J., Ravitz, A. D., Anderson, W. S.,

- Thakor, N. V., & Crone, N. E. (2014). Demonstration of a Semi-Autonomous Hybrid Brain-Machine Interface Using Human Intracranial EEG, Eye Tracking, and Computer Vision to Control a Robotic Upper Limb Prosthetic. *IEEE Transactions on Neural Systems and Rehabilitation Engineering*, 22(4), 784-796.
- McPherson, T., & Ueda, J. (2014). A Force and Displacement Self-Sensing Piezoelectric MRI-Compatible Tweezer End Effector With an On-Site Calibration Procedure. *IEEE/ASME Transactions on Mechatronics*, 19(2), 755-764.
- Measurement Specialties. Piezo Sensor-FDT Series. Retrieved from <http://www.meas-spec.com/>
- Miyamoto, A., Lee, S., Cooray, N. F., Lee, S., Mori, M., Matsuhisa, N., Jin, H., Yoda, L., Yokota, T., Itoh, A., Sekino, M., Kawasaki, H., Ebihara, T., Amagai, M., & Someya, T. (2017). Inflammation-free, gas-permeable, lightweight, stretchable on-skin electronics with nanomeshes. *Nature Nanotechnology*, 12, 907.
- Moheimani, S. O. R., & Fleming, A. J. (2006). Fundamentals of Piezoelectricity *Piezoelectric Transducers for Vibration Control and Damping* (pp. 9-35): Springer London.
- Mueller, J. K. P., Evans, B. M., Ericson, M. N., Farquhar, E., Lind, R., Kelley, K., Pusch, M., Marcard, T. v., & Wilken, J. M. (2011, 7-8 Nov. 2011). *A mobile motion analysis system using inertial sensors for analysis of lower limb prosthetics*. Paper presented at the Future of Instrumentation International Workshop (FIIW), 2011.
- Muheidat, F., & Tyrer, H. W. (2017, 17-19 July 2017). *Deriving Information from Low Spatial Resolution Floor-Based Personnel Detection System*. Paper presented at the 2017 IEEE/ACM International Conference on Connected Health: Applications, Systems and Engineering Technologies (CHASE).
- Murguialday, A. R., Aggarwal, V., Chatterjee, A., Cho, Y., Rasmussen, R., Rourke, B. O., Acharya, S., & Thakor, N. V. (2007, 13-15 June 2007). *Brain-Computer Interface for a Prosthetic Hand Using Local Machine Control and Haptic Feedback*. Paper presented at the 2007 IEEE 10th International Conference on Rehabilitation Robotics.
- Muthalif, A. G. A., & Nordin, N. H. D. (2015). Optimal piezoelectric beam shape for single and broadband vibration energy harvesting: Modeling, simulation and experimental results. *Mechanical Systems and Signal Processing*, 54-55, 417-426.
- Naik, G. R., Kumar, D. K., & Jayadeva. (2010). Twin SVM for Gesture Classification Using the Surface Electromyogram. *IEEE Transactions on Information Technology in Biomedicine*, 14(2), 301-308.
- Nakamura, B. H., & Hahn, M. E. (2016). Myoelectric activation differences in Transfemoral amputees during locomotor state transitions. *Biomedical Engineering-Applications Basis Communications*, 28(6), 8.

- Nandi, G. C., Iispeert, A. J., Chakraborty, P., & Nandi, A. (2009). Development of Adaptive Modular Active Leg (AMAL) using bipedal robotics technology. *Robotics and Autonomous Systems*, 57(6-7), 603-616.
- Nazmi, N., Abdul Rahman, M. A., Yamamoto, S., Ahmad, S. A., Zamzuri, H., & Mazlan, S. A. (2016). A Review of Classification Techniques of EMG Signals during Isotonic and Isometric Contractions. *Sensors (Basel)*, 16(8).
- Ng, T. H., & Liao, W. H. (2005). Sensitivity Analysis and Energy Harvesting for a Self-Powered Piezoelectric Sensor. *Journal of Intelligent Material Systems and Structures*, 16(10), 785-797.
- Nguyen, T. T., Feng, T., Häfliger, P., & Chakrabartty, S. (2014). Hybrid CMOS Rectifier Based on Synergistic RF-Piezoelectric Energy Scavenging. *IEEE Transactions on Circuits and Systems I: Regular Papers*, 61(12), 3330-3338.
- Novak, D., Rebersek, P., De Rossi, S. M., Donati, M., Podobnik, J., Beravs, T., Lenzi, T., Vitiello, N., Carrozza, M. C., & Munih, M. (2013). Automated detection of gait initiation and termination using wearable sensors. *Med Eng Phys*, 35(12), 1713-1720.
- Observational Gait Analysis Handbook*. (1989). CA, USA: Pathokinesiology Department & the Physical Therapy Department, Rancho Los Amigos Medical Center.
- Patterson, M. R., Delahunt, E., Sweeney, K. T., & Caulfield, B. (2014). An ambulatory method of identifying anterior cruciate ligament reconstructed gait patterns. *Sensors (Basel)*, 14(1), 887-899.
- Pfeifer, S., Pagel, A., Riener, R., & Vallery, H. (2015). Actuator With Angle-Dependent Elasticity for Biomimetic Transfemoral Prostheses. *IEEE/ASME Transactions on Mechatronics*, 20(3), 1384-1394.
- Pfister, A., West, A. M., Bronner, S., & Noah, J. A. (2014). Comparative abilities of Microsoft Kinect and Vicon 3D motion capture for gait analysis. *Journal of Medical Engineering & Technology*, 38(5), 274-280.
- Physiopedia contributors. (6 June 2017). Gait. Retrieved from <https://www.physiopedia.com/index.php?title=Gait&oldid=172822>
- Plauché, A., Villarreal, D., & Gregg, R. D. (2016). A Haptic Feedback System for Phase-Based Sensory Restoration in Above-Knee Prosthetic Leg Users. *IEEE Transactions on Haptics*, 9(3), 421-426.
- Popovic, D. B., & Kalanovic, V. D. (1993). Output space tracking control for above-knee prosthesis. *IEEE Transactions on Biomedical Engineering*, 40(6), 549-557.
- Popovic, D. B., Tomovic, R., Tepavac, D., & Schwirtlich, L. (1991). Control aspects of active above-knee prosthesis. *International Journal of Man-Machine Studies*, 35 (6), 751-767.
- Prakash, C., Mittal, A., Kumar, R., & Mittal, N. (2015, 19-20 March 2015). *Identification of spatio-temporal and kinematics parameters for 2-D optical gait analysis system*

using passive markers. Paper presented at the 2015 International Conference on Advances in Computer Engineering and Applications.

- Prendergast, P. J., Helm, F. C. T. V. D., & Duda, G. N. (2005). Analysis of muscle and joint loads. In V. C. Mow & R. Huiskes (Eds.), *Basic orthopaedic biomechanics and mechano-biology* (3rd ed., pp. 49). USA: LIPPINCOTT WILLIAMS & WILKINS.
- Presacco, A., Forrester, L. W., & Contreras-Vidal, J. L. (2012). Decoding Intra-Limb and Inter-Limb Kinematics During Treadmill Walking From Scalp Electroencephalographic (EEG) Signals. *IEEE Transactions on Neural Systems and Rehabilitation Engineering*, 20(2), 212-219.
- Ragnerius, A., & Widelund, F. (2016). *Automated foot strike pattern recognition using a smart sock with textile piezoelectric sensors*. (Master's Degree in Biomedical Engineering), Chalmers University of Technology, Gothenburg, Sweden.
- Ravi, N., Dandekar, N., Mysore, P., & Littman, M. L. (2005). *Activity recognition from accelerometer data*. Paper presented at the Proceedings of the 17th conference on Innovative applications of artificial intelligence - Volume 3, Pittsburgh, Pennsylvania.
- Rea, M., Rana, M., Lugato, N., Terekhin, P., Gizzi, L., Brotz, D., Fallgatter, A., Birbaumer, N., Sitaram, R., & Caria, A. (2014). Lower Limb Movement Preparation in Chronic Stroke: A Pilot Study Toward an fNIRS-BCI for Gait Rehabilitation. *Neurorehabil Neural Repair*, 28(6), 564-575.
- Ribeiro, D. M. S., Aguiar, P. R., Fabiano, L. F. G., D'Addona, D. M., Baptista, F. G., & Bianchi, E. C. (2017). Spectra Measurements Using Piezoelectric Diaphragms to Detect Burn in Grinding Process. *IEEE Transactions on Instrumentation and Measurement*, 66(11), 3052-3063.
- Romani, A., Filippi, M., & Tartagni, M. (2014). Micropower Design of a Fully Autonomous Energy Harvesting Circuit for Arrays of Piezoelectric Transducers. *IEEE Transactions on Power Electronics*, 29(2), 729-739.
- Roundy, S., Leland, E. S., Baker, J., Carleton, E., Reilly, E., Lai, E., Otis, B., Rabaey, J. M., Wright, P. K., & Sundararajan, V. (2005). Improving power output for vibration-based energy scavengers. *IEEE Pervasive Computing*, 4(1), 28-36.
- Ryu, J., Lee, B. H., & Kim, D. H. (2017). sEMG Signal-Based Lower Limb Human Motion Detection Using a Top and Slope Feature Extraction Algorithm. *IEEE Signal Processing Letters*, 24(7), 929-932.
- Salarian, A., Russmann, H., Vingerhoets, F. J. G., Dehollain, C., Blanc, Y., Burkhard, P. R., & Aminian, K. (2004). Gait assessment in Parkinson's disease: toward an ambulatory system for long-term monitoring. *IEEE Transactions on Biomedical Engineering*, 51(8), 1434-1443.
- Sanchis, A., Juan, A., & Vidal, E. (2012). A Word-Based Naïve Bayes Classifier for Confidence Estimation in Speech Recognition. *Audio, Speech, and Language Processing, IEEE Transactions on*, 20(2), 565-574.

- Sanei, S. (2013). Fundamentals of EEG Signal Processing *Adaptive Processing of Brain Signals* (pp. 37-44): John Wiley & Sons, Ltd.
- Schmalz, T., Blumentritt, S., & Jarasch, R. (2002). Energy expenditure and biomechanical characteristics of lower limb amputee gait:: The influence of prosthetic alignment and different prosthetic components. *Gait & Posture*, 16(3), 255-263.
- Segal, A. D., Orendurff, M. S., Klute, G. K., McDowell, M. L., & et al. (2006). Kinematic and kinetic comparisons of transfemoral amputee gait using C-Leg® and Mauch SNS® prosthetic knees. *Journal of Rehabilitation Research and Development*, 43(7), 857-870.
- Serra, R., Croce, P. D., Peres, R., & Knittel, D. (2014, 2-5 Nov. 2014). *Human step detection from a piezoelectric polymer floor sensor using normalization algorithms*. Paper presented at the IEEE SENSORS 2014 Proceedings.
- Seymour, R. (2002). *Prosthetics and Orthotics : Lower limb and spinal*. USA: Lippincott Williams & Wilkins.
- Shahmoradi, S., & Shouraki, S. B. (2017, 2-4 May 2017). *A Fuzzy sequential locomotion mode recognition system for lower limb prosthesis control*. Paper presented at the 2017 Iranian Conference on Electrical Engineering (ICEE).
- Shull, P. B., Jirattigalachote, W., Hunt, M. A., Cutkosky, M. R., & Delp, S. L. (2014). Quantified self and human movement: A review on the clinical impact of wearable sensing and feedback for gait analysis and intervention. *Gait & Posture*, 40(1), 11-19.
- Shull, P. B., Xu, J., Yu, B., & Zhu, X. (2017). Magneto-Gyro Wearable Sensor Algorithm for Trunk Sway Estimation During Walking and Running Gait. *IEEE Sensors Journal*, 17(2), 480-486.
- Shultz, A. H., Lawson, B. E., & Goldfarb, M. (2016). Variable Cadence Walking and Ground Adaptive Standing With a Powered Ankle Prosthesis. *IEEE Transactions on Neural Systems and Rehabilitation Engineering*, 24(4), 495-505.
- Simon, A. M., Ingraham, K. A., Fey, N. P., Finucane, S. B., Lipschutz, R. D., Young, A. J., & Hargrove, L. J. (2014). Configuring a Powered Knee and Ankle Prosthesis for Transfemoral Amputees within Five Specific Ambulation Modes. *PLoS ONE*, 9(6), e99387.
- Sordo, G., & Lorenzelli, L. (2016, May 30 2016-June 2 2016). *Design of a novel tri-axial force sensor for optimized design of prosthetic socket for lower limb amputees*. Paper presented at the 2016 Symposium on Design, Test, Integration and Packaging of MEMS/MOEMS (DTIP).
- Spanu, A., Pinna, L., Viola, F., Seminara, L., Valle, M., Bonfiglio, A., & Cosseddu, P. (2016). A high-sensitivity tactile sensor based on piezoelectric polymer PVDF coupled to an ultra-low voltage organic transistor. *Organic Electronics*, 36(Supplement C), 57-60.

- Stolyarov, R. M., Burnett, G., & Herr, H. (2018). Translational Motion Tracking of Leg Joints for Enhanced Prediction of Walking Tasks. *IEEE Transactions on Biomedical Engineering*, PP(99), 1-1.
- Suaste-Gomez, E., Rodriguez-Roldan, G., Reyes-Cruz, H., & Teran-Jimenez, O. (2016). Developing an Ear Prosthesis Fabricated in Polyvinylidene Fluoride by a 3D Printer with Sensory Intrinsic Properties of Pressure and Temperature. *Sensors*, 16(3), 11.
- Sun, Q., Seung, W., Kim, B. J., Seo, S., Kim, S.-W., & Cho, J. H. (2015). Active Matrix Electronic Skin Strain Sensor Based on Piezopotential-Powered Graphene Transistors. *Advanced Materials*, 27(22), 3411-3417.
- Sup, F., Bohara, A., & Goldfarb, M. (2007, 10-14 April 2007). *Design and Control of a Powered Knee and Ankle Prosthesis*. Paper presented at the Proceedings 2007 IEEE International Conference on Robotics and Automation.
- Suzuki, H., Soma, H., González, J., & Yu, W. (2012, Aug. 28 2012-Sept. 1 2012). *Using piezoelectric films for classification of upper arm motions: A preliminary report*. Paper presented at the 2012 Annual International Conference of the IEEE Engineering in Medicine and Biology Society.
- Takeda, R., Tadano, S., Todoh, M., Morikawa, M., Nakayasu, M., & Yoshinari, S. (2009). Gait analysis using gravitational acceleration measured by wearable sensors. *Journal of Biomechanics*, 42(3), 223-233.
- Tao, W., Liu, T., Zheng, R., & Feng, H. (2012). Gait Analysis Using Wearable Sensors. *Sensors*, 12(2), 2255.
- Tekscan Inc. Medical Sensor 9811e. Retrieved from <https://www.tekscan.com/products-solutions/medical-sensors/9811e>
- Thatte, N., & Geyer, H. (2016). Toward Balance Recovery With Leg Prostheses Using Neuromuscular Model Control. *IEEE Transactions on Biomedical Engineering*, 63(5), 904-913.
- Tkach, D. C., & Hargrove, L. J. (2013, 3-7 July 2013). *Neuromechanical sensor fusion yields highest accuracies in predicting ambulation mode transitions for trans-tibial amputees*. Paper presented at the Engineering in Medicine and Biology Society (EMBC), 2013 35th Annual International Conference of the IEEE.
- Tkach, D. C., Huang, H., & Kuiken, T. A. (2010). Study of stability of time-domain features for electromyographic pattern recognition. *J Neuroeng Rehabil*, 7(1), 21.
- Toledo, A. R., Fernandez, A. R., & Anthony, D. K. (2010). *A comparison of GA objective functions for estimating internal properties of piezoelectric transducers used in medical echo-graphic imaging*. Paper presented at the Pan American Health Care Exchanges, Peru.
- Torrealba, R. R., Cappelletto, J., Fermin-Leon, L., Grieco, J. C., & Fernandez-Lopez, G. (2010). Statistics-based technique for automated detection of gait events from accelerometer signals. *Electronics Letters*, 46(22), 1483-1485.

- Tucker, M. R., Olivier, J., Pagel, A., Bleuler, H., Bouri, M., Lambercy, O., Millan, J. D., Riener, R., Vallery, H., & Gassert, R. (2015). Control strategies for active lower extremity prosthetics and orthotics: a review. *J Neuroeng Rehabil*, 12, 29.
- Tura, A., Raggi, M., Rocchi, L., Cutti, A. G., & Chiari, L. (2010). Gait symmetry and regularity in transfemoral amputees assessed by trunk accelerations. *J Neuroeng Rehabil*, 7(1), 4.
- Ueberschlag, P. (2001). PVDF piezoelectric polymer. *Sensor Review*, 21(2), 118-126.
- Varol, H. A., Sup, F., & Goldfarb, M. (2010). Multiclass Real-Time Intent Recognition of a Powered Lower Limb Prosthesis. *IEEE Transactions on Biomedical Engineering*, 57(3), 542-551.
- Villalpando, E. C. M.-, Weber, J., Elliott, G., & Herr, H. (2008, 19-22 Oct. 2008). *Design of an agonist-antagonist active knee prosthesis*. Paper presented at the 2008 2nd IEEE RAS & EMBS International Conference on Biomedical Robotics and Biomechatronics.
- Waters, R. L., Perry, J., Antonelli, D., & Hislop, H. (1976). Energy cost of walking of amputees: the influence of level of amputation. *J Bone Joint Surg Am*, 58(1), 42-46.
- Wen-Yang, C., Chun-Hsun, C., & Yu-Cheng, L. (2008). A Flexible Piezoelectric Sensor for Microfluidic Applications Using Polyvinylidene Fluoride. *IEEE Sensors Journal*, 8(5), 495-500.
- Wentink, E. C., Beijen, S. I., Hermens, H. J., Rietman, J. S., & Veltink, P. H. (2013). Intention detection of gait initiation using EMG and kinematic data. *Gait & Posture*, 37(2), 223-228.
- Wentink, E. C., Prinsen, E. C., Rietman, J. S., & Veltink, P. H. (2013). Comparison of muscle activity patterns of transfemoral amputees and control subjects during walking. *Journal of NeuroEngineering & Rehabilitation (JNER)*, 10(87), 1-11.
- Wentink, E. C., Schut, V. G. H., Prinsen, E. C., Rietman, J. S., & Veltink, P. H. (2014). Detection of the onset of gait initiation using kinematic sensors and EMG in transfemoral amputees. *Gait & Posture*, 39(1), 391-396.
- Windrich, M., Grimmer, M., Christ, O., Rinderknecht, S., & Beckerle, P. (2016). Active lower limb prosthetics: a systematic review of design issues and solutions. *BioMedical Engineering OnLine*, 15(3), 140.
- Winter, D. (1991). The Biomechanics and Motor Control of Human Gait: Normal, Elderly and Pathological. *University of Waterloo Press*, 2.
- Wu, S.-K., Waycaster, G., & Shen, X. (2011). Electromyography-based control of active above-knee prostheses. *Control Engineering Practice*, 19 (8), 875-882.
- Xi, X., Tang, M., Miran, S. M., & Luo, Z. (2017). Evaluation of Feature Extraction and Recognition for Activity Monitoring and Fall Detection Based on Wearable sEMG Sensors. *Sensors (Basel)*, 17(6).

- Xie, H., Li, F., Sheng, Z., Xu, Z., & Liu, Y. (2009, 17-19 June 2009). *The gait system research of intelligent bionic leg*. Paper presented at the 2009 Chinese Control and Decision Conference.
- Xu, H., Liu, J., Hu, H., & Zhang, Y. (2016). Wearable Sensor-Based Human Activity Recognition Method with Multi-Features Extracted from Hilbert-Huang Transform. *Sensors*, 16(12), 2048.
- Yan, g., Lu, Q., Ding, G., & Yan, D. (2002, 2002). *The prototype of a piezoelectric medical microrobot*. Paper presented at the Proceedings of 2002 International Symposium on Micromechatronics and Human Science, 2002. MHS 2002. .
- Yang, U. J., & Kim, J. Y. (2015). Mechanical design of powered prosthetic leg and walking pattern generation based on motion capture data. *Advanced Robotics*, 29(16), 1061-1079.
- Ye, M., Yang, C., Stankovic, V., Stankovic, L., & Kerr, A. (2015, 14-16 Dec. 2015). *Gait analysis using a single depth camera*. Paper presented at the 2015 IEEE Global Conference on Signal and Information Processing (GlobalSIP).
- Young, A. J., & Hargrove, L. J. (2016). A Classification Method for User-Independent Intent Recognition for Transfemoral Amputees Using Powered Lower Limb Prostheses. *IEEE Transactions on Neural Systems and Rehabilitation Engineering*, 24(2), 217-225.
- Young, A. J., Simon, A. M., Fey, N. P., & Hargrove, L. J. (2013, 6-8 Nov. 2013). *Classifying the intent of novel users during human locomotion using powered lower limb prostheses*. Paper presented at the 6th International IEEE/EMBS Conference on Neural Engineering (NER), California, USA.
- Young, A. J., Simon, A. M., Fey, N. P., & Hargrove, L. J. (2014). Intent Recognition in a Powered Lower Limb Prosthesis Using Time History Information. *Ann Biomed Eng*, 42(3), 631-641.
- Young, A. J., Simon, A. M., & Hargrove, L. J. (2014). A Training Method for Locomotion Mode Prediction Using Powered Lower Limb Prostheses. *IEEE Transactions on Neural Systems and Rehabilitation Engineering*, 22(3), 671-677.
- Zhang, D., Han, X., Zhang, Z., Liu, J., Jiang, C., Yoda, N., Meng, X., & Li, Q. (2017). Identification of dynamic load for prosthetic structures. *International Journal for Numerical Methods in Biomedical Engineering*, 33(12).
- Zhang, F., Fang, Z., Liu, M., & Huang, H. (2011, Aug. 30 2011-Sept. 3 2011). *Preliminary design of a terrain recognition system*. Paper presented at the 2011 Annual International Conference of the IEEE Engineering in Medicine and Biology Society.
- Zhang, F., & Huang, H. (2013). Source Selection for Real-Time User Intent Recognition Toward Volitional Control of Artificial Legs. *Ieee Journal of Biomedical and Health Informatics*, 17(5), 907-914.

- Zhang, T. Y. (2016). *The research on motion recognition based on EMG of residual thigh*. Boca Raton: Crc Press-Taylor & Francis Group.
- Zhu, X. Y., Liu, J. W., Zhang, D. G., Sheng, X. J., & Jiang, N. (2017). Cascaded Adaptation Framework for Fast Calibration of Myoelectric Control. *IEEE Transactions on Neural Systems and Rehabilitation Engineering*, 25(3), 254-264.
- Zhuo, Q. F., Tian, L., Fang, P., Li, G. L., Zhang, X. Q., & Ieee. (2015). A piezoelectret-based approach for touching and slipping detection in robotic hands *2015 Ieee International Conference on Cyber Technology in Automation, Control, and Intelligent Systems* (pp. 918-921). New York: Ieee.

University of Malaya

LIST OF PUBLICATIONS

1. **Jasni, F.**, Hamzaid, N. A., Muthalif, A. G. A., Zakaria, Z., Shasmin, H. N., & Ng, S. C. (2016). In-Socket Sensory System for Transfemoral Amputees Using Piezoelectric Sensors: An Efficacy Study. *IEEE/ASME Transactions on Mechatronics*, 21(5), 2466-2476. doi:10.1109/TMECH.2016.2578679. (APPENDIX C).
2. **Jasni, F.**, Hamzaid, N. A., Mohd Syah, N. E., Chung, T. Y., & Abu Osman, N. A. (2017). Analysis of Interrelationships among Voluntary and Prosthetic Leg Joint Parameters Using Cyclograms. *Frontiers in Neuroscience*, 11(230). doi:10.3389/fnins.2017.00230. (APPENDIX D).
3. **Jasni, F.**, Hamzaid, N. A., Al-Nusairi, T. Y., Yusof, N. H. M., Shasmin, H. N., & Ng, S. C. (2018). Piezoelectric-based In-Socket Sensory System as A Gait Phase Identification Tool for Transfemoral Amputees: A Feasibility Study. *IEEE Sensors Journal* (**Under Review**).
4. **Jasni, F.**, & Hamzaid, N. A. (2018). Sensory System in Micro-Processor Controlled Prosthetic Leg: A Review. *IEEE Sensors Journal* (**Under Review**).
5. Yahya, T., Hamzaid, N. A., Ali, S., & **Jasni, F.** (2018). Standing and Sitting Variations Based on In-Socket Piezoelectric Sensors for Transfemoral Amputees. *BioMedical Engineering OnLine*. (**Under Review**).
6. Yusof, N. H. M., Hamzaid, N. A., **Jasni, F.**, & Lai, K. W. (2018). In-Socket Sensory System with Adaptive Neuro Based Fuzzy Inference System for Active Transfemoral Prosthetic Leg. *Journal of Electronic Imaging*. (**Under Review**).
7. **Jasni, F.**, Hamzaid, N. A., Mohamed Al-Nusairi, T. Y., Mohd Yusof, N. H., & Shasmin, H. N. Analysis on pattern recognition classifier optimal parameters for gait detection using in-socket sensory system signal. *IEEE Transactions on Biomedical Engineering*. (**In preparation**).

APPENDIX A: INTELLECTUAL PROPERTY

1. Hamzaid, N. A., Jasni, F., Shasmin, H. N., & Zakaria, Z., A prosthetic limb integrated with a sensory system, Malaysia (Patent filed on 22nd June 2017, Application No: PI 2017702344). (APPENDIX A)

 TRADEMARK2U INTELLECTUAL PROPERTY	
Our Ref : 2017/PT/TML/PTA9.08/APP/0446/KYS	By email, fax: 03-79676291
Date : 10 AUGUST 2017	(without enclosure)
UNIVERSITI MALAYA PUSAT INOVASI DAN PENGKOMERSILAN (UMCIC) ARAS 5 KOMPLEKS PENGURUSAN PENVELIDIKAN & INOVASI, UNIVERSITI MALAYA, 50603 KUALA LUMPUR. [Attn: PROF. LOO CHU KIONG/ PROF. DR. ROFINA YASMIN OTHMAN/ MDM MAWAR/ MS. AINOL]	
Dear Sir/Madam,	
Title	: A PROSTHETIC LIMB INTEGRATED WITH A SENSORY SYSTEM
Application Number	: PI 2017702344
Filing Date	: 22 JUNE 2017
Country	: MALAYSIA
Applicant	: UNIVERSITI MALAYA
Inventor	: NUR AZAH BINTI HAMZAID, FARAHIYAH JASNI, HANIE NADIA BINTI SHASMIN, ZAFIRAH BINTI ZAKARIA
We refer to the above matter.	
Kindly find enclosed herewith copies of:	
1. Certificate of Filing	
2. Preliminary Examination- Clear Formalities Report	
The request for substantive examination will be filed shortly. We shall attend to the necessary and keep you duly informed. Should you require further information, please do not hesitate to contact us. Kindly confirm upon receipt of this document by fax.	
Thank You.	
Yours sincerely,	
TRADEMARK2U SDN BHD	
	
KWEK YEN SAN [PATENT DEPARTMENT]	
<div>I/We hereby acknowledge receipt of the above stated document(s)</div> <div>(Signature & Company stamp)</div> <div>Name : _____</div> <div>NRIC No : _____</div> <div>Date : _____</div>	
<small>TRADEMARK2U SDN BHD (670910-M) Registered Trademark, Industrial Design, Patent Agent/Consultant No. 1, Block C, Jalan Dataran SD 1, Dataran SD PJU 9, Bandar Sri Damansara, 52200 Kuala Lumpur, Malaysia. Tel: (603) 6274 3352 Fax: (603) 6274 4795, 6273 6388 Email: info@trademark2u.com Website: www.trademark2u.com</small>	

APPENDIX B: ETHICS APPROVAL FOR THE STUDY

7/11/2017 Untitled Document



UNIVERSITY OF MALAYA
MEDICAL CENTRE

MEDICAL RESEARCH ETHICS COMMITTEE
 (Formerly known as Medical Ethics Committee)
UNIVERSITY OF MALAYA MEDICAL CENTRE

ADDRESS : LEMBAH PANTAL 59100 KUALA LUMPUR, MALAYSIA
 TELEPHONE : 03-79493209/2251 FAX/MILE : 03-79492030

NAME OF ETHICS COMMITTEE/IRB Medical Research Ethics Committee, University Malaya Medical Centre	MREC ID NO: 201755-5218
ADDRESS : LEMBAH PANTAL 59100 KUALA LUMPUR, MALAYSIA	
PROTOCOL NO(if applicable) :	
TITLE: Classification of Movements and Intentions of Transfemoral Amputees Using In-Socket Sensory System.	
PRINCIPAL INVESTIGATOR : Dr Sadeeq Ali	SPONSOR

The following items ☒ have been received and reviewed in connection with the above study to conducted by the above investigator.

<input checked="" type="checkbox"/> Application to Conduct Research Project(form)	Ver.No :	Ver.Date : 05-05-2017
<input checked="" type="checkbox"/> Study Protocol	Ver.No : 1	Ver.Date : 05-05-2017
<input checked="" type="checkbox"/> Patient Information Sheet	Ver.No : 1	Ver.Date : 05-05-2017
<input checked="" type="checkbox"/> Consent Form	Ver.No : 1	Ver.Date : 05-05-2017
<input type="checkbox"/> Questionnaire	Ver.No :	Ver.Date :
<input checked="" type="checkbox"/> Investigator's CV / GCP (Dr Sadeeq Ali, Dr Nur Azah Binti Hamzaid, Tanfik Yabrya Mohammmad Al-Nusairi, FARAHYAH BINTI JASNI, Nur Hidayah Mohd Yusof, SADEEQ ALI)	Ver.No :	Ver.Date :
<input type="checkbox"/> Insurance certificate	Ver.No :	Ver.Date :
<input checked="" type="checkbox"/> Other documents		

and the decision is ☒

☒ Approved (Full Board)

☐ Approved (Expedited)

☐ Rejected/reasons specified below or in accompanying letter)

Comments:

Satisfactory revision.

The Investigators are required to:

- 1) follow instructions, guidelines and requirements of the Medical Research Ethics Committee;
- 2) report any protocol deviations/violations to Medical Research Ethics Committee;
- 3) provide annual and closure report to the Medical Research Ethics Committee;
- 4) comply with International Conference on Harmonization – Guidelines for Good Clinical Practice (ICH-GCP) and Declaration of Helsinki;
- 5) obtain a permission from the Director of UMMC to start research that involves recruitment of UMMC patient;
- 6) ensure that if the research is sponsored, the usage of consumable items and laboratory tests from UMMC services are not charged in the patient's hospital bills but are borne by research grant;
- 7) note that he/she can appeal to the Chairman of Medical Research Ethics Committee for studies that are rejected;
- 8) note that Medical Research Ethics Committee may audit the approved study;
- 9) ensure that the study does not take precedence over the safety of subjects.

Date of meeting : 21-06-2017
 Date of approval : 10-07-2017

In-Socket Sensory System for Transfemoral Amputees Using Piezoelectric Sensors: An Efficacy Study

Farahiyah Jasni, Nur Azah Hamzaid, Asan Gani Abd Muthalif, Member, IEEE, Zafirah Zakaria, Hanie Nadia Shasmin, and Siew-Chek Ng

Abstract—This paper presents the design and evaluation of an in-socket sensory system for a transfemoral prosthetic leg using a set of piezoelectric sensors. The design process includes identifying the optimal mounting configuration of the sensors and determining their best placement. Two experiments were performed separately to address each objective. Results of the experiment suggested that cushion-all with fit size cantilever with elastic foundation should be adopted to mount the sensors on the socket's wall. As for the placement of the sensors, the result suggested that the sensors should be positioned in zig-zag orientation from top to bottom, which can cover all of the most active area on the quadriceps and hamstring muscle groups. With the identified design, the socket was fabricated and instrumented for a transfemoral amputee and the performance of the in-socket sensory system was evaluated. The amputee performed level walking at normal speed on a 5-m straight pathway multiple times while the output voltage signal from each sensor was recorded. The output signals consistency was assessed by calculating the cross correlation, r , within five trials. In order to measure the strength of the correlation matrix of each sensor, the Frobenius norm, $\|A\|_F$ was calculated. The high norm value for all sensors pattern ($\|A\|_F > 4.5$) for quadriceps implies that the mounting and placement of the sensors is most suitable for a consistent and reliable signal. For Hamstring, results inferred that except for the two sensors located on the top most position and the most bottom sensor, the other sensors showed good performance ($\|A\|_F > 4.4$). Thus, the proposed design of the in-socket sensory system using piezo sensors was proven to be effective for a transfemoral prosthetic leg.

Index Terms—Active-knee prosthetic leg, biomechanics, piezoelectric, sensor, transfemoral (TF).

I. INTRODUCTION

STUDIES have shown that transfemoral (TF) or above knee amputees utilize 60% more of their metabolic energy [1] and apply up to three times greater power and torque on the affected-side hip [2] as compared to nonamputees. A prosthetic leg could assist the amputees to regain back their normal life. In general, prosthetic legs can be divided into two types: passive and active. Popovic defined the passive type as a prosthesis that is controlled by synergy (i.e., the movements are mechanically preprogrammed to mimic trajectories of the sound joints), while active prostheses are referred as the ones equipped with adaptive electronics controllers and actuators in the joint [3].

Despite being very useful to amputees in stabilizing the body while standing and walking, passive prosthetic legs are constrained by some limitations. The three major limitations according to Kapti and Yuceturk [4] are as follows: 1) does not respond to the needs of daily living activities, such as climbing stairs and slope walking; 2) demands high amount of metabolic energy from the user; and 3) limited degree in ability of duplicating the normal kinematics and dynamics gait pattern.

On the other hand, active prosthesis offers a wider scope of usage to the amputees in which it is usually embedded with actuator to replace the missing knee joint. Hence, less energy is required by the user to do such movements. To date, a variety of methods to control the actuators and its feedback system in an active prosthesis were reported [5]–[7]. Electromyography (EMG)-based sensor was one prominent way used to identify the intention of the prosthesis user, first reported in 1991 [8]. Since then, there have been numbers of research proposing the use of EMG as the sensors in active prosthesis design [9]–[11]. Nonetheless, one of the unavoidable drawbacks of EMG-based sensory system is that it requires careful preparation on the skin in order to generate accurate result. Consequently, it complicates the donning process of the prosthetic devices [12], [13].

Besides EMG, there are other works proposing the usage of mechanical sensor to measure force or pressure in prosthetic design [14], [15]. Mueller *et al.* [16] suggested the inertial measurement unit (IMU) sensor to be used in lower limb prosthetic design to acquire kinematic and kinetic data when the amputee doing motion. On the other hand, Wheeler *et al.* [17] used microelectromechanical systems (MEMS)-based bubble pressure sensor to monitor interface pressure within the amputee's stump and the socket.

This study aimed to investigate the efficacy of utilizing piezoelectric (piezo) sensors as an alternative as input to control the

Manuscript received December 18, 2015; revised April 20, 2016; accepted May 24, 2016. Date of publication June 06, 2016; date of current version October 13, 2016. Recommended by Technical Editor L. Zuo.

F. Jasni, N. A. Hamzaid, Z. Zakaria, and S.-C. Ng are with the Biomedical Engineering Department, University of Malaya, Kuala Lumpur 50603, Malaysia (e-mail: farahiyahjasni@gmail.com; azah.hamzaid@um.edu.my; zzz@yahoo.com; slawong@um.edu.my).

H. N. Shasmin is with the Biomedical Engineering Department and the Centre for Applied Biomechanics, University of Malaya, Kuala Lumpur 50603, Malaysia (e-mail: hanie.nadia@um.edu.my).


A. G. A. Muthalif is with the Smart Structures, Systems, and Control Research Lab, Department of Mechatronics Engineering, International Islamic University Malaysia, Kuala Lumpur 53100, Malaysia (e-mail: asan@iium.edu.my).

Color versions of one or more of the figures in this paper are available online at <http://ieeexplore.ieee.org>.

Digital Object Identifier 10.1109/TMECH.2016.2578679

1093-4435 © 2016 IEEE. Personal use is permitted, but republication/redistribution requires IEEE permission. See http://www.ieee.org/publications_standards/publications/rights/index.html for more information.

APPENDIX D: PUBLICATION 2



ORIGINAL RESEARCH
published: 25 April 2017
doi: 10.3389/fnins.2017.00290

Analysis of Interrelationships among Voluntary and Prosthetic Leg Joint Parameters Using Cyclograms

Farahiyah Jasni^{1,2}, Nur Azah Hamzaid^{1*}, Nor Elloxiana Mohd Syah¹, Tze Y. Chung² and Noor Azuan Abu Osman¹

¹Department of Biomedical Engineering, Faculty of Engineering, University of Malaya, Kuala Lumpur, Malaysia; ²Department of Mechanical Engineering, Faculty of Engineering, International Islamic University Malaysia, Selangor, Malaysia; ³Department of Rehabilitation Medicine, Faculty of Medicine, University of Malaya, Kuala Lumpur, Malaysia

The walking mechanism of a prosthetic leg user is a tightly coordinated movement of several joints and limb segments. The interaction among the voluntary and mechanical joints and segments requires particular biomechanical insight. This study aims to analyze the inter-relationship between amputees' voluntary and mechanical coupled leg joints variables using cyclograms. From this analysis, the critical gait parameters in each gait phase were determined and analyzed if they contribute to a better powered prosthetic knee control design. To develop the cyclogram model, 20 healthy able-bodied subjects and 25 prosthesis and orthosis users (10 transtibial amputees, 5 transfemoral amputees, and 10 different pathological profiles of orthosis users) walked at their comfortable speed in a 3D motion analysis lab setting. The gait parameters (i.e., angle, moment and power for the ankle, knee and hip joints) were coupled to form 36 cyclograms relationship. The model was validated by quantifying the gait disparities of all the pathological walking by analyzing each cyclograms pairs using feed-forward neural network with backpropagation. Subsequently, the cyclogram pairs that contributed to the highest gait disparity of each gait phase were manipulated by replacing it with normal values and re-analyzed. The manipulated cyclograms relationship that showed highest improvement in terms of gait disparity calculation suggested that they are the most dominant parameters in powered-knee control. In case of transfemoral amputee walking, it was identified using this approach that at each gait sub-phase, the knee variables most responsible for closest to normal walking were: knee power during loading response and mid-stance, knee moment and knee angle during terminal stance phase, knee angle and knee power during pre-swing, knee angle at initial swing, and knee power at terminal swing. No variable was dominant during mid-swing phase implying natural pendulum effect of the lower limb between the initial and terminal swing phases. The outcome of this cyclogram adoption approach proposed an insight into the method of determining the causal effect of manipulating a particular joint's mechanical properties toward the joint behavior in an amputee's gait by delaminating the curve closeness, C, of the modified cyclogram curve to the normal conventional curve, to enable quantitative judgment of the effect of changing a particular parameter in the prosthetic leg gait.

Keywords: transfemoral, biomechanics, cyclogram, prosthesis

OPEN ACCESS

Edited by:
Wenwei Yu,
Osaka University, Japan

Reviewed by:
Giuseppe D'Astous,
Istituto Superiore di Sanità, Italy
Hans-Erik Schuster,
University of Stuttgart, Germany

***Correspondence:**
Nur Azah Hamzaid
azahhamzaid@um.edu.my

Specialty section:
This article was submitted to
Frontiers in Neuroscience,
a section of the journal
Frontiers in Neuroscience

Received: 10 December 2016
Accepted: 05 April 2017
Published: 25 April 2017

Citation:
Jasni F, Hamzaid NA, Mohd Syah NE,
Chung TY and Abu Osman NA (2017)
Analysis of Interrelationships among
Voluntary and Prosthetic Leg Joint
Parameters Using Cyclograms.
Front. Neurosci. 11:290.
doi: 10.3389/fnins.2017.00290

APPENDIX E: AWARDS RECEIVED

1. Bronze medal, Invention and Innovation Awards 2016, Malaysia Technology Expo (MTE) 2016, 18 – 20 February 2016, Kuala Lumpur. (APPENDIX G).
2. Silver medal, BioMalaysia & Asia Pacific Bioeconomy 2016 (BioMalaysia 2016), (Healthcare and Wellness category), 31st May – 2nd June 2016, Kuala Lumpur.

